Fatigue Behavior of CFRP Laminates with Initially Cut Fibers

by

SUDARSONO

A Dissertation Presented to
Department of Mechanical Engineering
Graduate School of Science and Engineering
Ehime University

June 2017

Summary

Recently, carbon fiber-reinforced plastics (CFRPs) have been widely applied to primary structure in the fields of transportation (aircraft and automobiles) and other fields as alternate materials of metals because a large fuel saving becomes possible by making structures light. When CFRP laminates are employed in automobiles structures, these components are frequently subjected to cyclic loads and vibrations, which may cause degradation of structural integrity because of fatigue damage. Thus, it is important to investigate the fatigue characteristics of CFRP laminates.

In addition, for design requirements and functional needs, an automobile is composed of many complexly shaped components. In general, it is quite difficult to fabricate such components using only conventional CFRP prepreg with continuous fiber owing to its poor formability. In contrast, discontinuous fiber-reinforced plastics fabricated by sheet molding compound (SMC) or injection molding have already been used as automotive parts since they have good molding flowability. However, their strength is much lower than that of composites reinforced with continuous fiber. Therefore, a new material, called unidirectionally arrayed chopped strands, was developed by introducing initially cut fibers (ICFs) into CFRP prepreg. The strength and uniformity of layer structure of the ICF laminate were found to be superior to those of SMCs. CFRP laminates with ICFs have good formability without large degradation of static strength, however, their fatigue behavior has not thoroughly been investigated thus far.

In this dissertation, first, fatigue behavior and damage progress of open-holed CFRP laminates with ICFs having interlayers are investigated. Three types of CFRP laminates were employed; a laminate without ICF fabricated using an autoclave (Continuous-A), a laminate with ICF fabricated using an autoclave (ICF-A) and a laminate with ICF fabricated using press molding (ICF-P). First, fatigue test was conducted to obtain *S* (maximum stress)-*N* (the number of cycles to failure) curves in order to reveal fatigue strength. The fatigue tests for several specimens were interrupted at three prescribed numbers of cycles to observe damage progress. It is found that the Continuous-A laminate shows little strength degradation in the *S*-*N* curve by approximately 5 % at *N* of 10^6 while the fatigue strength of the ICF-P laminate is higher than that of the ICF-A laminate. Fatigue strength in both ICF laminates is decreased by approximately 30 % at *N* of 10^6. In contrast, the damage progress of the ICF-P laminate is the least among the three laminates while the delamination progress at both edges and around the hole in the Continuous-A laminate is the most prominent.

Second, the effects of fiber cutting angle on the fatigue behavior of open-holed CFRP laminates with ICFs are also investigated. Three kinds of fiber cutting angles (θ = 22.5,

45, and 90°) were applied to two types of quasi-isotropic ICF laminates; ICF-A and ICF-P. First, fatigue tests were conducted to obtain *S-N* curves in order to reveal fatigue strength. The fatigue tests of one specimen for each configuration were interrupted at three prescribed numbers of cycles to observe damage progress. Finally, a semi-empirical equation was proposed to predict delamination area just before the final failure against normalized applied stress. It is found from the experiment result that the fatigue strength in both laminates is the highest when the θ is the smallest (22.5°) although the static strength is the highest when the θ is 90°. In contrast, both laminates with the biggest θ (90°) exhibit the greatest delamination growth around the hole by cyclic loading.

Finally, fatigue behavior and damage progress of non-holed CFRP laminates with ICFs having interlayers are also investigated. Three types of CFRP laminates were employed; Continuous-A, ICF-A and ICF-P. First, fatigue test was conducted to obtain *S-N* curves in order to reveal fatigue strength. The fatigue tests for several specimens were interrupted at three prescribed numbers of cycles to observe damage progress. The results obtained from the fatigue test and damage progress observation of non-holed CFRP laminates indicated that the fatigue strength of the Continuous-A laminate is the highest among the three laminates while the fatigue strength of the ICF-P laminate is higher than that of the ICF-A laminate. However, the decrease ratio of fatigue strength at N of 10^6 is about 35% of its static strength, which is almost the same in the three laminates. In addition, the degree of damage in the ICF-P laminate is the smallest among the three laminates while the increase rate of the crack density and edge delamination is the greatest in the ICF-A laminate with thicker plies.

In conclucion, comparing the two ICF laminates in this study, it concluded that the fatigue strength of the ICF-P laminate in both open-holed and non-holed specimens had the greater fatigue strength compared to the ICF-A laminate. In addition, the fatigue damage progress in the ICF-P laminate is smaller than ICF-A laminate. Moreover, the ICF-P laminate with the smallest θ (22.5°) exhibited the greatest fatigue strength, while the ICF-A laminates with the largest θ (90°) exhibited the greatest delamination growth around the hole in open-holed specimens.

Acknowledgments

In the name of Allah SWT, the Most Gracious and the Most merciful. I would like to express my deepest gratitude to my supervisor, Prof. Dr. Keiji Ogi, not only for accepting me as a doctor student but also for his guidance, support and encouragement given throughout my years at Ehime University. I would also like to express my gratitude to Prof. Dr. Manabu Takahashi and Prof. Dr. Kazuyuki Nakahata for their valuable input and review to improve the content of my dissertation.

I am grateful to Associate Professor Dr. Mitsuyoshi Tsutsumi, Assistant Professor Dr. Koichi Mizukami and the members of Mechanic of Materials Laboratory for numerous helpful discussions, suggestions, assistance, cooperation and friendship. I would like to express my gratitude to all those who helped me during the research and writing of this dissertation. I would like to acknowledge the Scholarships Program of Ministry of Research, Technology and Higher Education of the Republic of Indonesia for providing financial support.

Finally, I would like to thank to my father Ane Ipo, my mother Maskunu and my brothers/sisters (Dani, Sona, Anti and Eby) for their love, support, and words of encouragement throughout my pursuit of my education. A special appreciation to my beloved wife Irma Nurjannah and my lovely children Adzka Rahadatul Aisy and Muh. Akhtar Aydin Khalfani for all the care, love, support and understanding thorough these long and hard year.

Sudarsono

Matsuyama, June 2017

List of Figures

List of Tables

Table of Contents

Chapter 1

Introduction

This chapter describes the general background of the short carbon fiber reinforced polymers (CFRP), the origination of laminate with initially cut fiber (ICF), and the review of previous study in improving the mechanical properties of ICF laminate, as well as the main objective and outline of this study.

1.1 General Background

A composite material is a mixture of two or more constituent materials, commonly consisting of a continuous matrix in which reinforcing filler has been embedded. Carbon-fibre reinforced plastic (CFRP) laminates constitute an important class of composite materials. They are produced by combining carbon fibers as reinforce and resin as matrix. Carbon fibers consist of small crystallites of 'turbostratic' graphite, one of the allotropic forms of carbon [1].

CFRP laminates have a heterogeneous laminated structure, consisting of individual layers of high-modulus, high-strength carbon fibers in a thermoplastic or thermoset matrix. The individual layers that make up the laminates are known as laminae or plies and are generally orthotropic or transversely isotropic, with the laminate then exhibiting anisotropic, orthotropic or quasi-isotropic behavior depending on its stacking sequence.

CFRP laminates have frequently been applied to various structures in wide range of industrial fields such as aircraft and aerospace, automotive, sport and recreations, civil engineering, environment and energy and, electronic, and medical science. They have become increasingly popular in almost every field associated with high performance. Their popularity is due to the fact that when compared to many other engineering materials, they offer superior stiffness, strength and fatigue properties at relatively low

density. They also have stable tensile strength, excellent corrosion resistance and dimensional stability.

Composites and more specifically, CFRP lie close to the top left corner of both charts: they have a high specific stiffness and a high specific strength, as can be seen in the Ashby [2] plots of Figure 1-1. This attractive combination of stiffness, strength and low mass has seen CFRP laminates experience steady growth and increased market penetration in industries such as aircraft [3–7], automotive[8–12], construction [13–15] and renewable energy[16–18].

The application of CFRP to various transportation vehicles, such as aircrafts and automobiles, has attracted more attention with the increasing requirements of energy saving vehicles and clean living environment. CFRP has been successfully applied to the primary structures, such as the wings and fuselage, of latest series civilian airplanes such as the Airbus A380 and the Boeing 787 [19], as shown in Fig. 1-2.

Recent years, more researchers and automobile manufacturers are interested with the application of CFRP to mass-produced automobiles due to the rapid increase of fuel prices and the increasing world-wide requirements of clean-air environment. For example, a CFRP automobile model with has been introduced by Japan Carbon Fiber Manufacturers Association (JCMA) [20], as shown in Fig. 1-3. The model shows that the

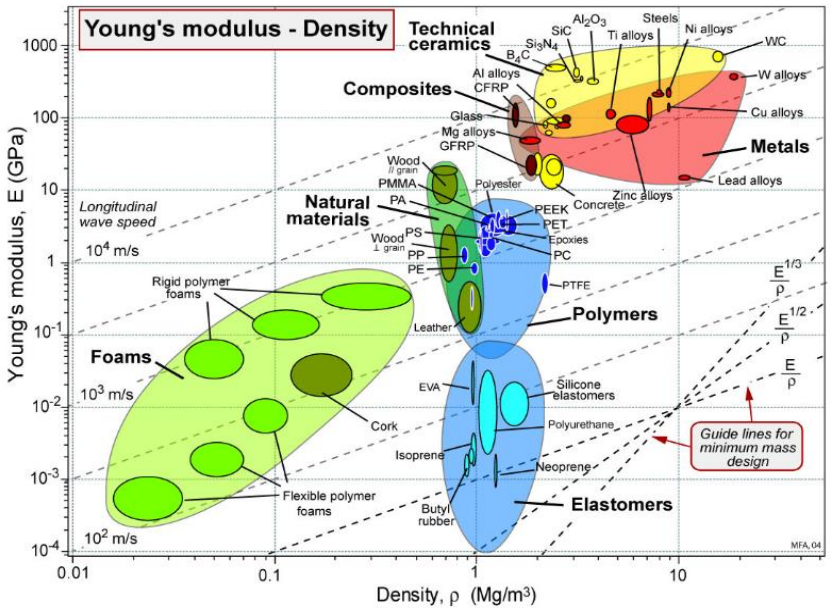

(a)

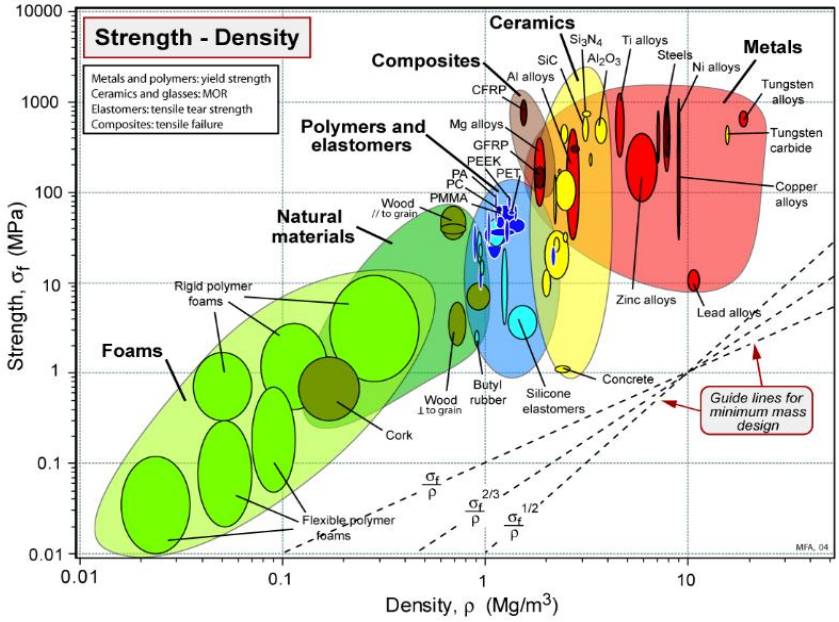

(b)

Figure 1-1: Ashby plots of (a) Young's modulus and density, and (b) strength and density for a range of engineering materials [2].

application of CFRP for 17% of total automobile weight will reduce the weight by 30% compared to the conventional model. Consequently, it can improve fuel efficiency and as well as substantially reduce CO_2 emission by equivalent of 50 tons over life cycle.

So far, the automobile components such as body panel, windshield frame, door

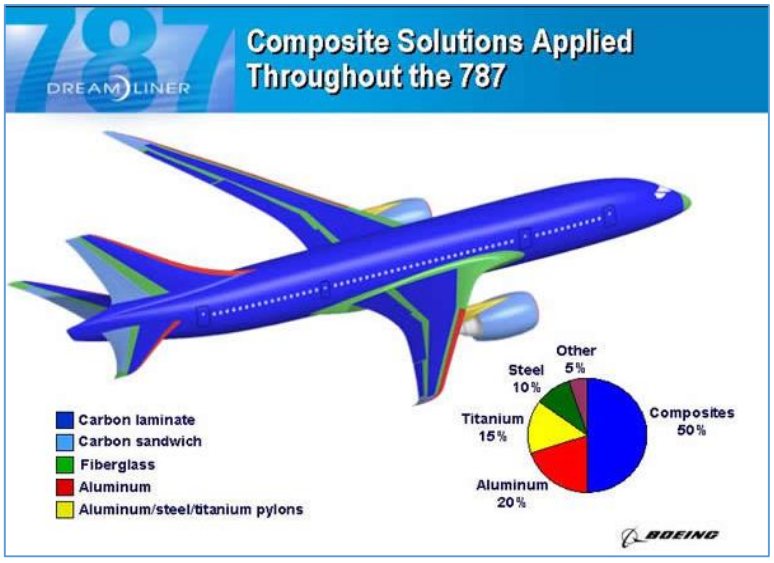

(a)

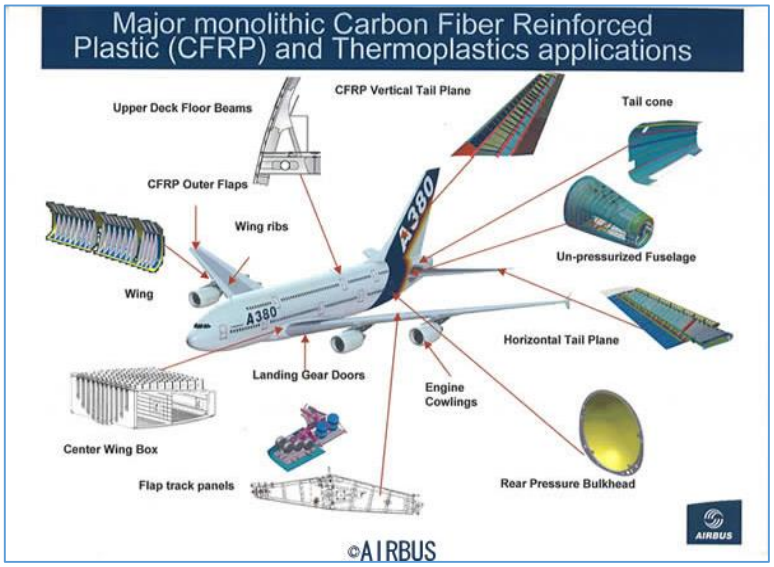

(b)

Figure 1-2: Overview of material application in the Boeing 787 and the Airbus A380 [19].

.

panel, hood, front crash structure, front end structure, real spoiler, tunnel, pillar, engine subframe, drive shaft, rear engine cover inner panel have been commercially produced by car manufacturer for exclusive and racing cars in limited edition. Now, there is a tendency to try to use the fiber for commercial, mass production cars in full scale in order to reduce production costs to a minimum practical level. In addition, this material has four advantages over every other type of material for automobile structure: super lightweight, super strong, super stiff and easy to mold into all kinds of different shape.

On the other hand, the application of CFRP to automobiles must consider different requirements compared to aircraft applications because the structural components of automobiles are relatively small and their geometries are more complicated. Generally,

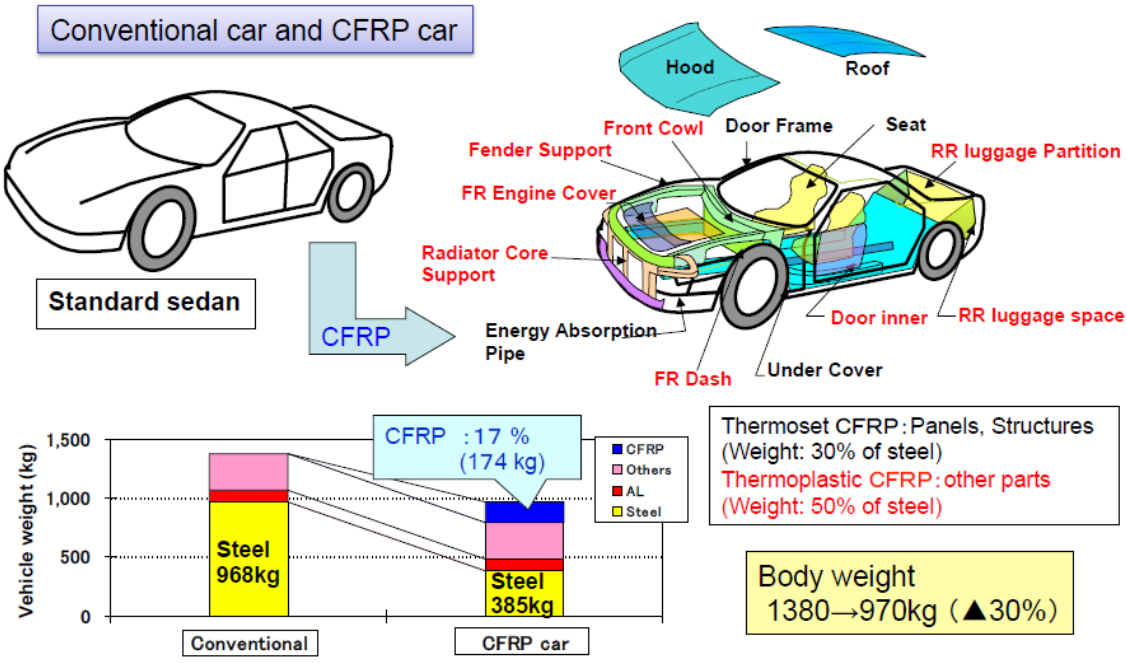

Figure 1-3: Comparison of body weight between conventional car and CFRP car [20].

complex-shaped components are manufactured through resin transfer molding (RTM) and sheet molding compound (SMC). However, In the case of RTM components, they contain discontinuities of reinforcing fibers. For example, fibers in prepreg sheets might be bent and broken at a sharp corner. For SMC components, they have large variation due the many ends of fiber bundles. Thus, such composite components fabricated by two methods may have broken and initially cut fibers that degrade the mechanical properties of CFRP.

In order to improve the mechanical properties for such components, Taketa et al. [21] developed a new molding sheet by regularly introducing slits into the conventional prepreg sheets. CFRP laminates with initially cut fibers (ICF) achieved higher strength than both conventional materials (RTM and SMC) through control of the fiber cutting angle and pattern, fiber direction and the position of fiber ends, as well as the shaping performance of molding sheet.

On the other hand, in the application of CFRP laminates for structural components, circular holes are needed for several technical reasons such as joining, weight reduction and functional needs. In addition, these components are frequently subjected to cyclic loads and vibrations, which may cause degradation of structural integrity because of fatigue damage, which is known to be responsible for the majority of failures in structural

components and machinery [22]. Furthermore, the fatigue damage behavior of CFRPs must be evaluated quantitatively for their application in production automobiles, because automobile structures are required to adopt a wide safe-life design.

The fatigue behavior and damage progress of open-holed CFRP laminates have been an extensively-researched topic. The growth of damage in such laminates with variability of fibers, matrices, manufacturing methods, lamination stacking sequences and geometries under fatigue loading is known to affect the fatigue performance of the material and ultimately, the structure. Therefore, a better understanding of the fatigue behavior and failure mechanisms is crucial to improve composite laminate design.

The fatigue behavior of CFRP laminates containing a stress concentrator is of particular importance. It is recognized that subcritical damage evolves from these stress raisers under increasing load cycles, until an instability occurs and catastrophic failure ensues. Therefore, it is important to understand the general fatigue response of CFRP laminates with ICF containing a circular hole.

1.2 Introduction of the First of ICF Laminates

In order to enhance the strength and stiffness of short fiber reinforced polymers, many studies [23–26] have been performed at the enhancement of fiber volume fraction and the high alignment of fibers. Highly aligned discontinuous fiber yarn and prepreg

with highly aligned unidirectional short fibers were developed in [23,24] using the technology of stretch-broken carbon fibers. This technology can fabricate short fiber composites with highly aligned fibers and high fiber volume fraction. However, it is difficult to control the fiber length by this technology.

A different method was developed using random chopped strands made by cutting the conventional CFRP prepreg with continuous carbon fibers in [25,26]. This method can fabricate short fiber composites with high fiber volume fraction which is near the original composites with continues fibers, but the chopped strands are randomly distributed in the composites. On other hand, high porosity and random distribution of chopped strands result in much lower strength than conventional CFRP.

Recently, a new method was developed, a new short fiber reinforced polymer made by laminate with ICF has been developed [21,27–30]. The laminate is made by introducing specific slits into a conventional prepreg with continuous carbon fibers. The experimental results showed that the ICF laminates have higher strength and modulus than conventional short fiber reinforced polymers due to the high aligned fibers and high fiber volume fraction. it also has superior formability and is suitable to fabricate structural components in complex geometries.

In the early study on the ICF laminates, two kinds of ICF prepregs are investigated

[21,27,28]. The first kind of ICF prepreg has staggered short slits perpendicular to the fibers [21], and the second one has continuous slits with a small angle to the fiber direction [28]. Much higher strength is obtained for the second kind of ICF laminates than the first kind.

The schematic diagram of the first designed ICF laminate is shown in Fig. 1-4, proposed in [21]. The continuous and discontinuous slits of 12.5 mm in length at an interval of 25 mm are introduced into the prepreg. All the slits are perpendicular to the fiber direction and loading direction and all the fiber are cut into 25 mm in length in the ICF prepreg. This constitution allows the fiber strands flowing smoothly during molding

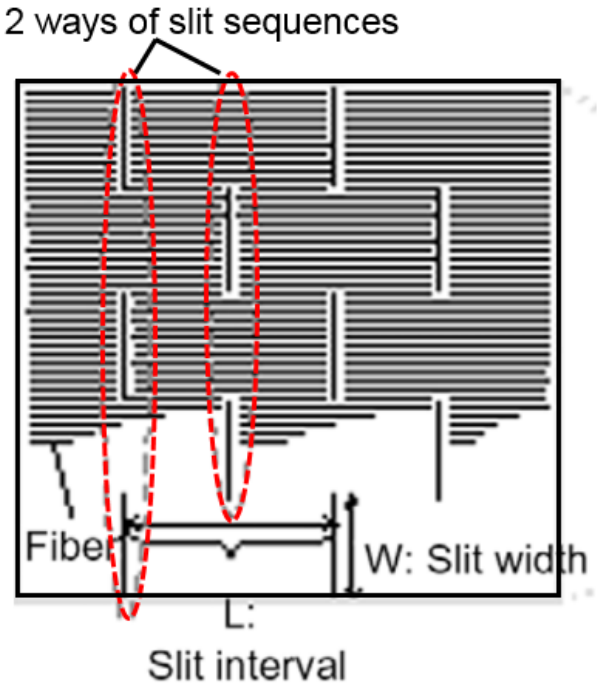

Figure 1-4: Schematic of first ICF laminates created by introducing slits in arrayed continuous fibers of prepreg [21].

while the stress concentration is minimized by isolating the mutual position of the strands-ends. Thus, components with complex geometry such as rib structures can be fabricated by ICF plies. Compared with short fiber reinforced polymers fabricated by SMC and injection molding methods, the layer structure and the high fiber volume (about 60%) of conventional CFRP laminates are maintained and the fiber directions are uniform in a single ply of ICF laminates.

Figure 1-5 shows the experiment results of the tensile strength and modulus of the quasi-isotropic laminate stacked by ICF plies together with those of SMC and conventional CFRP laminate without slits for a comparison. The strength of ICF laminate was twice of SMC and the scatter range was much narrower similar to that of the conventional laminate. In addition, the tensile modulus, which is close to that of conventional CFRP laminate, was much higher than that of SMC.

Figure 1-6 presents the photographs of the cross-sections and the fractured specimens obtained from the SMC, ICF and conventional CFRP laminates. In the case of SMC, the chopped strands are crimped in the thickness direction, and several resin-rich regions are seen. In contrast, ICF laminate does not include any resin-rich regions, except for just around the slits. This is the main reason for the high modulus of the ICF laminate.

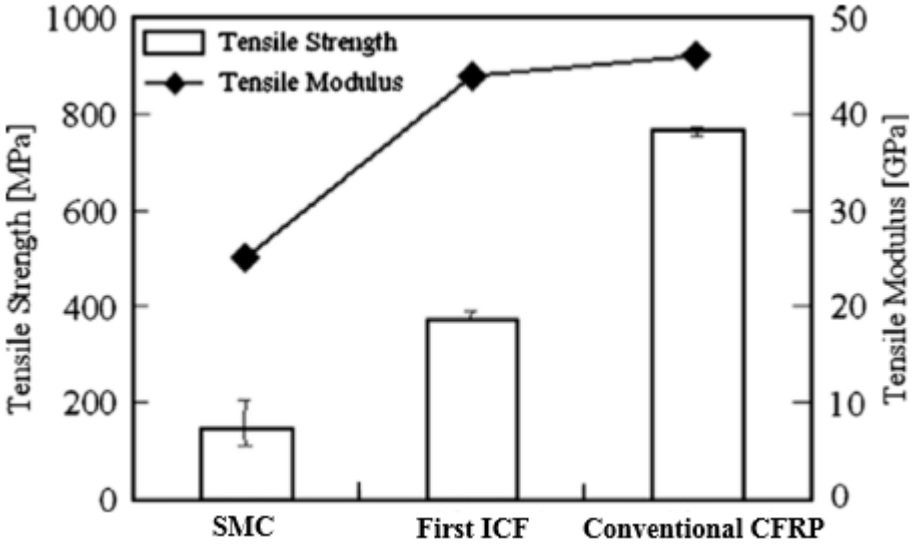

Figure 1-5: Comparison of tensile strength and modulus between SMC, the first ICF and conventional CFRP [21].

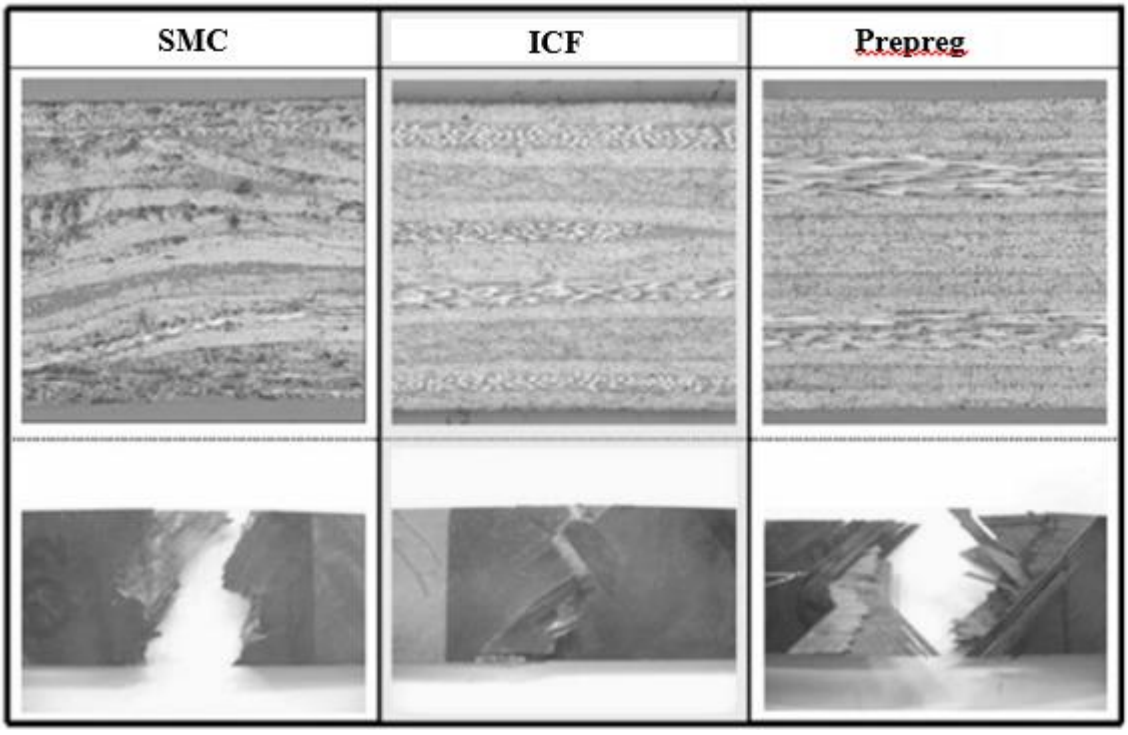

Figure 1-6: Comparison of cross-sections and fractured coupons of SMC, first ICF and conventional CFRP [21].

Additionally, observed from the fractured of various specimens, SMC is seen to have a zigzag fracture plane, implying that the crack generated in the resin-rich regions grows in the specimen, avoiding the chopped strands, and causes the final failure. In contrast, a large delamination is generated in the initial ICF laminate, in spite of matrix cracking observed before the delamination. Delamination was assumed to be induced only by the shear stress concentration around the slits, without the matrix cracking effect. No fiber breakage occurs even near the slits in the ICF laminate. It concluded that the interlaminar delamination caused the final failure of the ICF. Although it is revealed that the first ICF laminate has better mechanical properties than the injection molding and SMC, the flowability of the ICF laminate should also be clarified.

In order to clarify the flowability of the ICF laminate, a stretched ICF laminate was fabricated by hot pressing at 3 MPa pressure and 150 ºC for 30 minutes, As a result, the

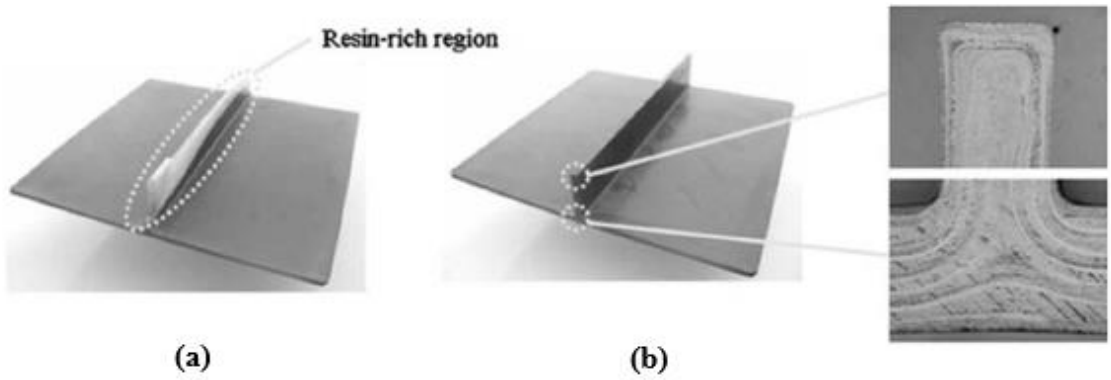

Figure 1-7: A T-shaped rib structure made from (a) conventional prepreg and (b) ICF prepreg [21].

area of the ICF laminate increased by 31% after hot pressing, compared to the original ICF ply before hot pressing. This fact demonstrated that this ICF laminate has the same excellent flowability as SMC. Furthermore, in order to investigate the layer structure of the ICF laminated component, T-shaped rib components with present ICF prepreg and conventional prepreg without slits are fabricated, as shown in Fig. 1-7. It is found large resin-rich region in the case of rib component fabricated by conventional prepreg. In contrast, no such resin-rich region is seen in the case of the component fabricated by present ICF prepreg and the layer structure of ICF plies is still maintained even in the rib part.

1.3 Review of Previous Study

As mentioned in previous subsection, initial ICF laminates performs higher strength compared with previous short carbon fiber reinforced polymers. But the strength of the early ICF is relatively low compared to conventional CFRP laminate due to that delamination is the principal cause of the final failure, subsequently, the early ICF laminate only can be fabricated as the no-bearing structures and secondary-bearing structures. In order to improve the strength of ICF laminate without reducing the flowability, many researches are conducted. The main studies in improving the strength of ICF laminate are interlaminar toughening and adjusting of the slit angle.

1.3.1 Interlaminar Toughening of ICF Laminates

Based on the consideration of inhibiting the delamination in the ICF laminate, the following three interlaminar toughening methods are tried [27]: (1) Toughening the matrix resin; (2) Inserting a toughened interlaminar layer into plies; (3) Localizing the toughened layer only around the ends of the chopped strands.

1. Toughening the matrix resin

In the first trial of interlaminar toughening, the matrix of the ICF itself was exchanged for toughened resin. A fresh prepreg of P3252S-15 (Toray Industries), made of carbon fiber T700S and epoxy resin #2521R is used for fabricating ICF laminate. The ICF laminate with the toughened matrix #2521R improves the strength by 14%. It is noted that a conventional CFRP laminate with #2521R also improved the strength by 9%. On contrary, the fracture morphologies of the first ICF laminate and the ICF laminate with #2521R closely resemble. This demonstrates that the strength of ICF is strongly dependent on the damage progress due to the delamination.

2. Inserting a toughened interlaminar layer into plies

The purpose of a toughened interlaminar layer is to suppress the progress of interlaminar delamination, caused primarily by out-of-plane impact, and to maintain the

compression strength of the laminates. In order to improve the interlaminar toughness, the thermoplastic non-woven fabric is used as the toughened interleaves. As a result of the tensile modulus and strength, inserting polyamide nonwoven fabrics improves the strength by up to 17%. The ICF laminate with polyamide non-woven fabrics in an areal weight of 30 g/m2 has less strength than that in an areal weight of 20 g/m2. Thus, an optimized interlaminar thickness for the toughened layer with regard to tensile strength seems to exist. In contrast, inserting polyolefin non-woven fabrics reduces the strength. It decreases the interlaminar toughness because polyolefin has poor adhesion to carbon fibers and the epoxy resin matrix. Consequently, it was concluded through this study that inserting appropriately toughened interleaves into ICF plies can improve the tensile

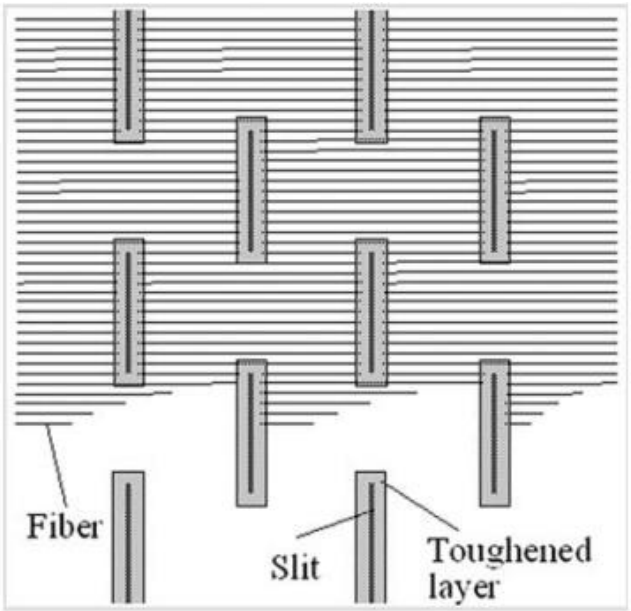

Figure 1-8: Schematic diagram of ICF laminate with interlaminar toughened layers only around the slits. [21].

strength.

This study also confirmed that delamination was still the principle damage which caused the final failure of the ICF laminate. However, the tensile modulus is significantly reduced. For example, inserting polyamide non-woven fabric in 20 g/m2 improved the strength by 17%, but reduced the modulus by 18%. This is because the toughened interleaves decreased the volume fraction of fiber of the ICF laminate.

3. Localizing toughened layer around the ends of chopped strands.

As the final trial, instead of inserting the toughened interleaf into every interface

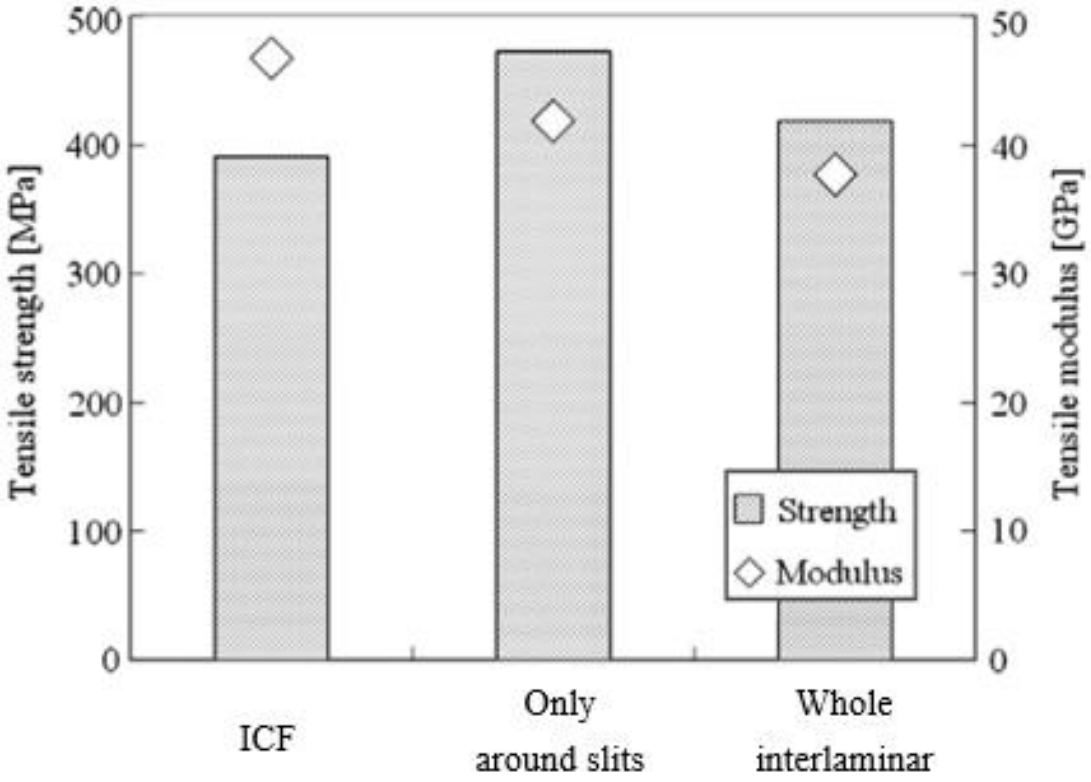

Figure 1-9: Comparison of tensile strength and modulus of quasi-isotropic laminates with different areas of toughened layers. [21].

between the ICF plies, this trail tried a locally toughening method only around the ends of the slits, as shown schematically in Fig. 1-8.

The tensile strength of ICF is improved by 21%, and the tensile modulus was reduced by only 10%, using locally toughening method, as summarized in Fig. 1-9. Although a locally toughened interleaf can only suppress the onset of delamination, it directly and positively affects the strength. In addition, the relatively small amount of toughened interleaf layer inserted minimizes the decline in the fiber volume fraction and the modulus of the ICF laminate.

1.3.2 ICF with Continuous and Angled Slits

From above subsections, it is seen that the slits are still perpendicular to the fibers. The problem of high stress concentration around the tips of slits in the ICF laminate is still unsolved. To reduce the stress concentration around the tips of slits in the ICF laminate and to further improve the strength of early ICF laminates, Taketa et al. [28] proposed a second design of ICF ply by introducing continuous and angled slits into the prepreg. The optical image of the second designed ICF ply and the schematics of the relative ICF laminate are given in Fig. 1-10. The angle between the fiber direction and

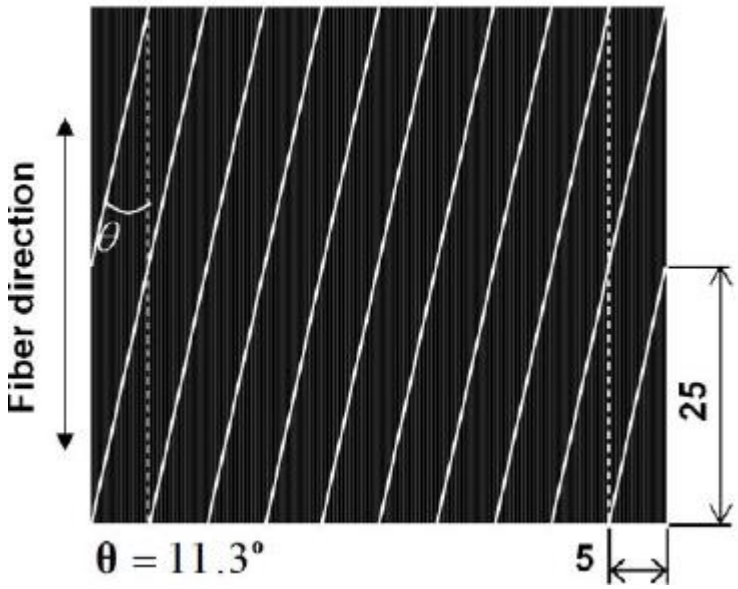

Figure 1-10: Schematic diagrams of Enhanced ICF by introducing continuous angled slits in prepreg [28].

the slit is about 11° and the fiber length are 25 mm in length which is as same as the early ICF ply.

The mechanism of why the small angle can reduce the stress concentration and suppressing the initiation of delamination is described in Fig. 1-11. A local square region is selected as an analysis model and the average in-plane stresses occurred due to the tensile stress σ applied in the fiber direction are expressed by axial stress σ_x, σ_y and shear stress τ_{xy},

$$\sigma_x = \sigma \cos^2\theta,\ \sigma_y = \sigma \sin^2\theta,\ \sigma_{xy} = \sigma \cos 2\theta/2 \quad \text{.....(1)}$$

In the case of first ICF (θ= 90°), $\sigma_x = 0$, $\tau_{xy} = 0$, and $\sigma_y = \sigma$. Therefore, the stress σ_y applied to the slit in the direction perpendicular to the slit is maximized, so the shear stress

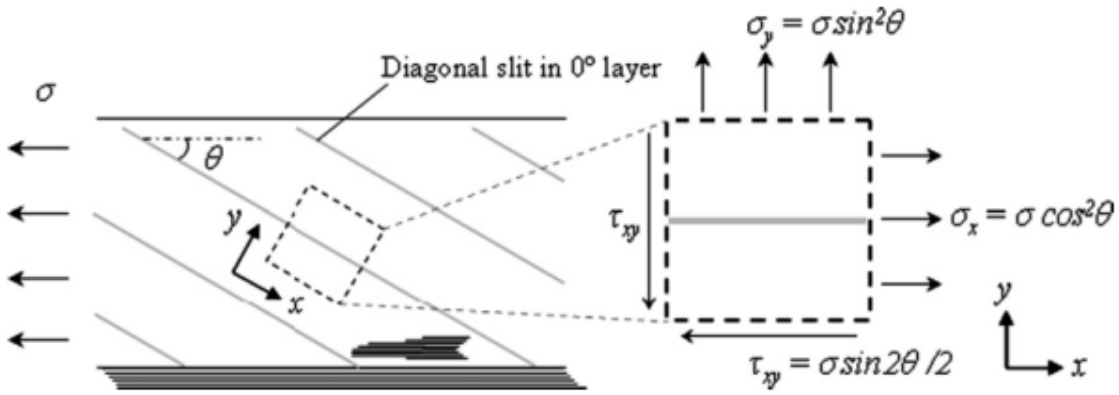

Figure 1-11: Schematic diagram of stress distribution around an angled slit in the 0 layer. [28]

around the slit is also maximized due to load transfer at the interface. In contrast, in the case of ICF with a slit small angled at a smaller θ, σ_x becomes larger and σ_y and τ_{xy} become smaller. σ_x does not contribute to the initiation of delamination from the slit because σ_x is parallel to the slit, while the shear stress around the slit caused by σ_y and τ_{xy} are responsible for delamination in modes II and III. Therefore, the initiation of delamination around slits is not as so severe as the early ICF laminates.

In this study, effects of the slit angle on the strength of the ICF laminates are investigated. The ICF plies with angled slits were stacked in a quasi-isotropic lamination of $[45/0/-45/90]_{2S}$ and cured by a hot pressing. Two kinds of ICF laminates with 31% stretched and non-stretched shapes are fabricated to investigate the flowability during the curing process. The stretch of ICF occurred due to the flowability of chopped strands under the pressure of 3 MPa in hot pressing process. The angled slit direction was $+\theta$ on

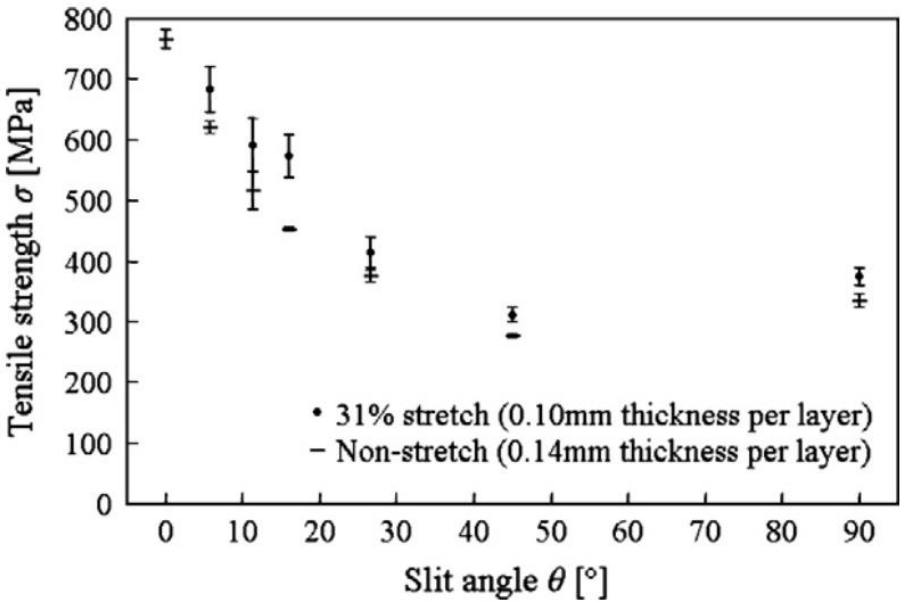

Figure 1-12: Relation between tensile strength of quasi-isotropic ICF laminates and the slit angle [28]

the upper half of the laminate $[45/0/-45/90]_2$ and $-\theta$ on the lower half.

Tensile tests of the secondly designed ICF laminates are also conducted. The relation between the tensile strength of quasi-isotropic ICF laminates and the slit angle θ are presented in Fig. 1-12. As the slit angle becomes smaller than 45°, the tensile strength dramatically increases, approaching that of conventional laminate without slits (θ = 0°). The ICF laminates with an area increase (31% stretched) exhibit higher strength than those of non-stretched ICF laminates for each slit angle because the each ply in stretched laminates becomes thinner than original ply.

1.3.3 ICF Laminate with Staggered Angle Slits and Bi-angled Slits

Although the above mentioned early ICF laminates exhibit better mechanical

properties and similar flowabilty compared to traditional short fiber reinforced composites made by such as injection molding and SMC, the final failure of the early ICF laminates even the secondly designed ICF laminate with continuous angled slits are still dominated by the delamination progression and fiber breakage is rarely observed. It means that the high strength advantage of the carbon fiber is still not efficiently utilized. Large delamination easily occurs and extends along the continuous slits due to the stress concentration along the slits. In order to improve simultaneously mechanical propertries and flowability, two newly designed ICF prepregs, namely, with discontinuous staggered angled slits and with discontinuous bi-angled slits (See Fig. 1-13), are proposed and investigated experimentally and numerically [29,30].

New designs of ICF laminates are proposed to improve existing ICF laminates with

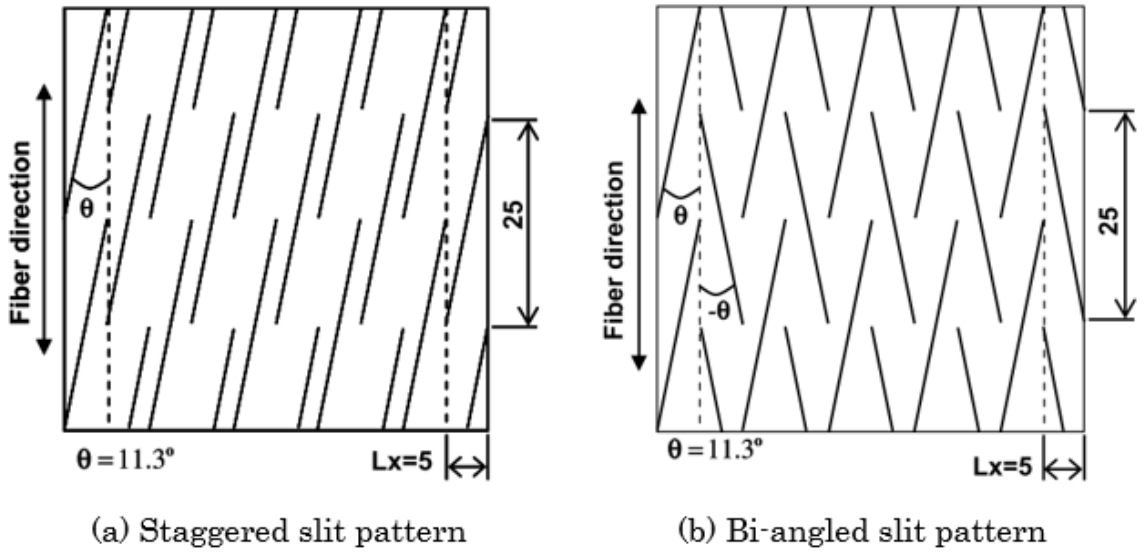

Figure 1-13: Schematic of newly designed discontinuous angled slit patterns [29]

continuous angled slits by introducing discontinuous angled slits into a unidirectional prepreg. Two slit patterns of staggered angled slits and bi-angled slits are designed. A paper cutter is employed to introduce slits into the prepreg. Quasi-isotropic ICF laminates

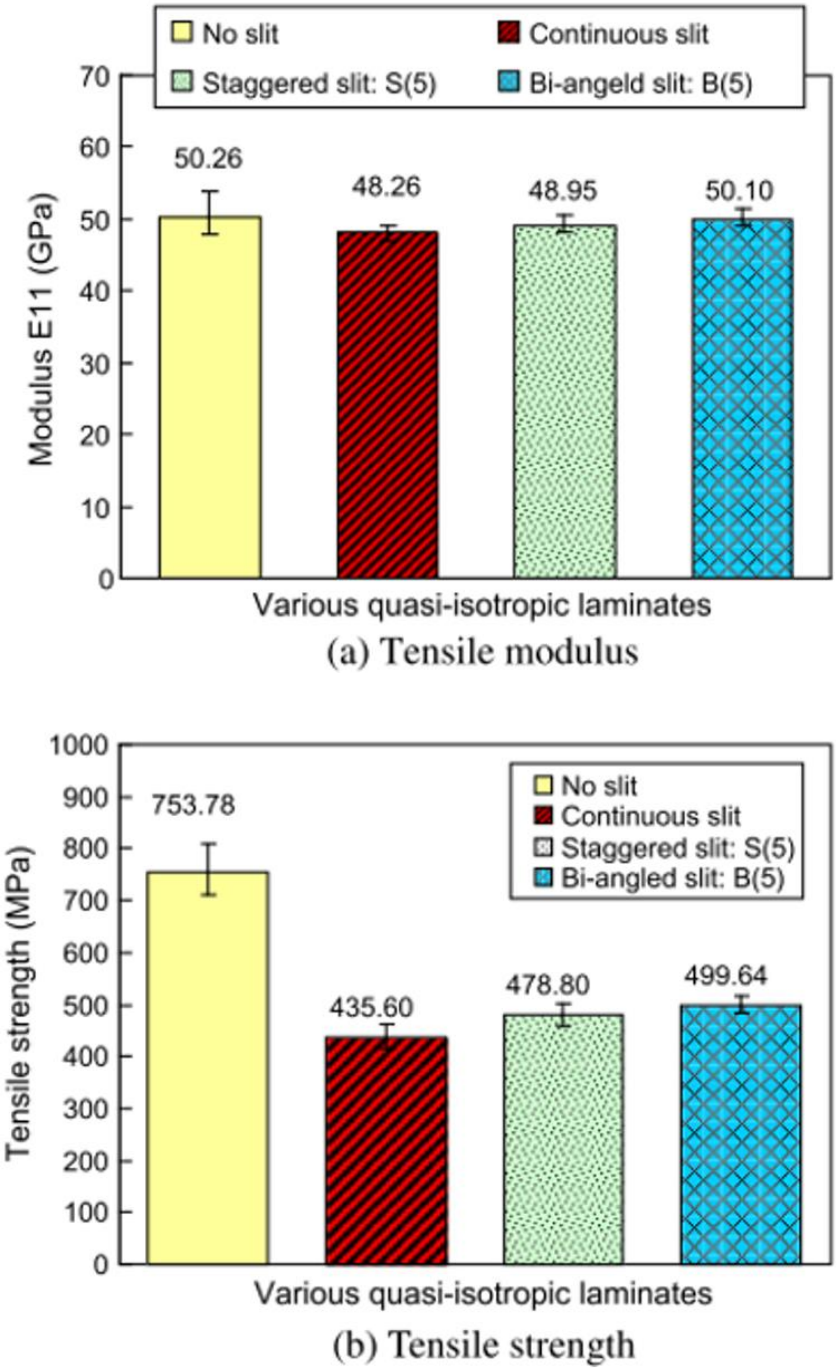

Figure 1-14: Tensile properties of various quasi-isotropic laminates [29]

with new slit patterns and existing continuous angled slits together with the conventional laminate without slits are fabricated for tensile tests. Hybrid laminates [90/0/90] with two unidirectional glass-fiber/epoxy plies and one ICF ply are fabricated for flowability tests.

Figure 1-14 presents the detailed values of the tensile modulus and strength. Comparing with a laminate without slits, the modulus and strength of ICF laminate with continuous slits reduces by 4% and 42.2%, the laminate with staggered slits reduces by 2.6% and 36.5%, and the laminate with bi-angled slits reduces by 0.3% and 33.7%, respectively. Comparing with an existing ICF laminate with continuous slits, newly designed ICF laminates with bi-angled slits and with staggered slits enhance the tensile strength by 14.7% and 9.9%, respectively. Evidently, out of the three types of laminates studied, the ICF laminate with bi-angled slits gives the best tensile properties among the ICF laminates. Experimental results reveal that newly designed ICF laminates possess higher strength and better flowability than existing ICF laminate

1.3.4 Fatigue Behavior of Open-Holed CFRP Laminates

CFRP laminates, despite still being viewed by some as cutting-edge technology, have actually long existed as an engineering material. The study of their mechanical properties, fracture behavior and response to stress raisers performed by researchers almost half a century ago. Considerable experimental research has been done to investigate the damage

mechanisms in CFRP laminates when subjected to different types of loading, including tension, compression, impact and fatigue. A better understanding of the damage mechanisms will assist in improving composite laminate designs.

Fibre-reinforced composites laminates are increasingly being used to manufacture load bearing primary structures in the aerospace industry as composites offer a much greater strength to weight ratio than metals. The initial perception was that composite materials do not suffer from the effects of fatigue, however in recent years it has become well established that composites can exhibit damage under cyclic loading conditions. Laminates with stress concentrations have complex damage sequences and failure events, and show a wide variety of effects not observed in unnotched laminates. The notch sensitivity of a laminate in terms of mechanical properties, depends on various factors, such as: laminates sequences, laminate thickness, ply orientations, laminate size, notch size, fabrication method, and machining quality. These factors all affect the way damage propagates, their interactions and the final mode of failure.

1.3.4.1 Tension-Tension

Investigations into the fatigue behavior of open-holed CFRP laminates subjected to tension-tension loading have been performed. Many of the studies in the literature have concentrated on the macroscopic effects of fatigue damage on fatigue performance and there have been some studies into the detailed damage mechanisms and sequence of

events occurring, such as in [31–50]. There has also been few works describing various failure fatigue models for prediction of fatigue behavior and fatigue life and their fit to experimental data.

Few studies describing effect of matrix toughness, fiber-matrix adhesion on the fatigue strength and failure mechanism of notched CFRP laminates have been performed. For example, Aymerich and Found [31] investigated and compared fatigue behavior of

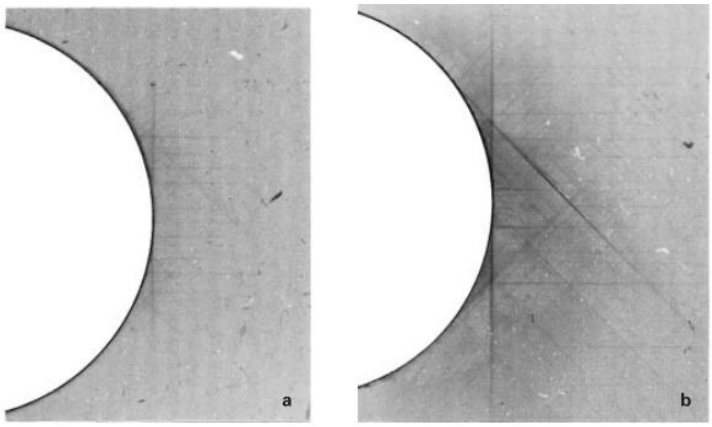

Figure 1-15: Fatigue damage progression in a notched carbon/epoxy specimen; (σ_{max}= 0.95.σ_{static}, R=0.1). (a). *N*=10 000 cycles; (b). *N*=30 0000 cycles. [31]

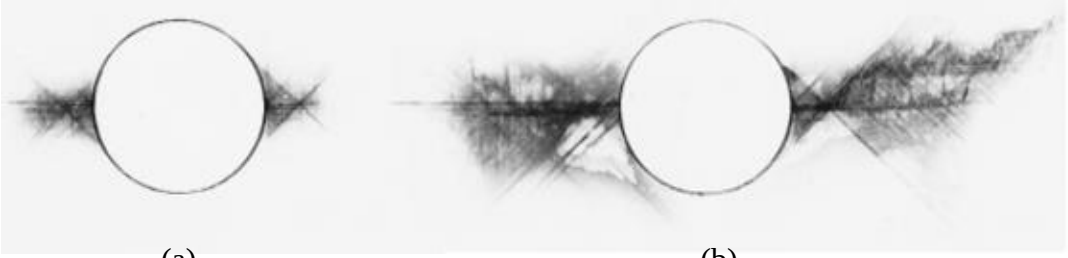

(a) (b)

Figure 1-16: Fatigue damage progression in a notched carbon/PEEK specimen (σ_{max}= 0.84.σ_{static}, R=0.1). (a). *N*=2727 cycles; (b). *N*=14180 cycles. [31]

quasi-isotropic carbon/PEEK and carbon/epoxy open-holed laminates, chosen as representative of the two classses of tough and britlle matrix composite. They found that fatigue damage in carbon/epoxy laminate consists of a combination of matrix cracks, longitudinal splitting and delaminations, which attenuate the stress concentration and suppress fibre fracture at the hole, as a consequence, fatigue failure can be reached only after very high number of cycles. In contrast, carbon/PEEK laminates, the behavior of fatigue damage in carbon/PEEK laminates strongly depend on the stress level due to the superior matrix toughness and the high fibre-matrix adhesion. At high stresses the absence of early splitting and delaminations promotes the propagation of fibre fracture therefore resulting in poor fatigue performance; while at low stress levels, damage modes are matrix controlled and this again translate into very long fatigue life. Typical differences of fatigue damage progression in notched specimens of two material systems are shown in Fig. 1-15 and Fig. 1-16.

Afaghi et al. [32] investigated the effect of fibre–matrix interfacial adhesion on fatigue strength of a cross-ply polymer matrix composite laminates containing a circular hole under tensile-tensile cyclic fatigue loading. They found that the fatigue life of notched cross-ply laminates is sensitive to the level of adhesion between fibre and matrix. The fatigue life of laminates with strong fibre-matrix adhesion was higher than that of

laminates with low-fibre-matrix adhesion. Damage analysis results showed that the composite system exhibit longitudinal splitting, delamination and transverse ply cracking at all load level. However, laminate with strong fibre-matrix adhesion reveals much extensive longitudinal splitting and local delamination. These results confirmed that the fatigue life of notched laminated composites is dependent on fiber–matrix interfacial adhesion. In addition, fractographic analysis on the failure section shows that primary damage mode in laminate having a poor fibre-matrix adhesion, are fibre-matrix splitting and fibre bundle pullout that extended to the end-tabs. However, laminate with the strong

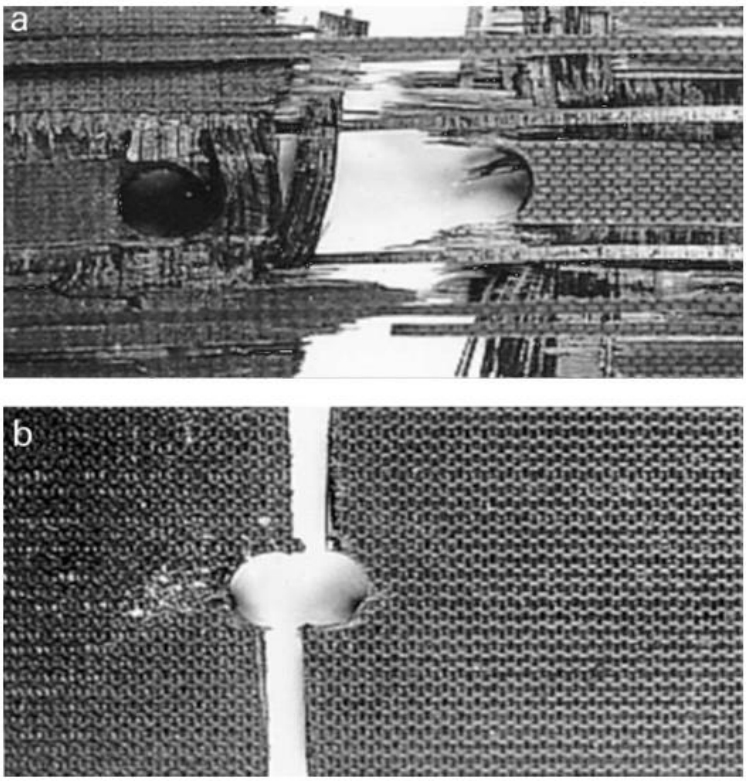

Figure 1-17: Typical fracture patterns of fatigue $(0/90)_{4s}$ notched laminates (σ_{max}= $0.85.\sigma_{static}$, $N = 10^5$ cycles) (a). Laminate with poor fibre-matrix adhesion and (b). Laminate with strong fibre-matrix adhesion [32]**.**

fibre-matrix adhesion exhibit catastrophic brittle failure with little apparent evidence of longitudinal splitting. Photograph of failure section of fatigue notched specimens of two laminates are shown in Fig. 1-17.

Vieille and Albouy [33] also investigated the influence of matrix ductility on the tensile fatigue behavior in notched and unnotched woven-ply C/PPS (thermoplastic) and C/Epoxy (thermoset) laminates under high temperature condition. The obtained results show that matrix ductility is prominent to rule the fatigue response of notched woven-ply laminates at high temperature. They applied a simple analytical model to test its predictive capabilities to evaluate the fatigue damage accumulation in both materials. The model proved to be applicable to C/PPS composites with a good agreement between experimental and model responses. However, it does not seem relevant to predict damage accumulation within C/Epoxy notched laminates subjected to tensile fatigue loadings.

Few studies have addressed the characterization of detailed damage mechanisms and sequence of events occurring. Kawai and Shiratsuchi [34] studied the effects of centrally located circular holes on the constant amplitude fatigue behavior of cross-ply CFRP laminates of various stacking sequences. They showed how the notched fatigue strength of cross ply laminates becomes lower than for un-notched specimens in the range of short fatigue life. However for the long life range this notch sensitivity becomes insignificant.

They also proposed a new method for prediction of fatigue strengths of composites with the assumption that notch sensitivity reduces during fatigue loading.

Nixon-Pearson et al. [35] carried out an extensive experimental and program to investigate and understand the sequence of damage development throughout the life of open-hole quasi-isotropic IM7/8552 carbon-fibre/epoxy laminates loaded in tension–tension fatigue. They used X-ray Computed Tomography (CT) in order to determine the 3D sequence of damage events. The results showed that matrix cracking at the surface ply and initiation of matrix cracks in the subsequent plies lead to delaminations that progress through the thickness, and ultimately to the propagation of delamination at the -45/0 interface all the way back towards the end tabs. The number of cycles to failure decreased linearly as the maximum fatigue stress level increased.

Nixon-Pearson and Hallett [36,37] carried out an extensive experimental program to investigate and understand the sequence of damage development throughout the life of open-hole carbon/epoxy laminates of various quasi-isotropic stacking sequences loaded in tension–tension fatigue. They showed that a delamination dominated failure mode is observed in all quasi-isotropic stacking sequences but the highest of severities tested. Tests showed that initially damage starts to propagate out from the hole edge in terms of matrix cracks and delamination. Asymmetric -45/0 delaminations cause a large drop in

stiffness. This is the dominant failure event for both the ply level and sub-laminate level specimens. The failure events for the ply level specimens are more localized around the hole, giving a more abrupt decrease in stiffness from the initial plateau. For the baseline sub-laminate level specimens, damage occurs in the outer sub-laminates first and then passes through into the central sub-laminates with a greater degree of distributed matrix cracking.

Aidi et al. [38] carried out an extensive experimental program to investigate and quantify the damage development by measuring the residual properties throughout the fatigue life of open-hole quasi-isotropic carbon-fiber/epoxy laminates loaded in tension–tension fatigue using two combined non-contact methods digital image correlation (DIC) and optic based vibrations. The results provide an important step in the validation of DIC and vibration response as a powerful combined non-destructive evaluation tool for monitoring the development of fatigue damage as well as predicting the damage level of notched composite materials.

The predicting fatigue life and damage development were also studied extensively. Spearing and Beaumont [39,40] performed fatigue studies of notched carbon fiber composite materials by predominantly using cross ply laminates. They developed a new approach to modelling the post fatigue strength and stiffness in notched composites

showing how the observation of notch tip damage can be quantified by the extent of individual failure processes. They found that damage at a notch tip in a laminate under cyclic tensile loading consists of splits, delamination and transverse ply cracks. The notch tip damage zone grows under tensile cyclic loading in a stable manner, with the shape and size of the damage zone depending on the laminate geometry, fibre, matrix and interfacial properties.

1.3.4.2 Tension-Compression

An extensive literature also exists on the compressive fatigue behavior of open holed CFRP laminates. Mohlin et al. [41] studied fatigue delamination growth in notched carbon/epoxy laminates under compressive fatigue loading using tetrabromoethane (TBE) enhanced X-ray radiography. They performed tests with amplitude range from 48% to 88% of the static fracture compressive load. They showed that matrix cracks in the 0° ply orientations (along the direction of loading) occur tangential to the hole roots below 10^3 cycles. After further cycling, delamination begin to propagate outwards between the interfaces of the off axis plies until catastrophic failure occurs.

Kellas et al. [42] studied fatigue behavior and damage development in a sixteen-ply 0°, and +/−45° notched-carbon fiber composites subjected to tension-compression fatigue loading. Tension-compression fatigue of the notched laminates produces a complex interaction of damage modes which give rise to fatigue failures. They noted that the first

sort of damage observed consisted of splitting at notch tips in the loading direction. They found very limited amount of matrix micro-cracking in the outer-most pairs of 45 fibre plies. The C-scans observation indicated a growth in the delamination damage development at the notch tip and in the loading axis direction. Further increase in the number of fatigue cycles leads to the development of further fibre cracks through the thickness near the notch tip. Both the delamination area and the number of splits also increase rapidly. Final failure appears to be initiated by a rapid growth of the delamination damage in the transverse direction. Fatigue extends the slits in the load direction but the development of parallel sets of splits probably results from the matrix micro-cracking and subsequent delamination followed by microbuckling of bands of 0° fibers at the notch tip in the outermost layers.

Morton J et all [43] investigated the effect of absorbed moisture and/or heat on the tension-compression fatigue properties of notched (sharp slits and circular holes) 0°and +/−45° carbon fiber reinforced plastic laminates using several destructive and non-destructive methods. It was found that the shape and extent of fatigue damage around the notches were highly dependent upon the environments considered (temperature and absorbed moisture). The effects of environment and loading upon the fatigue behavior are: (1). A reduction of the constraint between 0 and 45 layers by means of shear stiffness

changes, leads to effective blunting of the notches (by longitudinal splitting) and, consequently, improved residual strengths. (2). Softening of the matrix as well as lateral (widthwise) delamination growth lead to 0° fiber failure by buckling and hence poor residual compressive strengths. Furthermore, it was shown that the residual strength or fatigue life depended upon the lay-up for a given environment.

Kellas et al. [44] examined the effects of hygrothermal environments upon the fatigue behavior of notched fiber-reinforced plastic laminates subjected to reversed axial loading. They isolated a physical parameter related to fatigue damage characteristics around stress concentrators. This parameter was defined as the damage transition stress, denoted S_t. It was found that the magnitude of S_t constitutes a measure of the fatigue performance of a particular material system. They found that the magnitude of *St* in dry-conditioned specimens depends upon lay-up, loading regime and notch geometry. However, the magnitude of *St* for a different stacking sequence and notch geometry remained approximately constant under the wet environments conditions. The fatigue performance of the wet-conditioned specimens is slightly improved relative to that of the dry specimens.

Soutis et al. [45] studied compression fatigue behavior for cross ply carbon fiber-epoxy laminate containing either a single hole or two closely spaced hole. They showed

the similar fatigue damage behavior for both single-hole and two-hole specimens, the fatigue damage consists of ply cracking, delamination and fiber microbuckling at loads approaching the static compressive strength. They also confirmed that the applied maximum compressive stress is below 85% of the static compressive strength, no fatigue failure occurs prior to reaching 10^6 cycles. However, at the peak fatigue loads equal to 90% of the static compressive strength, fatigue failure occurs as result of microbuckle initiation and growth.

Mall et al. [46] carried out experiments to study the fatigue behavior of both notched and unnotched carbon/epoxy composites manufactured from the H-VaRTM (heated-

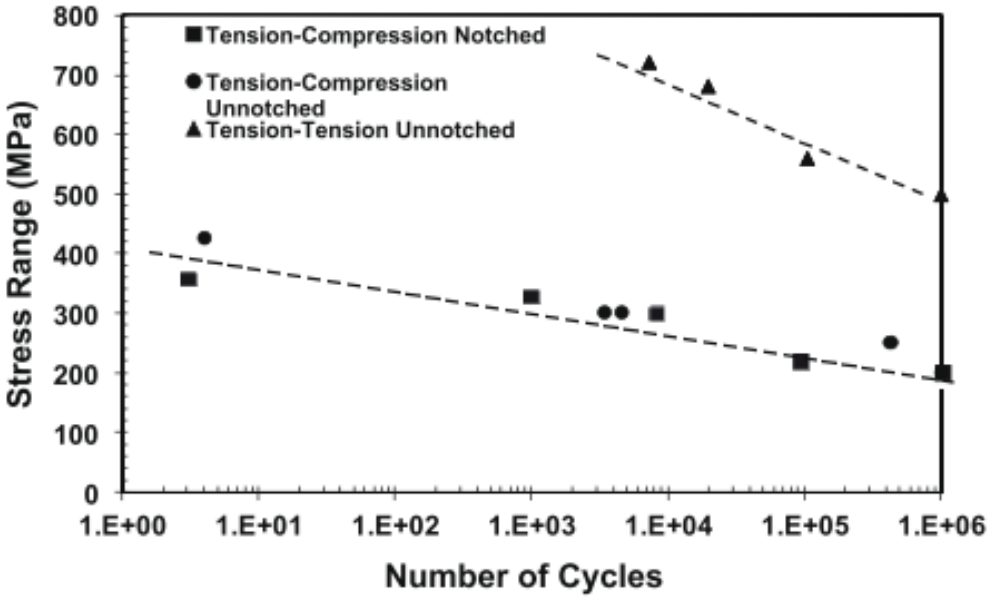

Figure 1-18: Stress range versus fatigue life [46].

vacuum assisted resin transfer molding) process under tension–compression loading. They showed that the fatigue lives of the unnotched composites in the fully reversed

tension–compression fatigue testing condition were significantly shorter than in the tension–tension fatigue testing condition. However, there was no effect of the notch on the fatigue life/strength, as illustrated in Fig. 1-18. This is due to the development of localized damage at minimum cross-section which eliminated the stress concentration. This damage again started in the form of matrix cracks followed by delamination at the location of maximum stress concentration, i.e. at the edge of the hole. Damage mechanisms involved initial matrix cracking followed by delamination, microbuckling, fiber kinking and finally fiber breakage. The final fracture of the tension–compression fatigue specimens was a compressive failure in the shear mode.

Yashiro and Okabe [47] numerically estimated the damage states in CFRP cross-ply laminates contain a hole under fatigue loading by using an fiber Bragg grating (FBG) sensor. They observed debonding of the FBG sensor in the fatigue test. Shear-lag analysis for calculating the strain distribution of the debonded optical fiber was combined with damage analysis using cohesive elements and optical analysis for an FBG sensor to calculate the reflection spectrum. The damage pattern in the laminate and the debonding length were estimated from the reflection spectrum by an optimization technique with numerical analyses. They found that the appropriate damage pattern was required for accurately estimating the debonding length. The damage-pattern estimation using FBG

sensors was therefore applied in experiments with little debonding. However, greater debonding induced invalid damage-pattern estimates. These estimates indicated that information on the damage pattern disappeared from the spectrum shape because of both debonding of the optical fiber and delamination near the hole.

1.3.4.3 Predicting Fatigue behavior

Huh and Hwang [48] proposed fatigue failure criteria for predicting fatigue life of circular notched carbon fiber reinforced plastic laminates using residual strength degradation model and assumptions on the stress redistribution. They resulted six equations for fatigue life prediction of notched laminates based on the fatigue failure criteria and fatigue life equations of unnotched laminates. They found that proposed fatigue life prediction equations (FLPEs) are in good agreement with fatigue experimental data from circular notched

Other work, Satapathy et al. [49] proposed a modified fiber failure fatigue model for prediction of fatigue behavior and fatigue life of notched composites under in-plane uniaxial and multiaxial loading. They used three types (i.e. cross-ply, quasi-isotropic and angle ply) laminated composites contain a central circular hole. They showed a good agreement between the analytical predictions and the experimental observations in terms of fatigue life for both uniaxial and multiaxial loading cases. They also showed that the

fatigue life is lower with uniaxial compression–compression loading compared with that for uniaxial tension–tension loading.

Nixon-Pearson et al. [50] performed a numerical study to investigate the capability of a cohesive interface element formulation with fatigue damage capability to predict the damage development and failure of open-holed carbon/fiber laminates. They combine modelling techniques developed for predicting the static strength of open hole tensile specimens with the extended capability of interface elements to predict damage accumulation under fatigue loading. They found that the predicted damage process had a close match to that observed experimentally. Matrix cracking at the surface ply and initiation of matrix cracks in the subsequent plies lead to delamination through thickness, and ultimately to failure at the -45/0 interface. The model could predict an *S*–*N* curve which had good agreement to tests when run at different severities.

1.4 Objectives

Almost all studies conducted on the topic of laminates with initially cut fiber have been limited to the case of pure tension. In addition, all studies of fatigue behavior of open-holed CFRP laminates have been performed to the conventional prepregs (i.e. unidirectional and woven). To the author's knowledge, equivalent work for fatigue behavior of open-holed CFRP laminate with initially cut fibers has not been reported in

the literature. This dissertation aims to explore fatigue strength and fatigue damage progress in open-holed and non-holed CFRP laminates with ICF under tension-tension loading, and to investigate the effect of slit angle to the fatigue behavior and damage progress of such laminates.

The primary objectives of this dissertation are to: (i) investigate fatigue strength and damage progress of open-holed CFRP laminates with ICF toughened with interlayers subjected to tension-tension fatigue loading; (ii) investigate the effects of fiber cutting angle on the fatigue behavior of open-holed CFRP laminates with ICFs subjected to tension-tension fatigue loading; (iii) investigate fatigue strength and damage progress of non-holed CFRP laminates with ICF toughened with interlayers subjected to tension-tension fatigue loading.

1.5 Outline

The outline of this dissertation is listed as below:

Chapter 1 introduced the general background of CFRP and their application in aircraft and automobile components. This chapter also reviews the previous studies in CFRP laminates with initially cut fibers (ICF) as well as the previous studies in fatigue and damage behavior of open-holed CFRP laminates.

Chapter 2 investigates fatigue behavior and damage progress of open-holed CFRP

laminates with ICFs. Two kinds of staggered angled ICF CFRP laminates are fabricated for fatigue tests, one laminate is fabricated using autoclave (ICF-A laminate) and the other laminate is fabricated using press molding method (ICF-P laminate). As benchmark, CFRP laminate with the conventional laminate without ICFs (Conventional-A) is fabricated. Additionally, fatigue damage progress is observed for the three laminates.

Chapter 3 investigates the effect of fiber cutting angle on the fatigue behavior of open-holed CFRP laminates with ICFs. Three types of laminates with three kinds of fiber cutting angle (θ = 22.5, 45 and 90°) are made for fatigue tests. Additionally, fatigue damage progress is observed for the three laminates. Finally, a semi-empirical equation is proposed to predict delamination area just before the final failure against.

Chapter 4 investigates fatigue behavior and damage progress of non-holed CFRP laminates with ICFs. Two kinds of staggered angled ICF CFRP laminates are fabricated for fatigue tests, one laminate is fabricated using autoclave (ICF-A laminate) and the other laminate is fabricated using press molding method (ICF-P laminate). As benchmark, CFRP laminate with the conventional laminate without ICFs (Conventional-A) is fabricated. Additionally, fatigue damage progress is observed for the three laminates.

Chapter 5 summarizes the conclusions of the dissertation

Chapter 2

Fatigue Behavior of Open-Holed CFRP Laminates with Initially Cut Fibers

In this chapter, we investigated fatigue behavior and damage progress of open-holed CFRP laminates with ICFs having interlayers. Three types of CFRP laminates were employed; a laminate without ICF fabricated using an autoclave (Continuous-A), a laminate with ICF fabricated using an autoclave (ICF-A) and a laminate with ICF fabricated using press molding (ICF-P). First, fatigue test was conducted to obtain *S* (maximum stress)-*N* (the number of cycles to failure) curves in order to reveal fatigue strength. The fatigue tests for several specimens were interrupted at three prescribed numbers of cycles to observe damage progress.

2.1 Introduction

Recently, carbon fiber-reinforced plastics (CFRPs) have been widely applied to primary structural components of aircraft and automobiles because of their contribution to higher fuel efficiency and lower emission of CO_2. Such structural components often have circular holes for several technical reasons such as joining, weight reduction and functional needs. In addition, these components are frequently subjected to cyclic loads and vibrations, which may cause degradation of structural integrity because of fatigue damage. In particular, for design requirements and functional needs, an automobile is composed of many complexly shaped components. It is quite difficult to fabricate such components using only conventional CFRP prepreg with continuous fiber owing to its poor formability. In contrast, discontinuous fiber-reinforced plastics fabricated by sheet molding compound (SMC) or injection molding have already been used as automotive parts since they have good molding flowability. However, their strength is much lower than that of composites reinforced with continuous fiber. Therefore, a new material, called unidirectionally arrayed chopped strands, was developed by Taketa et al. [21] by introducing initially cut fibers (ICFs) into CFRP prepreg. The strength and uniformity of layer structure of the ICF laminate were found to be superior to SMCs.

Several experimental results have been reported on ICF laminates thus far. In the

subsequent paper by Taketa et al. [27], the effects of interlaminar toughening on suppression of delamination in ICF laminates were experimentally studied. Yashiro & Ogi [51] investigated the effects of ICFs on fracture behavior in CFRP cross-ply laminates, having alternate or identical ICF angle $\pm\theta$ in the 0° plies. Next, Taketa et al. [52] proposed a technique for enhancing strength and uniformity of layer structure in ICF laminates by introducing ICFs with small angles for the fiber direction. Furthermore, Taketa et al. [28] also investigated mechanical properties of ICF laminates for the application as structural material for complex geometry. They found that the ICF laminates maintain high mechanical properties after forming to complex shapes. Li et al. [29] proposed two newly designed ICF prepregs with discontinuous staggered angled ICFs and discontinuous bi-angled ICFs. Li et al. [30] also studied the damage progression in three kinds of ICF quasi-isotropic (QI) laminates under tension by finite element simulation based on a multiscale analysis.

Meanwhile, numerous studies have been performed on fatigue behavior of various kinds of open-holed CFRP composites under a variety of loading conditions. O'Higgins et al. [53] studied the open hole tension (OHT) characteristics of CFRP and glass fiber reinforced plastic (GFRP). Mall et al. [46] investigated the tension–compression fatigue behavior of unnotched and notched carbon/epoxy composites manufactured using the H-

VaRTM (heated vacuum-assisted resin transfer molding). Yashiro and Okabe [47] studied fatigue damage identification in open-holed CFRP laminates by using embedded fiber Bragg grating (FBG) sensors. Kawai and Shiratsuchi [34] investigated the effect of notch on fatigue behavior of CFRP laminates with different stacking configurations. More recently, Fujita et al. [54] investigated mechanical properties such as compression after impact and compressive strength with OHT specimens of ICF laminates with toughened interlayers. Most of the above studies on open-holed laminates have been performed on continuous CFRP laminates while very little attention has been paid to fatigue behavior of open-holed ICF CFRP laminates.

The objective of the present study is to investigate fatigue behavior and damage progress of open-holed ICF CFRP laminates with toughened interlayers. Two kinds of QI ICF laminates were fabricated by autoclave and hot press molding methods. For comparison, a QI laminate made of continuous prepreg is also manufactured by the autoclave method. First, S (maximum stress)-N (the number of cycles to failure) curves were measured for the above three laminates. Second, the internal fatigue damage progress was observed using optical microscopy and radiography. Finally, the effect of interlayers on fatigue progress was discussed based on the microscopic observation of the damages.

2.1 Experimental Procedure

The prepreg used in this study is made of carbon fiber (volume fraction 0.58) and epoxy resin with interlayers, (T800S/#3900-2B, Toray Industries). This prepreg system contains about 30 μm thick interlayers including tough thermoplastic particles on the 150 μm thick base CFRP layer. A micrograph on the cross-section of the laminate is presented in Fig. 2-1.

In this study, we made ICF sheets as proposed by Taketa et al. [21]. An automatic cutting machine with a special tangential blade was employed to mechanically introduce ICFs into the prepreg. The schematic of the ICF patterns in this study is illustrated in Fig. 2-2. 1 mm-long staggered ICFs were arrayed at an interval of 25 mm in the fiber direction. Two types of ICF laminates with an ICF angle θ of 22.5° were fabricated by using the

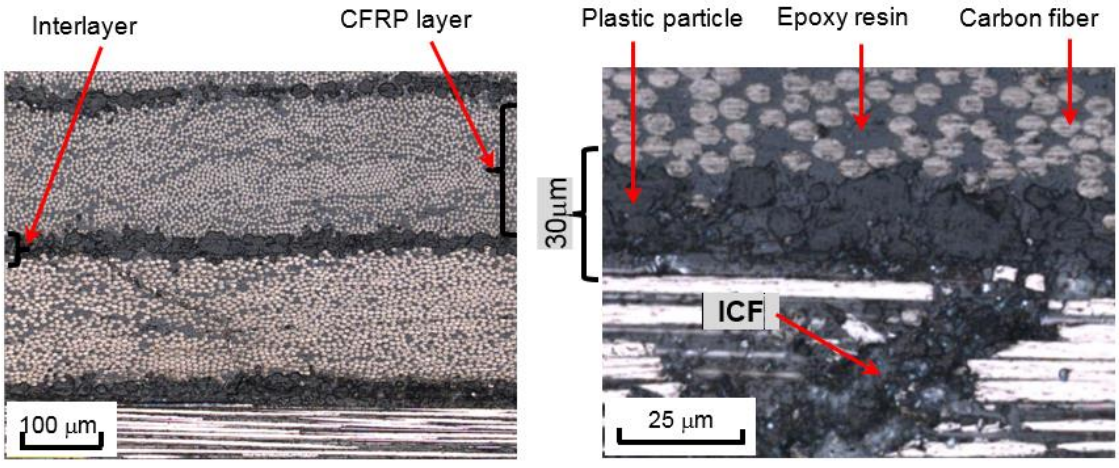

Figure 2-1: Microstructure of the CFRP laminate used in the fatigue test [71].

autoclave method (ICF-A) and press molding method (ICF-P). The ICF plies were prepared by cutting 300 mm and 250 mm square prepreg sheets for the ICF-A and ICF-P laminates, respectively.

An ICF-A QI laminate was built by stacking ICF plies in a sequence of $[45/0/-45/90]_s$ and then cured in the autoclave. The schematic of the press molding process is illustrated in Fig. 2-3. An ICF-P QI laminate was made by stacking ICF plies in a sequence of $[45/0/-45/90]_{2s}$ into a mold (300 mm square) and cured at a pressure of 0.3 MPa and a temperature of 150° C for 30 min, during which its area increases from 70 % to 100 % of the mold. For comparison, a Continuous-A QI laminate was also fabricated by stacking the conventional prepreg (250 mm square) without ICFs in a sequence of $[45/0/-45/90]_s$ and then cured using autoclave method.

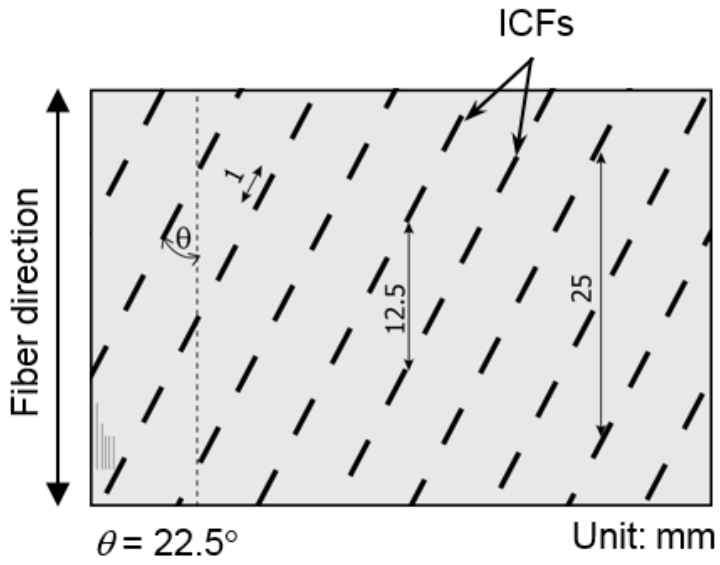

Figure 2-2: Schematic of ICF patterns introduced in the prepreg [71].

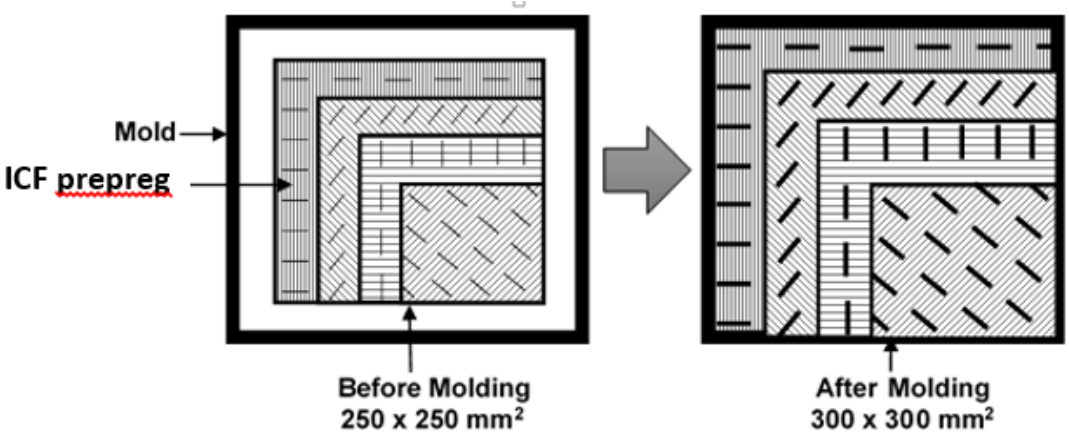

Figure 2-3: Schematic of an ICF-P laminate before and after press-molding [71].

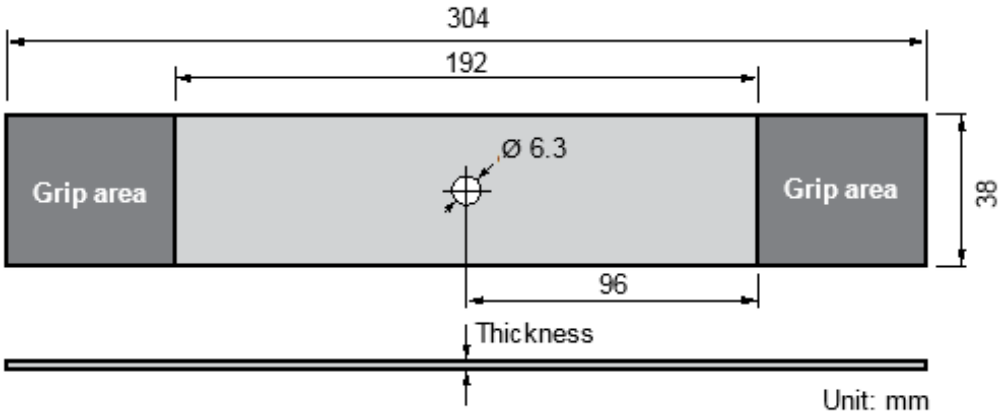

Figure 2-4: Dimensions of the open hole tension (OHT) specimen [71].

OHT specimens were then cut out from laminates according to the ASTM standard (D5766). The dimensions and geometry of OHT specimens are shown in Fig. 2-4. The specimen is 304 mm long and 38 mm wide. A 6.3 mm diameter hole was made at the center of the specimen by using a drilling machine. No end tabs were bonded on the specimen because fracture did not occur near the grip area. Table 2-1 summarizes the stacking sequence, the thickness and static tensile strength of the Continuous-A, ICF-A

Table 2-1: Stacking sequence, thickness and static tensile strength of OHT specimens [71].

Laminate	Stacking sequence	Thickness		Static tensile strength (MPa)
		Laminate (mm)	Ply (mm)	
Continuous-A	$[+45/0/-45/90]_s$	1.55	0.194	531.2
ICF-A	$[+45/0/-45/90]_s$	1.56	0.195	432.7
ICF-P	$[+45/0/-45/90]_{2s}$	2.16	0.135	531.6

and ICF-P OHT specimens.

The tensile fatigue tests were conducted at a room temperature with a sinusoidal waveform under a load-control condition using a hydraulic testing machine (8516 INSTRON). All the tests were performed at a stress ratio of 0.1 and at a frequency of 3 Hz. The maximum stress σ_{max} was varied between 60 and 95 % of the static tensile strength σ_{OHT} of each ICF OHT specimen. The tests were terminated at N of 10^6 cycles even if no failure occurred. In order to quantitatively evaluate the magnitude of damage, fatigue tests ($\sigma_{max} = 0.73\ \sigma_{OHT}$) of one specimen for each laminate was interrupted at the prescribed numbers of cycles ($N = 10^3, 10^4, 10^5$) before final failure. The internal damage progress during the fatigue test was observed using transmissive radiography (SOFTEX M-100) with the aid of zinc iodide as a contrast medium. The projected internal damage area was then quantitatively measured using commercial imaging software.

2.3 Results and Discussion

2.3.1 *S-N* Curves

Figure 2-5 shows the *S-N* curves for the Continuous-A, ICF-A and ICF-P laminates. The *S-N* curve of the Continuous-A laminate shows the least reduction of fatigue strength among the three laminates (approximately by 5% of the static tensile strength at 10^6 cycles). In contrast, the *S-N* curve behavior of the ICF-A and ICF-P laminates was similar although the static strength of the ICF-P laminate was higher than that of the ICF-A laminate. The fatigue strength in both laminates decreased approximately by 30 % of their static tensile strength at *N* of 10^6 cycles. Comparing the results of Continuous-A and ICF-A laminates,

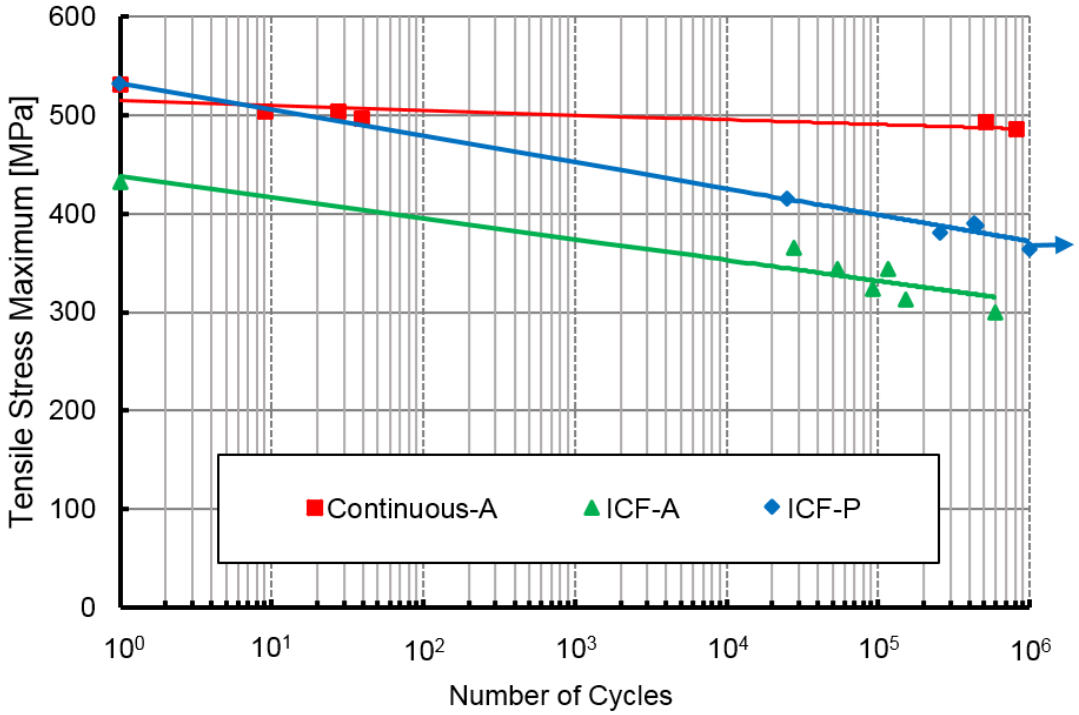

Figure 2-5: *S-N* curves of three types of OHT specimens [71].

both the static tensile strength and fatigue strength of the ICF-A laminate are smaller than those of the Continuous-A laminate. This indicates that damage are easily initiated from ICFs at relatively low stress levels or low numbers of cycles, as shown later. Moreover, comparing the ICF-A and ICF-P laminates, both the static tensile strength and fatigue strength of the ICF-P laminate (ply thickness 1.56 mm) were higher than those of the ICF-A laminate (ply thickness 2.16 mm). The main reason for higher strength of the ICF-P laminate is the thinner plies as has been analytically explained by Taketa et al. [21].

2.3.2 Damage Progress

Figures 2-6a, 2-6c, 2-7a, 2-7c, 2-8a and 2-8c depict the schematics of damage progress viewed from the top and projected soft X-ray photos for the Continuous-A, ICF-A and ICF-P laminates, respectively. Figures 2-6a, 2-7a, and 2-8a are illustrations based on the X-ray photos while Figs. 2-6b, 2-7b and 2-8b are ones based on the optical micrographs on the edge surfaces. Figures 2-9 and 2-10 present the crack density and delamination area around the hole, respectively, for the three laminates at three numbers of cycles. The measurement area around the hole for crack density and delamination is 293 mm^2.

First, at N of 10^3, transverse cracks in the ±45° and 90° plies and splitting cracks in the 0° plies are initiated from the hole roots (arrows A) as well as from the both edges in

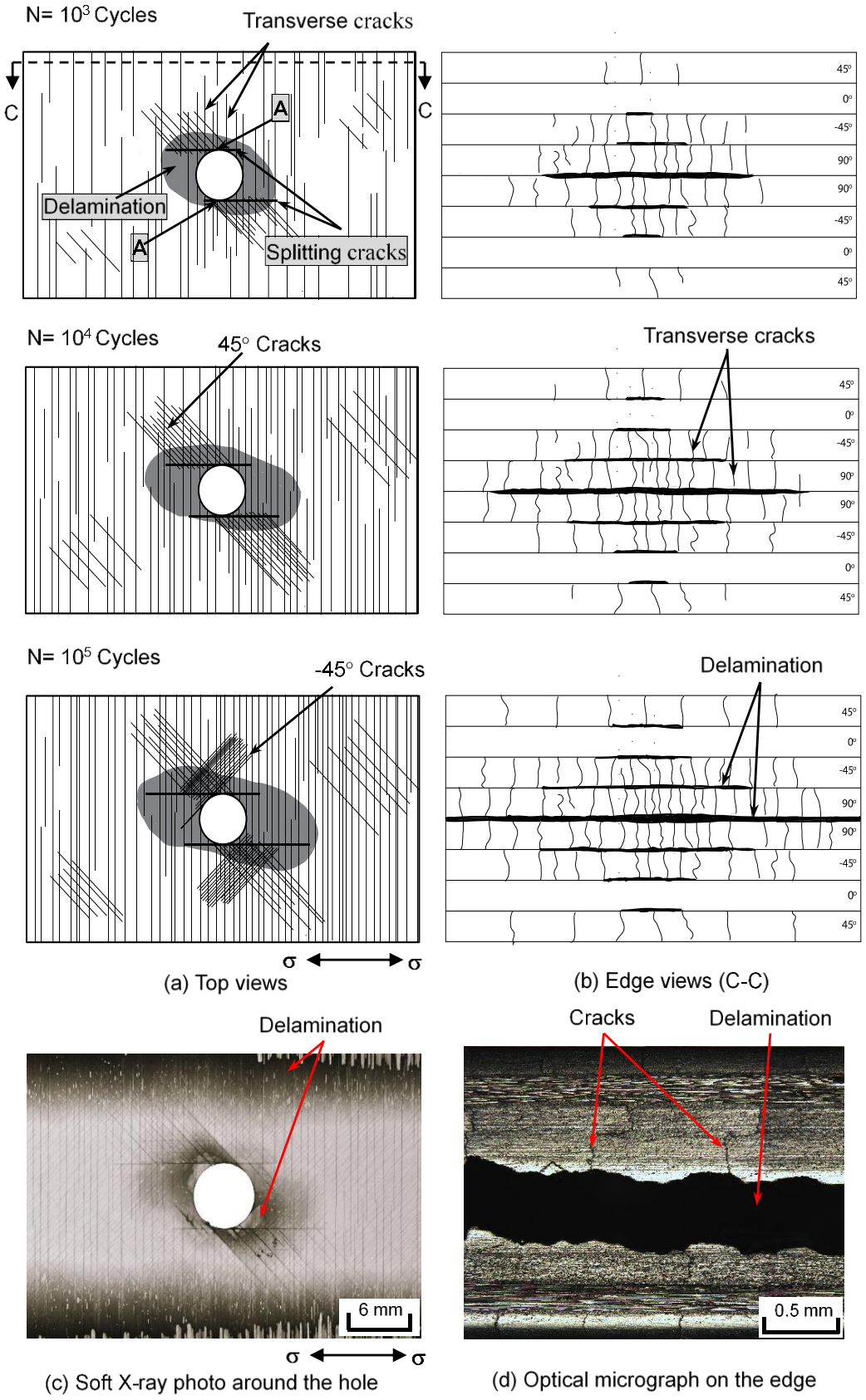

Figure 2-6: (a) Top and (b) edge views of schematic damage progress, (c) an X-ray photo and (d) and an optical micrograph on the edge in the Continuous-A specimen [71].

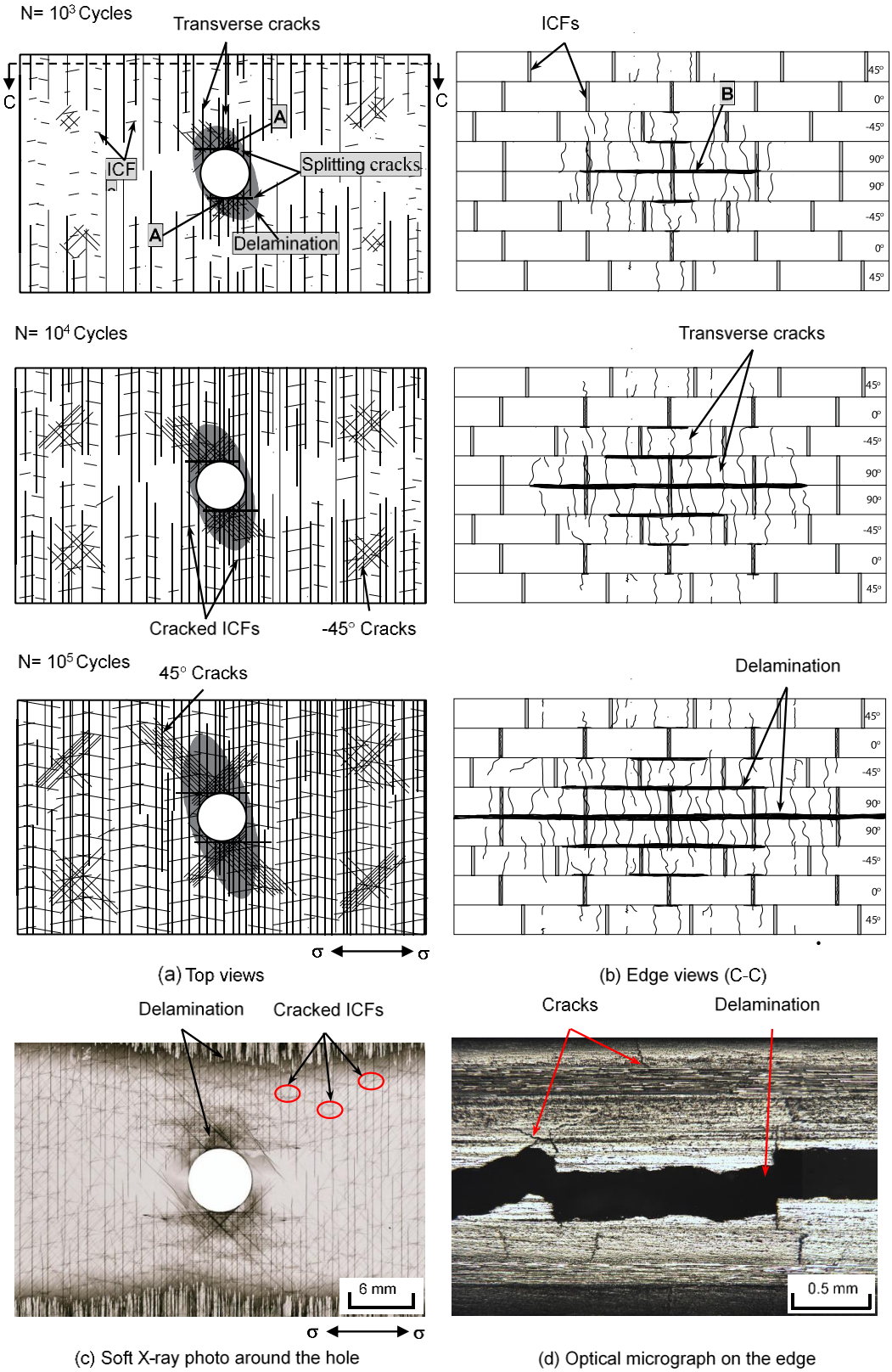

Figure 2-7: (a) Top and (b) edge views of schematic damage progress, (c) an X-ray photo and (d) and an optical micrograph on the edge in the ICF-A specimen [71].

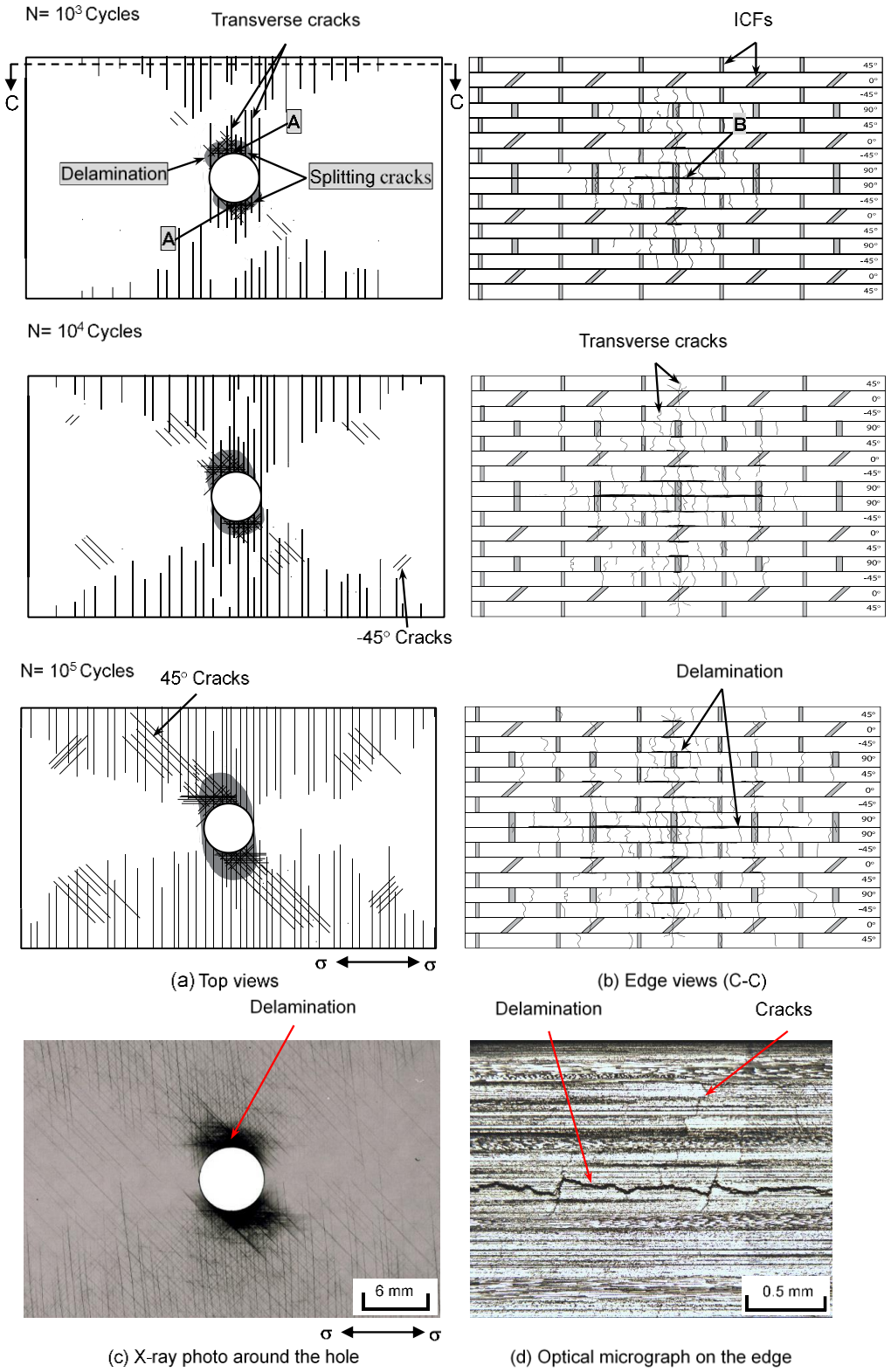

Figure 2-8: (a) Top and (b) edge views of schematic damage progress, (c) an X-ray photo and (d) and an optical micrograph on the edge in the ICF-P specimen [71].

all the laminates. The crack density, which is defined as the sum of the crack length per unit area around the hole, in the Continuous-A laminate is the largest among the three laminates as shown in the Fig. 2-9. This is mainly due to a lot of cracks propagating from the splitting cracks in the longitudinal ply. Comparing both ICF laminates, the crack density in the ICF-P laminate is smaller than that in the ICF-A laminate since the ply is thinner in the ICF-P laminate. On the other hand, the delamination area is comparable in the three laminates.

Second, at N of 10^4, the transverse cracks from the both free edges propagated and were connected with each other across the width of the specimens. In the ICF-A laminate (Fig. 2-7), a lot of cracks were newly generated from ICFs existing not only around the hole but also away from the hole. Consequently, the crack density in the ICF-A laminate is the largest among the three laminates. In contrast, the crack density and delamination area are the smallest in the ICF-P laminate.

Third, at N of 10^5, the density and length of cracks increase rapidly, especially in the Continuous-A and ICF-A laminates (Fig. 2-9). The delamination propagating around the hole in the Continuous-A and ICF-A laminates are more remarkable than that in the ICF-P laminate as shown in Fig. 2-10. As a result, the ICF-P laminate shows the smallest damage growth among the three laminates. This is because the initiation and propagation

of matrix cracking are suppressed as the ply becomes thinner. In addition, the area of the cracking and delamination is limited near the hole roots as shown in Fig. 2-8c.

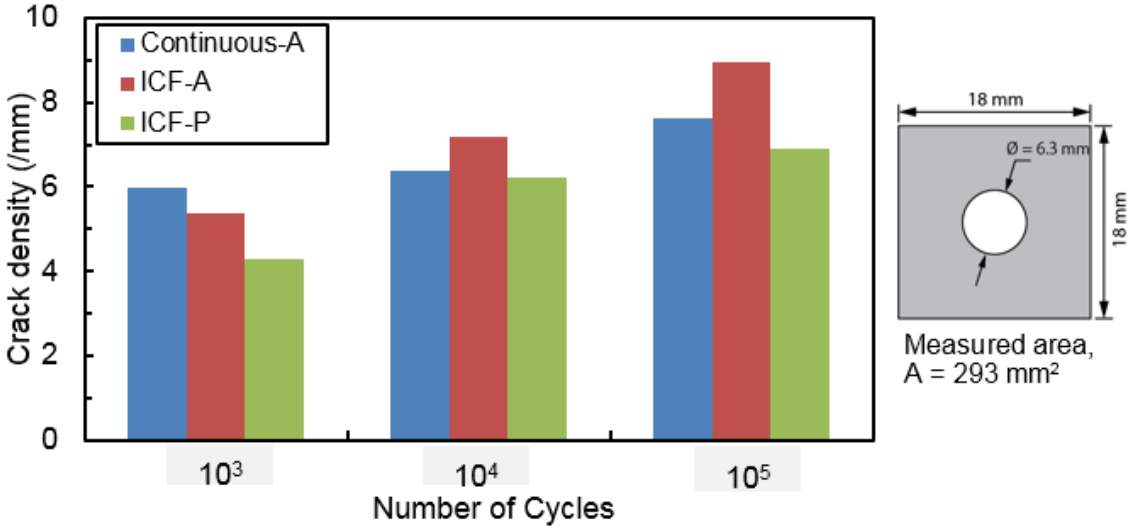

Figure 2-9: Crack density around the hole at three numbers of cycles for the three laminates [71].

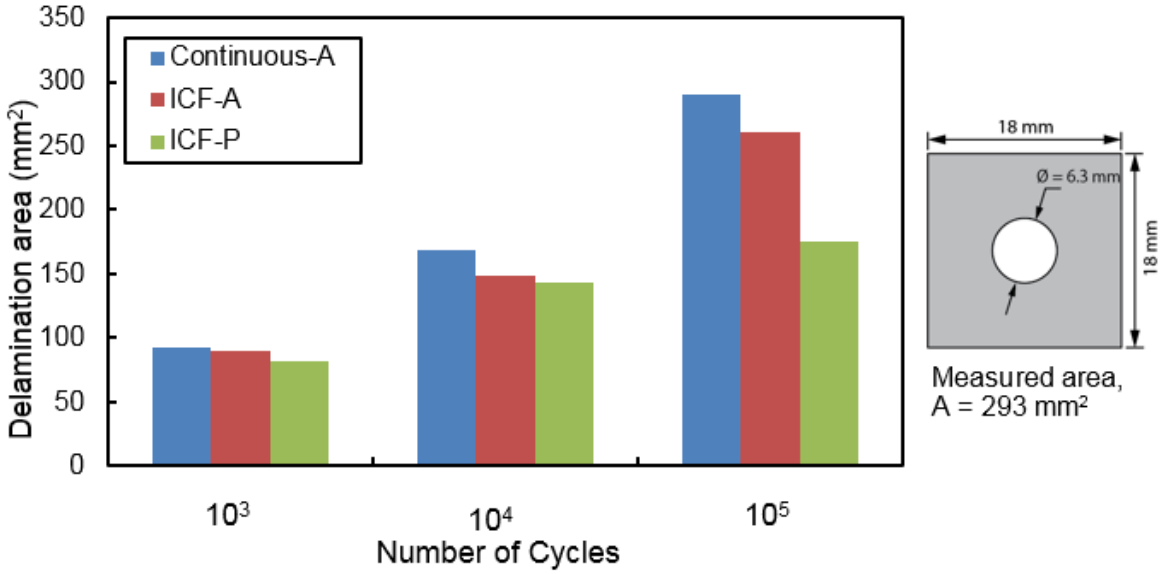

Figure 2-10. Delamination area around the hole at three numbers of cycles for the three laminates [71].

Figures 2-6b, 2-7b and 2-8b schematically show the damage progress on the free edge surfaces of the three laminates. In the Continuous-A laminate (Fig. 2-6), the damage scenario is as follows: (1) Transverse cracks are initiated in the 90° and ±45° plies. (2) The number of transverse cracks increases with increasing *N*. (3) Adjacent transverse cracks are connected with each other by way of the ply interfaces. (4) Delamination is generated and extends along the specimen length and across the specimen width. The delaminations are mainly caused by the interlaminar shear stress at the both free edges (Figs. 2-6d, 2-7d and 2-8d) and the hole roots (Figs. 2-6a, 2-7a and 2-8a). On the other hand, the damage progress in the ICF-A (Fig. 2-7) and ICF-P laminates (Fig. 2-8) are summarized as follows: (1) Transverse cracks independent of ICFs occur in the 90° and ±45° plies. (2) New cracks extend from the tips of ICFs only in the ICF-A laminate. (3) Adjacent transverse cracks are connected with each other through the ply interfaces. (4) Delamination is generated and extends at the ply inter faces. In particular, the delamination occurs at the ply interfaces near ICFs at the early stage of cycles (arrows B).

From the above schematics, it is found that the delamination in the Continuous-A laminate is more prominent than that in the ICF-A laminate. Contrarily, relatively small delamination locally extends around the hole in the ICF-P laminate (Fig. 2-8d). It is revealed that matrix cracks are relatively difficult to propagate in the ICF-P laminate with

thinner plies.

The final fracture behavior for the three types of laminates are schematically shown in Fig. 2-11. All the specimens exhibit a brittle fracture manner. In the Continuous-A

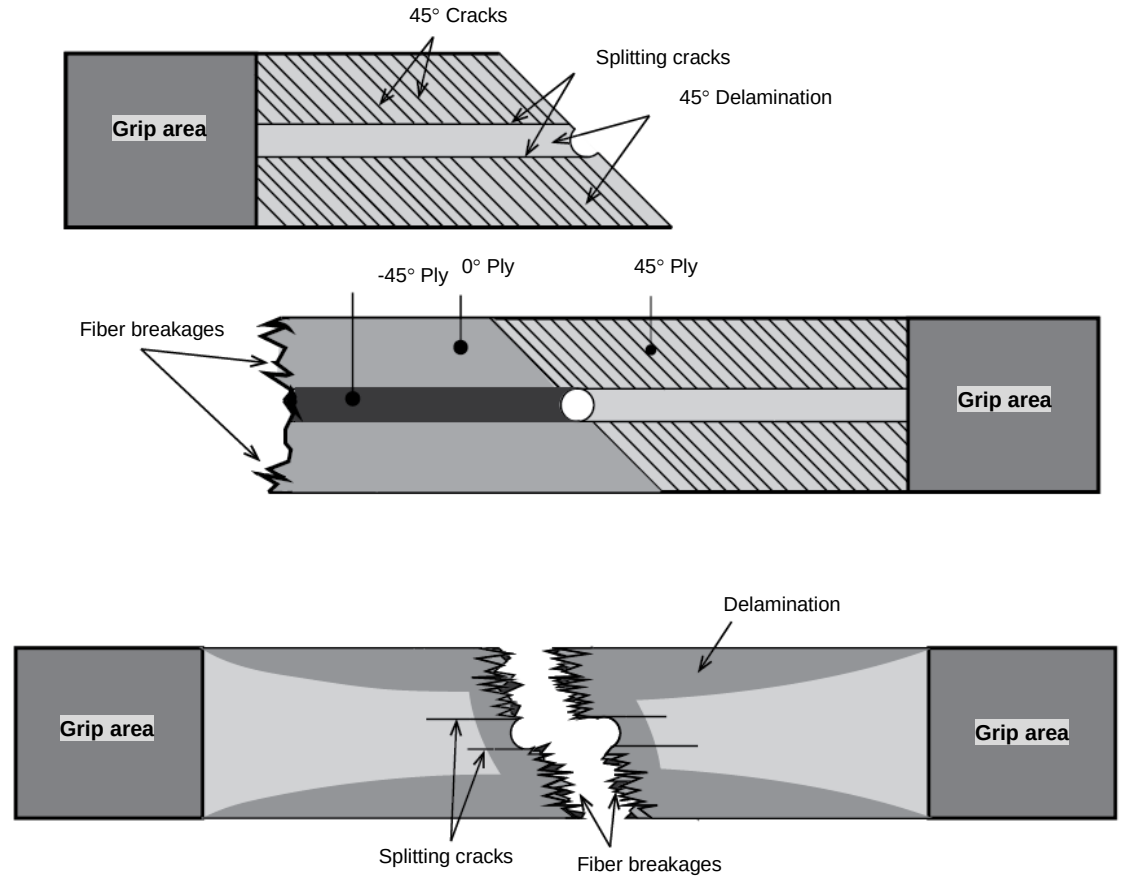

Figure 2-11. Schematics of final fracture behavior of the three OHT specimens **[**71**]**.

laminate, the delamination at the interface between the 45° and 0° plies dominates the final failure. The splitting cracks generated from the hole roots in the 0° plies propagate along the specimen length to induce the delamination, which causes full peel-off of the plies at the 0°/-45° interfaces. The delamination starting from the hole propagates in the

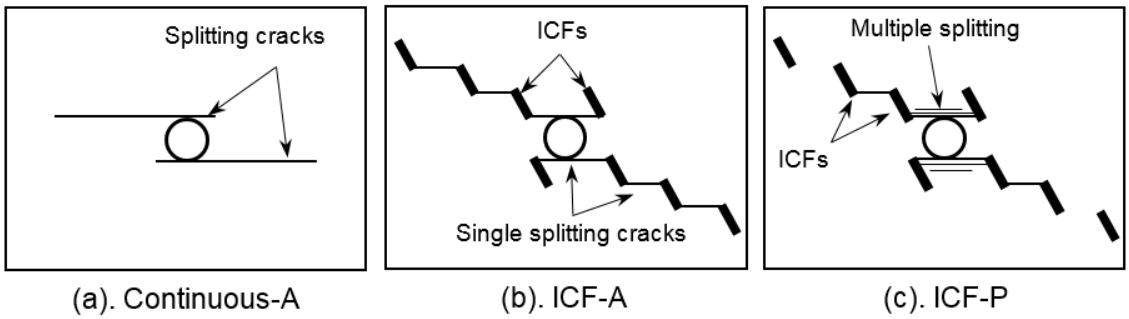

Figure 2-12: Schematics of split progress in 0° ply: (a). Continuous-A, (b). ICF-A, and (c). (ICF-P) laminates [71].

loading (longitudinal) direction and reaches both ends of the specimen at the final failure stage. In contrast, in the both ICF laminates, the final fracture mode is fiber breakage around the hole, although free-edge delamination is more remarkable in the ICF-A laminate. In addition, the damages including delamination and fiber breakage in the both ICF laminates tend to extend in the transverse direction rather than in the longitudinal direction. The propagation behavior of the splitting cracks in the 0° plies in the Continuous-A, ICF-A, and ICF-P laminates is illustrated in Fig. 2-12. The ICFs hinder propagation of the splitting cracks in the ICF laminates and induce the crack deflection (Fig. 2-12b and c). Consequently, the splitting cracks initiated around the hole in the ICF

laminates (Figs. 2-7a and 2-8a) are shorter than those in the Continuous-A laminate (Fig. 2-6a). In addition, multiple splitting cracks are only generated in the ICF-P laminate (Fig. 2-12c). Figure 2-12 also explains the decrease of the fatigue strength in the *S-N* curves for the ICF-A and ICF-P laminates, where the intact ligament width becomes smaller by the connection of ICFs. In addition, comparing the present result with the result of static tensile test for the similar OHT specimens [12], it is found that the delamination is more predominant in the fatigue failure. This is presumably because the fatigue delamination propagation occurs during cyclic loading.

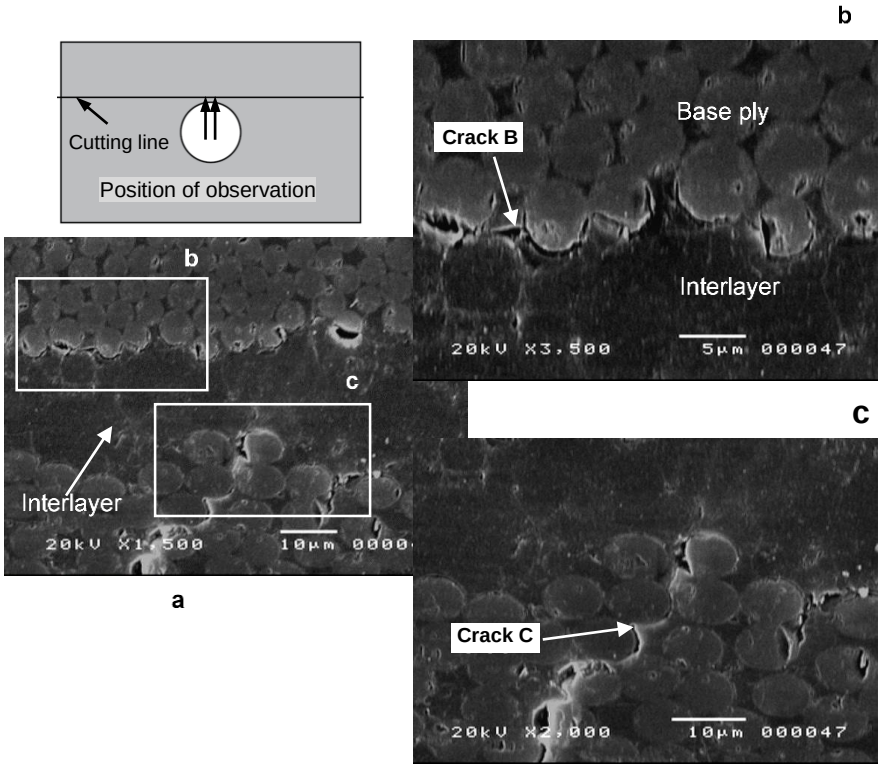

Figure 2-13: SEM photos of cross-sections near the hole of the specimen after fatigue test; (a) cracks around interlayer (b) crack at interface, and (c) transverse crack [71**]**.

2.3.3 The Effect of Interlayers

Figure 2-13 depicts the scanning electron micrographs of cross-sections near the hole of the specimen after the fatigue test. Two types of cracks are observed; one is generated at the interface between the base ply and the interlayer (Crack B, Fig. 2-13b) and the other is initiated in the matrix of the base ply (Crack C, Fig. 2-13c). Cracks B and C extend in the directions parallel and perpendicular to the interlayer, respectively. Both cracks are arrested by the interlayer as depicted in Figs. 2-13b and c. This result testifies that the interlayer plays a role of a crack arrestor also for fatigue crack propagation even near the hole. Namely, propagation of the cracks generated in the base plies stop near the interfaces between the base plies and the interlayers, resulting in suppression of delamination.

2.4 Conclusions

The fatigue behavior and damage progress in open-holed CFRP laminates with ICF toughened with interlayers are presented. From the experimental results, the following conclusions are derived:

1. The fatigue strength of the Continuous-A laminate is the highest among the three laminates. The decrease ratio of fatigue strength at N of 10^6 is only 5% of its static strength.
2. The fatigue strength of the ICF-P laminate is higher than that of the ICF-A laminate.

However, the decrease ratio of fatigue strength at N of 10^6 is about 30% of its static strength, which is almost the same in the both ICF laminates.

3. The degree of damage in the ICF-P laminate is the smallest among the three laminates while the increase rate of the crack density is the greatest in the ICF-A laminate with thicker plies.
4. The damage propagation direction around the hole in the Continuous-A laminate is rather longitudinal while that in the both ICF laminates is transverse.
5. The interlayer acts as a crack arrestor for fatigue crack propagation even near the hole.
6. Further work is still required to quantitatively predict fatigue damage development in both ICF laminates by finite element analysis.

Chapter 3

Effect of Fiber Cutting Angle on The Fatigue Behavior of Open-Holed CFRP Laminates with Initially Cut fibers

This study investigated the effects of fiber cutting angle on the fatigue behavior of open-holed carbon fiber-reinforced plastic (CFRP) laminates with initially cut fibers (ICFs). Three kinds of fiber cutting angles (θ = 22.5, 45, and 90°) were applied to two types of quasi-isotropic ICF laminates: one was fabricated using autoclave (ICF-A) and the other was fabricated using press molding (ICF-P). First, fatigue tests were conducted to obtain *S* (maximum stress)-*N* (the number of cycles to failure) curves in order to reveal fatigue strength. The fatigue tests of one specimen for each configuration were interrupted at three prescribed numbers of cycles to observe damage progress. Finally, a semi-empirical equation was proposed to predict delamination area just before the final failure against normalized applied stress.

3.1 Introduction

Recently, researchers are concerned with the application of carbon fiber-reinforced plastics (CFRPs) to aircraft and automobiles structural components for the purpose of higher fuel consumption efficiency and the further requirements of environment protection. Such structural components often have circular holes for several technical reasons such as joining, weight reduction and functional needs. These components are frequently subjected to cyclic loads and vibrations, which may cause degradation of structural integrity owing to fatigue damage.

It is quite difficult to fabricate such components using only conventional CFRP prepreg with continuous fiber because of its poor formability. In contrast, discontinuous fiber-reinforced plastics fabricated by sheet molding compound (SMC) or injection molding have already been used as automotive parts since they have good molding flowability. However, their strength is much lower than that of composites reinforced with continuous fiber. Therefore, a new material, called unidirectionally arrayed chopped strands, was developed by Taketa et al. [21] by introducing a regular fiber cutting pattern into CFRP prepreg. The laminates with inititially cut fibers (ICFs) possess higher strength and uniformity of layer structure than SMCs. In their subsequent paper [27], they investigated the effect of interlaminar toughening on suppression of delamination in ICF

laminates. They found that ICF laminates with interlaminar toughening achieve higher strength than conventional ICF laminates. Yashiro & Ogi [51] investigated the effects of ICF on fracture behavior in CFRP cross-ply laminates, having alternate or identical ICF angle $\pm\theta$ in the 0° plies. They observed the damage progress during tensile tests for several geometries of ICF and evaluated fracture behavior in ICF laminates by a layer-wise finite element (FE) model using cohesive elements. They confirmed that the longitudinal stress concentrates at the central line of ICF and the damage of laminates occurred mostly near the highest stress concentration. Next, Taketa et al. [28,52] proposed a technique for enhancing strength and uniformity of layer structure in ICF laminates by introducing small cutting angles to the fiber direction. They also studied the flowability of structure made of a flat plate and a T-shaped rib using ICF, and visualized the movement of the chopped strands. More recently, Fujita et al. [54] investigated mechanical properties of ICF laminates and found that the ICF laminates maintained high mechanical properties after forming to complex shapes.

In order to improve the strength and material symmetry of ICF laminates, two newly designed ICF prepregs with discontinuous staggered angled ICFs and with discontinuous bi-angled ICFs are proposed by Li et al. [29]. They revealed that such ICF laminates possessed higher strength and better flowability than existing ICF laminates. Li et al. [30]

also studied the damage progression in three kinds of ICF quasi-isotropic laminates under tension by FE simulation based on multiscale analysis.

Fatigue properties are important in real structures, and numerous studies have been performed on fatigue behaviour of various kinds of open-holed CFRP composites under a variety of loading conditions [34,36,38,46,47,53,55,56]. However, as far as the authors know, almost all the previous studies have performed for conventional composites (i.e. unidirectional or woven). Although static, tensile and compressive strength of open-holed ICF laminates have been reported [54], *S-N* curves and fatigue damage progress of open-holed ICF laminates have not been sufficiently studied so far.

In the presents study, the effect of fiber cutting angle θ on the fatigue behavior and damage progress in open-holed ICF laminates is investigated. In order to validate the effect of ICF angle θ and laminate thickness on fatigue damage behavior, we prepared two kinds of quasi-isotropic ICF laminates with three staggered cutting line patterns. First, *S-N* curves were measured for the above six ICF laminates. The microscopic fatigue damage progress was then investigated using optical microscopy and radiography. Finally, a semi-empirical equation was proposed to predict delamination area just before the final failure against normalized applied stress.

3.2 Experimental Procedure

The composite laminates were fabricated using the prepreg made of carbon fiber (volume fraction 0.58) and epoxy resin with interlayers, (T800S/#3900-2B, Toray Industries). This prepreg system contains about 30 μm thick interlayers including tough thermoplastic particles on the 150 μm thick base CFRP layer. A micrograph on the cross-section of the laminate is presented in Fig. 3-1.

In this study, we made ICF sheets as proposed by Taketa et al. [21]. An automatic cutting machine with a special tangential blade was employed to mechanically introduce fibers cutting into the prepreg. The ICF patterns are illustrated in Fig. 3-2. 1 mm-long staggered fibers cutting were arrayed at an interval of 25 mm in the fiber direction. Two types of ICF laminates with three kinds of θ (22.5°, 45°, and 90°) were fabricated by

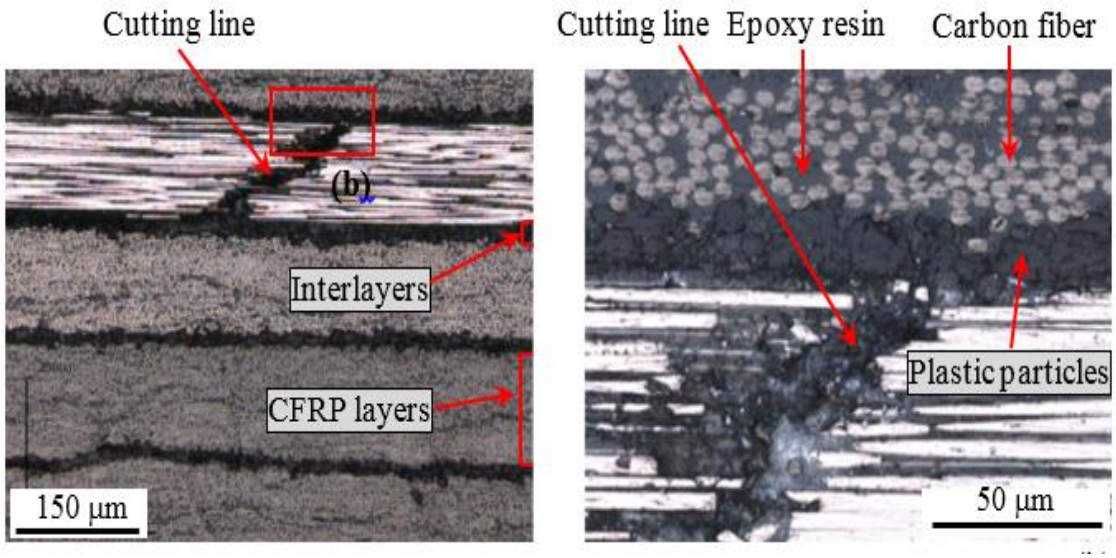

Figure 3-1: Microstructure of T800S/3900-2B laminates with ICFs [72].

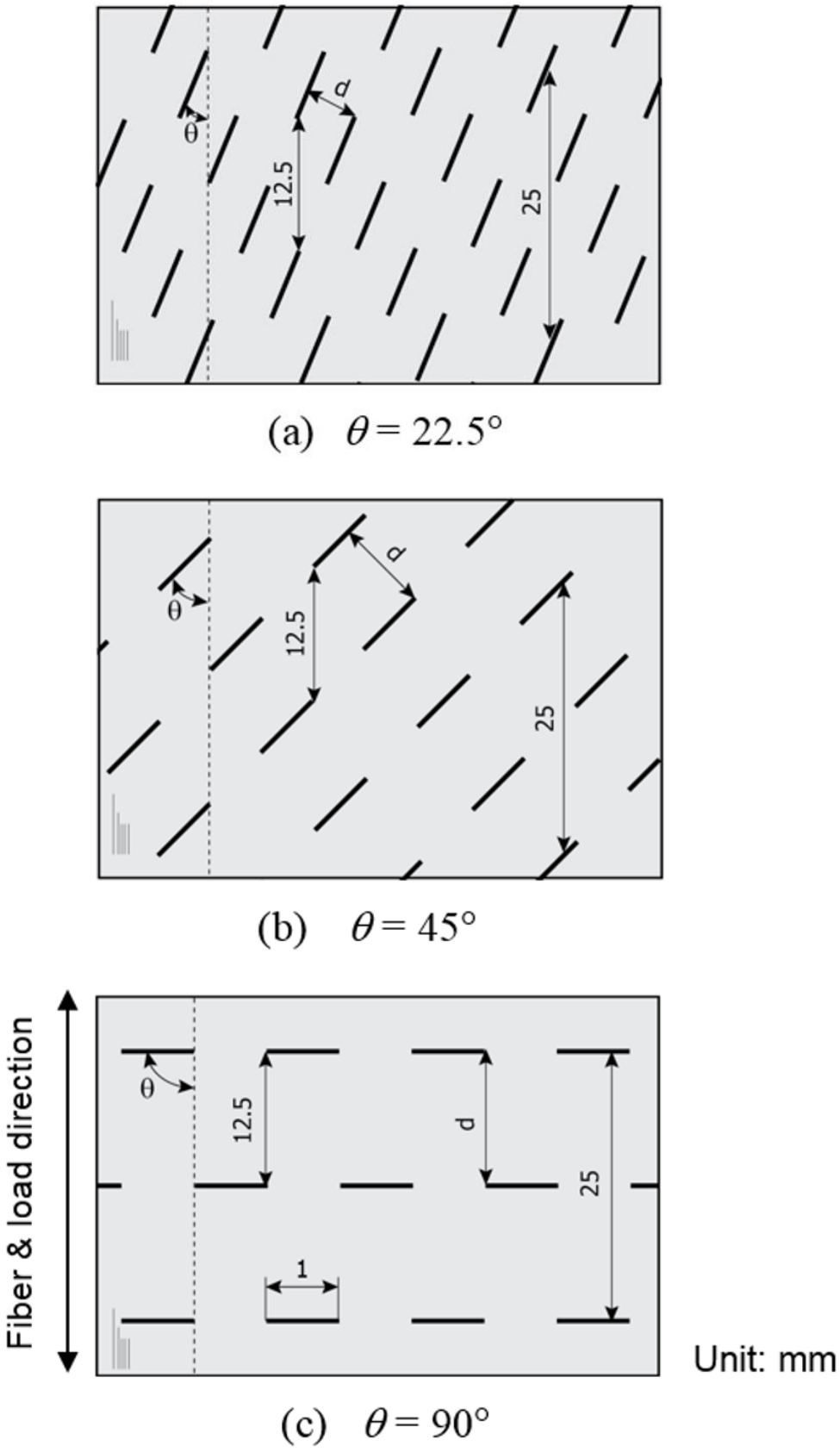

Figure 3-2: Schematics of the three cutting patterns [72].

using autoclave method (ICF-A) and press molding method (ICF-P). The ICF plies were prepared by cutting prepreg sheets 300 mm and 250 mm square for ICF-A and ICF-P laminates, respectively.

An ICF-A laminate was built by stacking ICF plies in the quasi-isotropic sequence of $[45/0/-45/90]_s$ and then cured in the autoclave. The thickness of cured laminates and each ply was 1.56 mm and 0.2 mm, respectively. The press molding process is schematically

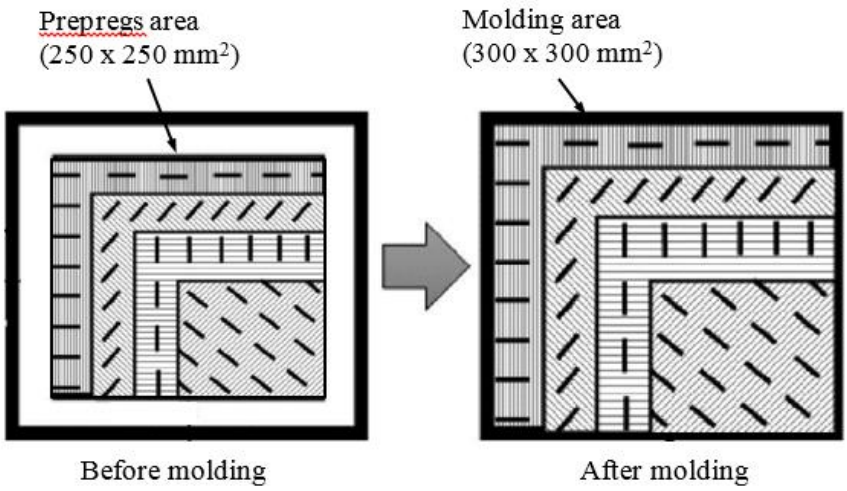

Figure 3-3: Schematics of press molding [72].

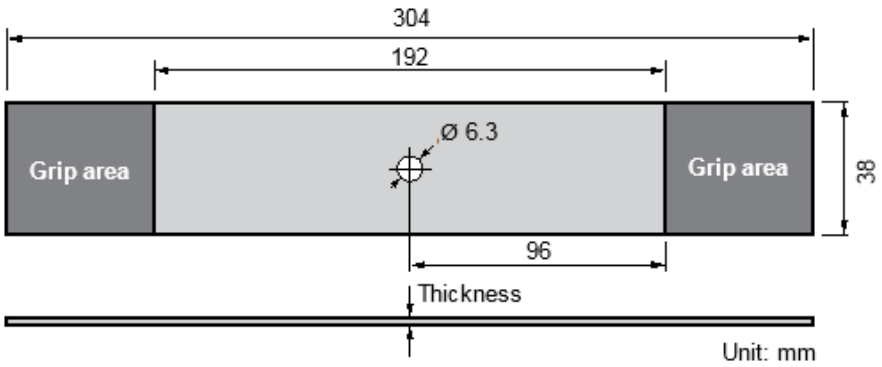

Figure 3-4: Dimensions of the open hole tension (OHT) specimen [72].

shown in Fig. 3-3. An ICF-P laminate was made by stacking ICF plies with a sequence of $[45/0/-45/90]_{2s}$ into a mold cavity (300 x 300 mm) and cured at a pressure of 0.3 MPa and a temperature of 150° C for 30 min, where its area increased from 0 to 100 % of the mold. The thickness of cured laminates and each layer was 2.16 mm and 0.14 mm, respectively.

Open hole tension (OHT) specimens were then cut out from the cured laminates according to the ASTM standard (D5766). The dimensions and geometry of OHT specimens are shown in Fig. 3-4. The specimen is 304 mm long and 38 mm wide. A 6.3 mm diameter hole was made at the center of the specimen by using a drilling machine.

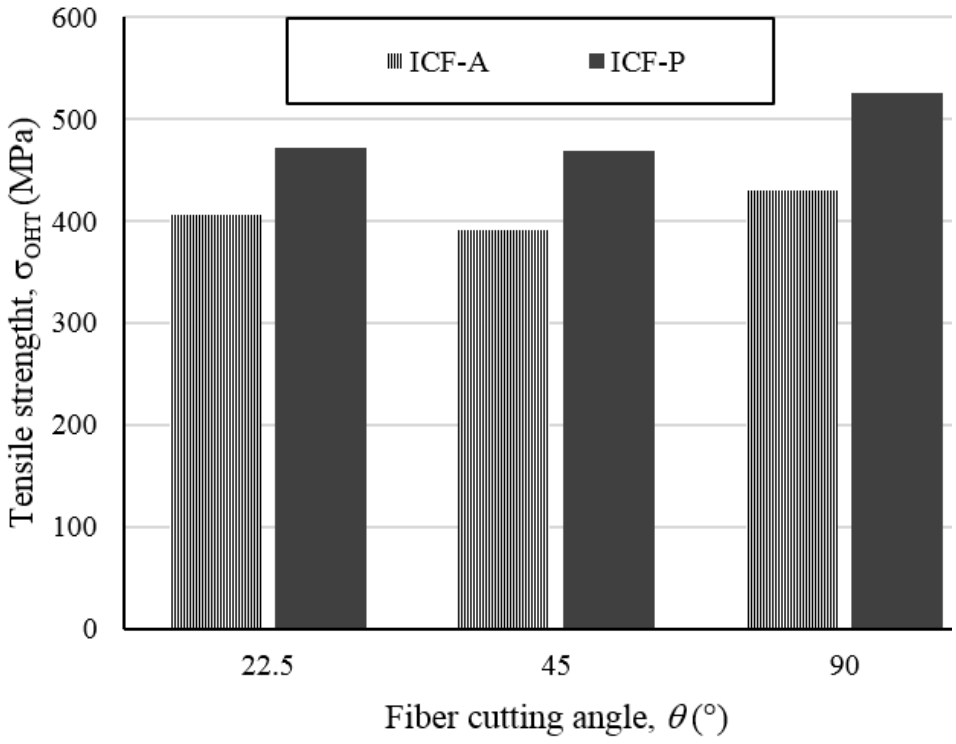

Figure 3-5: Static tensile strength of two types of open holed specimens [72].

The static tensile strength of the ICF-A and ICF-P specimens with the three θ are shown in Fig. 3-5.

The tensile fatigue tests were conducted at room temperature with a sinusoidal waveform under load-control conditions using a hydraulic testing machine (8516 INSTRON). All the tests were performed at a stress ratio of 0.1 and at a frequency of 3 Hz. The maximum stress, σ_{max}, was varied between 60 and 85 % of the static tensile strength, σ_{OHT}, of each ICF laminate. The tests were terminated at one million cycles even if no failure occurred. In order to quantitatively evaluate the magnitude of damage, fatigue tests (σ_{max}= 0.65.σ_{OHT}) were interrupted for several additional specimens at three prescribed numbers of cycles (N =10^3, 10^4, 5x10^4). The damage progress during the fatigue test was observed using penetrant radiography technique. A penetrant made of zinc iodide, as a contrast medium, was infiltrated into the specimens. The projection image of internal damage was then captured using soft X-ray radiography (SOFTEX M-100).

3.3 Results and Discussion

3.3.1 *S*-*N* Curves

Figure 3-6 shows the normalized *S*-*N* curves for ICF-A and ICF-P laminates. Here, *S*

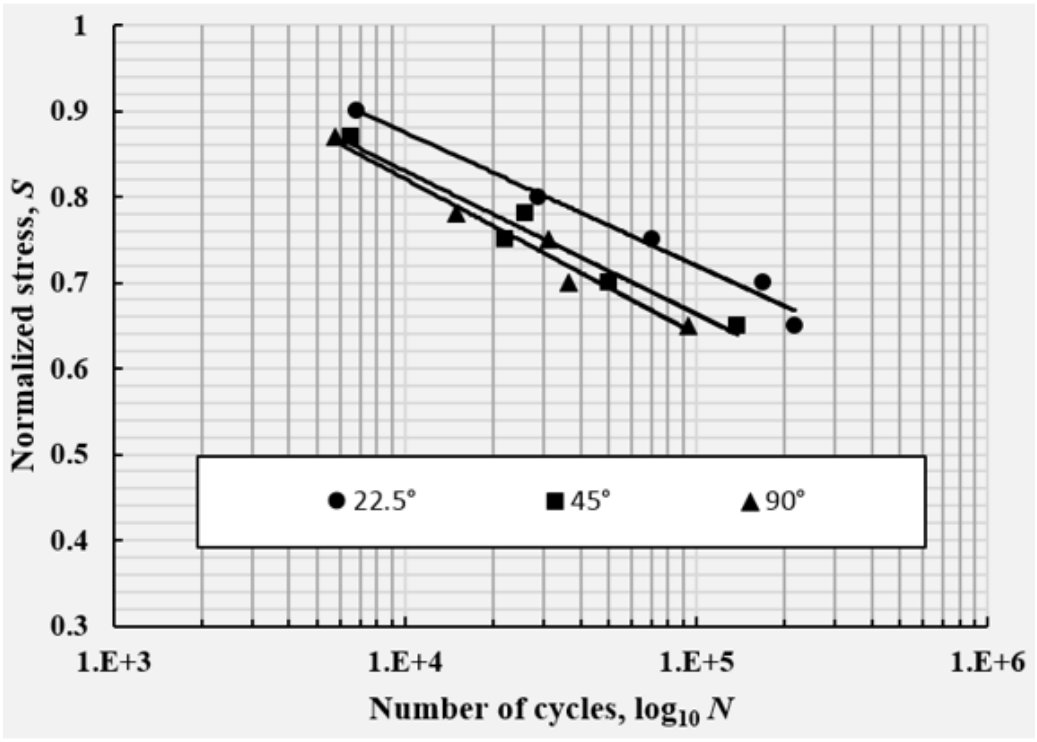

(a) ICF-A

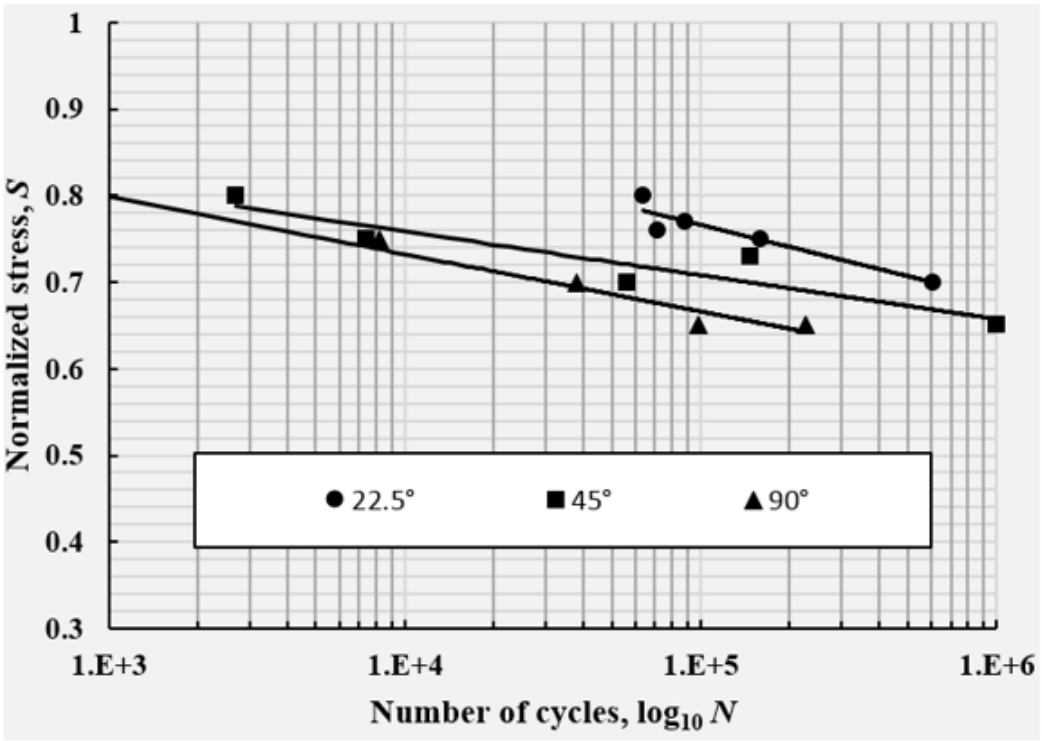

(b) ICF-P

Figure 3-6: *S-N* curves of two types of open-holed ICF laminates with the three fiber cutting patterns [72].

represents the maximum tensile stress normalized by the static tensile strength of each laminate. In ICF-A laminates (Fig. 3-6(a)), the *S-N* curves for θ = 90° and 45° exhibit similar tendency although the static strength for θ = 90° is higher than that for θ = 45°. The normalized fatigue strength in both laminates decreases gradually to approximately 60 % at 10^6 cycles. Comparing with the laminates having larger θ, the slope of the *S-N* curve for θ = 22.5° is slightly smaller and its fatigue strength decreases to approximately 70 % of the static strength at 10^6 cycles. In the ICF-P laminates (Fig. 3-6(b)), the normalized fatigue strength for θ = 90° and 45° is almost the same. However, the decline of fatigue strength in the laminates with θ = 90° is larger than that of the laminates with θ = 45°.

The fatigue strength for θ = 90° and θ = 45° is approximately 62 % and 70% of their static tensile strength, respectively, at 10^6 cycles. Contrarily, the slope of the *S-N* curve for θ = 22.5° is the smallest among the three ICF laminates where the fatigue strength is kept to be relatively high (approximately 72 % of the static strength) even at 10^6 cycles.

Based on the results in both ICF laminates, the fatigue strength is the highest for θ = 22.5° among the three θ. This indicates that damage progress is more suppressed as the θ becomes smaller. It is supposed that stress distribution around ICF depends on fiber cutting angle and plays a significant role in the damage progress. Moreover, comparing

the ICF-A and ICF-P laminates, the fatigue strength of ICF-P laminates (ply thickness 0.14 mm) was slightly higher than that of ICF-A laminates (ply thickness 0.2 mm) for all the fiber cutting angles (see Fig. 3-6). The main reason for higher strength in the ICF-P laminates is smaller thickness of plies as has been analytically explained by Taketa et al. [21].

3.3.2 Damage Progress

Figure 3-7 depicts the projected images of fatigue damage progress in open-holed ICF-A laminates for the three θ at the three N. Hereafter, the locations of cracked ICFs were identified from the initial ICF pattern. The sequence of damage around the hole common to all the laminates was as follows. At $N = 10^3$ cycles, transverse cracks in the 90° plies are generated from the hole boundary followed by off-axis cracks, which are matrix cracks in the ±45° plies along the splitting cracks in the 0° plies propagating from the hole roots (arrows A). Such cracks and ICFs concentrate in the vicinity of the two hole roots. A few cracked ICFs also appear around the hole. At $N = 10^4$ cycles, the transverse cracks, off-axis cracks, and splitting cracks extend and are connected with each other. Moreover, the delamination is induced by splitting cracks at the (45°/0°) and (0°/-45°) ply interfaces near the hole roots and extends in the transverse direction. At $N = 5 \times 10^4$ cycles, the crack length as well as the number of cracks rapidly increases together

with further delamination growth. Final failure of the specimen occurs due to the fiber fracture in the 0° plies.

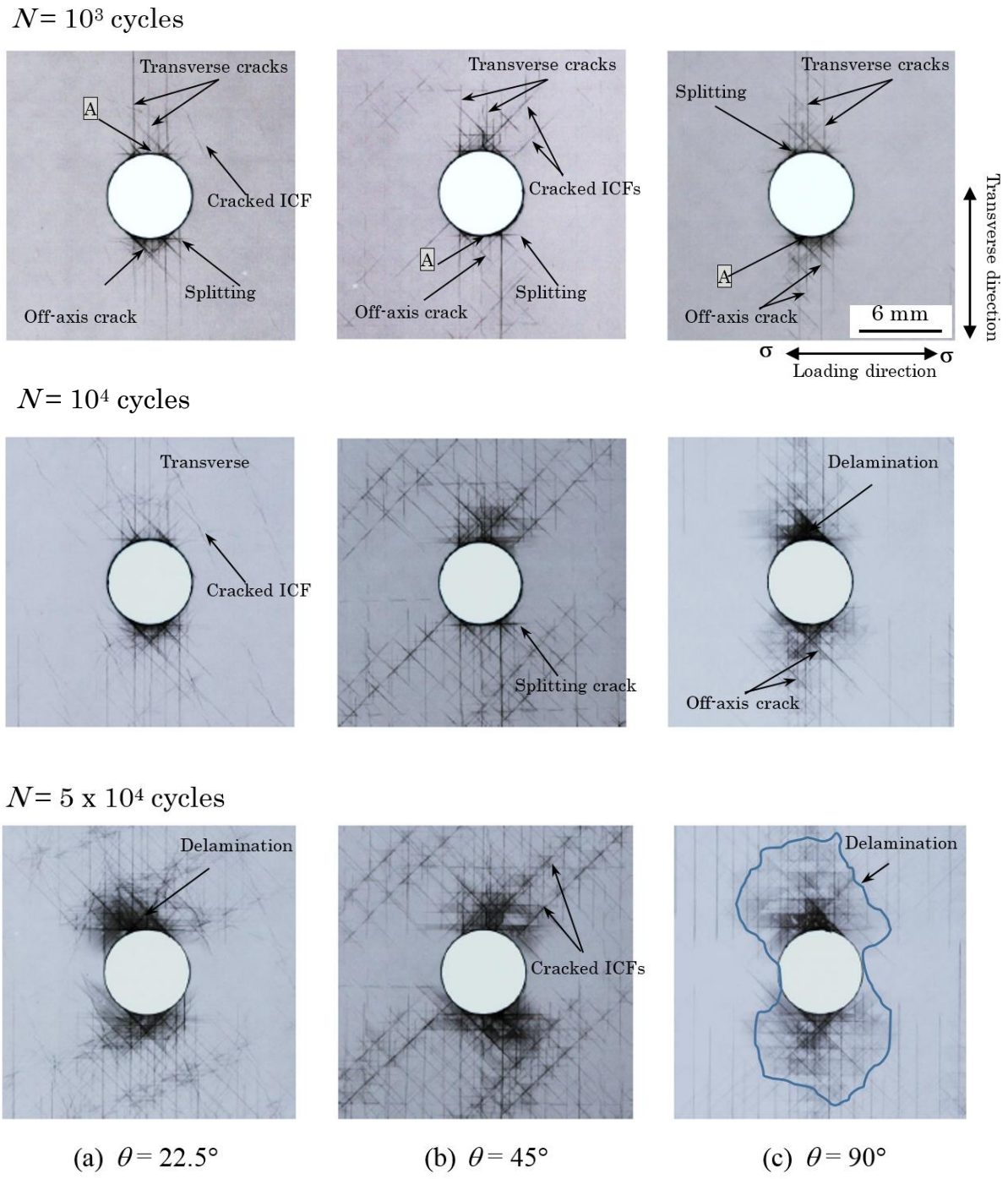

Figure 3-7: Soft X-ray photographs showing projected damage in holed ICF-A laminates for the three θ at the three number of cycles [72].

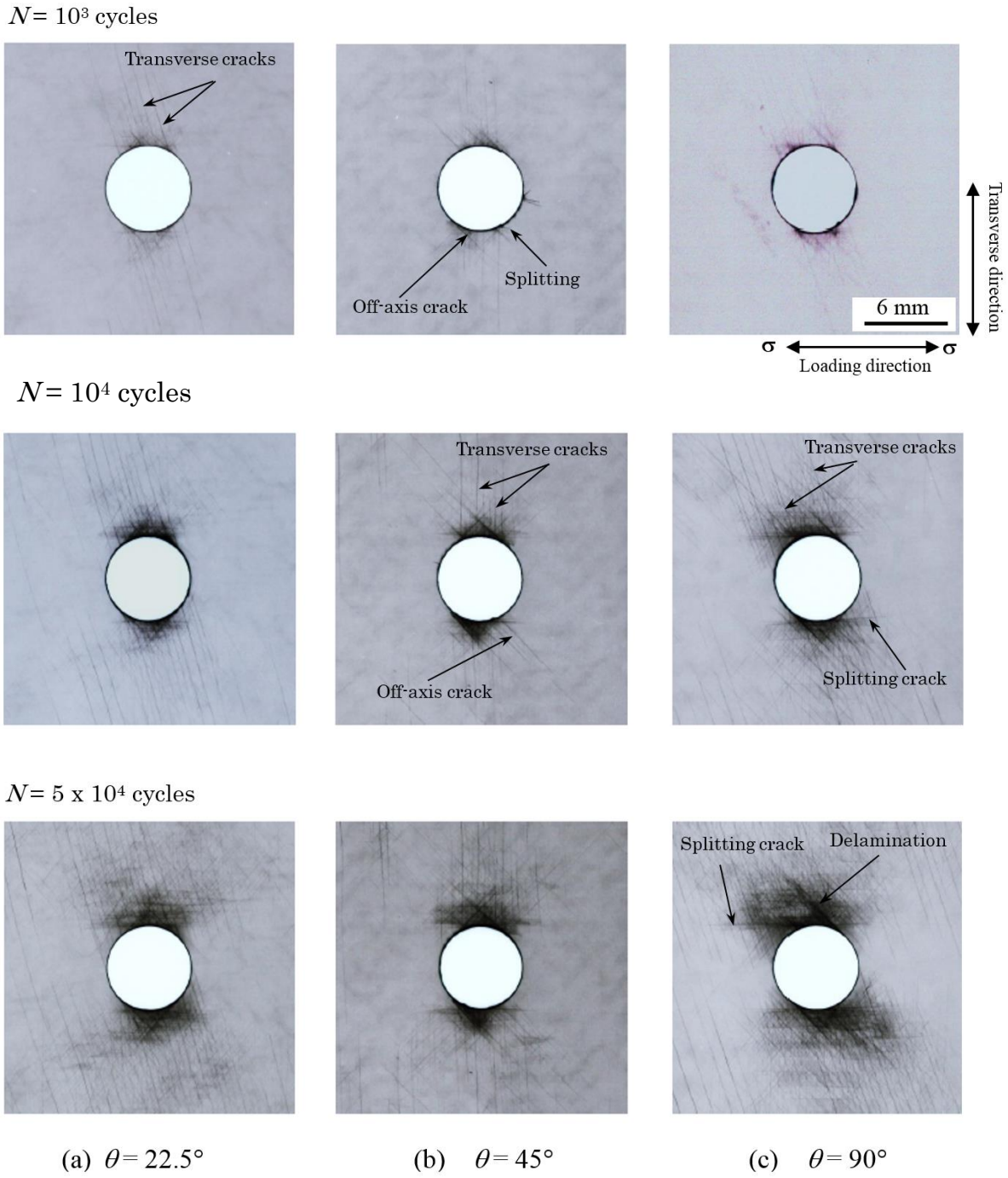

Figure 3-8: Soft X-ray photographs showing projected damage in holed ICF-P laminates for the three θ at the three number of cycles [72].

The difference of damage progress among the three fiber cutting angles is as follows. More cracked ICFs are initiated in the laminates with θ = 22.5° and 45° than in the laminate with θ = 90°. This is because the distance between the ICFs (d = 12.5 sinθ mm) becomes shorter as θ becomes smaller. Figure 7 also shows that the delamination in the laminates with θ = 90° and θ = 45° is greater than that in the laminate with θ = 22.5°. Consequently, it is found that the matrix cracking is a major damage mode in the laminates with smaller θ while the delamination becomes dominant with increasing θ.

Figure 3-8 presents the fatigue damage progress of open-holed ICF-P laminates for the three θ at the three N. At the earliest stage of fatigue ($N = 10^3$ cycles), the predominant damage mode is transverse cracking at the hole roots in the 90° plies for all θ although short splitting cracks tangent to the hole are also initiated. However, there are few off-axis cracks in the ±45° plies at this stage. Next, at $N = 10^4$ cycles, the transverse and off-axis cracks are generated from the splitting cracks that become longer. In addition, the delamination starts to develop from the two splitting cracks. At the later stage (N = 5 x 10^4 cycles), the delamination continues to grow across the width in all the laminates. The laminates with θ = 90° exhibit wider delamination compared with two other laminates having smaller θ. This result means that the damage progress rate in the ICF-P laminate with θ = 90° is the highest among the three θ because the stress concentration generated

around the fiber cutting lines is the highest in this laminate. The above damage progress in the ICF-P laminate is similar to that in the ICF-A laminate, where the damage progress rate is the highest in the laminate with $\theta = 90°$ as shown in Fig. 3-8(c).

From the above result, it is found that the fatigue damage mechanisms of the ICF-A and ICF-P laminates are almost the same as follows: (1) Transverse cracks independent of ICFs occur in the 90° and ±45° plies. (2) New cracks extend from the tips of ICFs only in the ICF-A laminate. (3) Adjacent transverse cracks are connected with each other through the ply interfaces. (4) Delamination is generated and extends at the ply interfaces. However, the damage area including delamination, matrix cracks, splitting cracks in the ICF-P laminate is smaller than that in the ICF-A laminate.

Figures 3-9 and 3-10 present the ICF-A and ICF-P laminates with the three θ after fatigue failure, respectively. All the laminates exhibit a brittle fracture mode accompanied by fiber breakage after unstable delamination growth. More fiber breakages are observed in the fractured laminate with $\theta = 22.5°$ than in the laminates with $\theta = 90°$ and 45°. In contrast, delamination is more dominant in the laminates with $\theta = 45°$ and 90° compared with the laminate with $\theta = 22.5°$. This is mainly because the in-plane shear stress, causing delamination, becomes larger as θ becomes greater. Main difference between the ICF-A and ICF-P laminates is the delamination area after final failure as shown later.

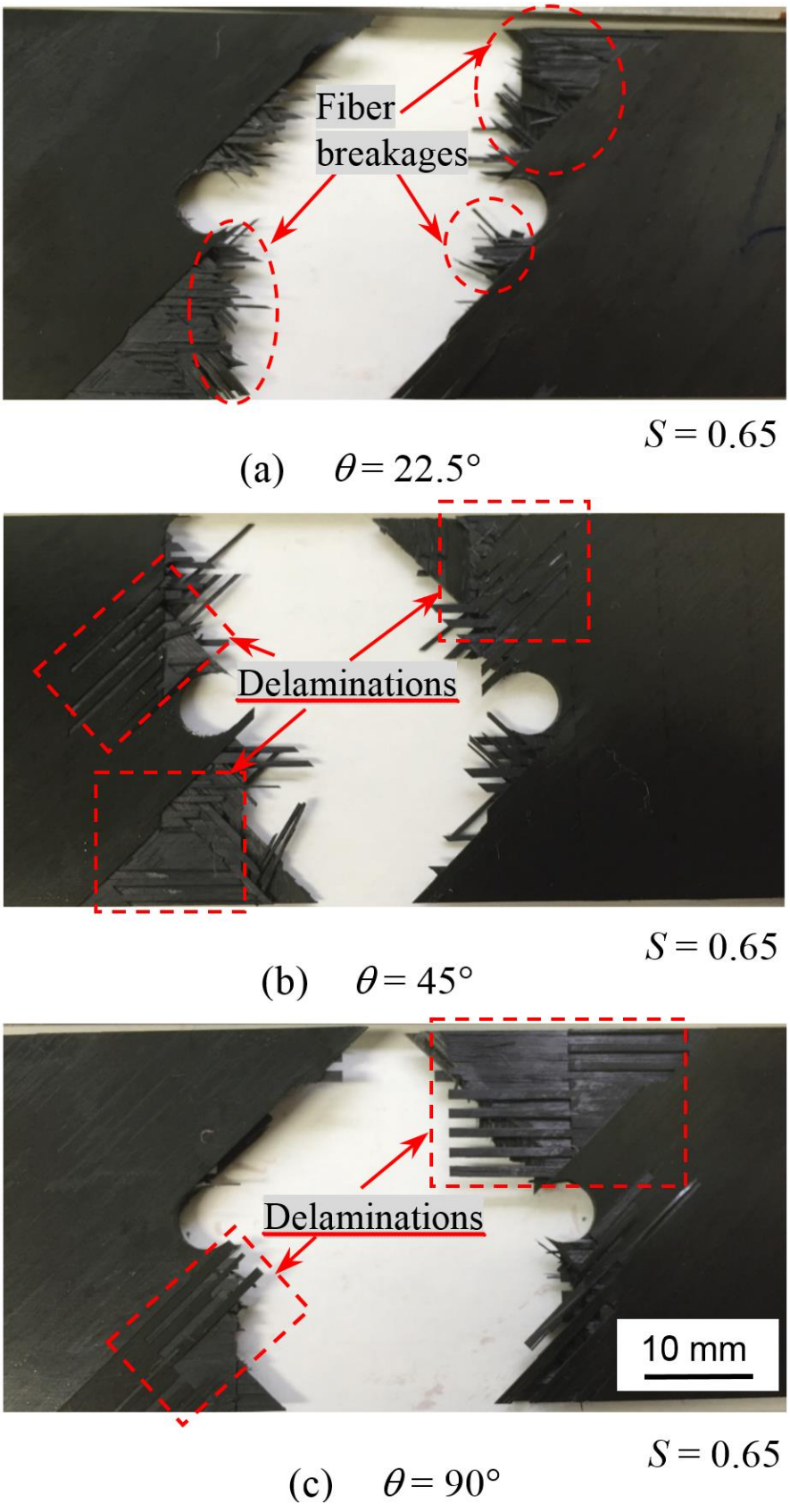

Figure 3-9: Typical images of fractured specimens of ICF- A laminates with the three θ [72].

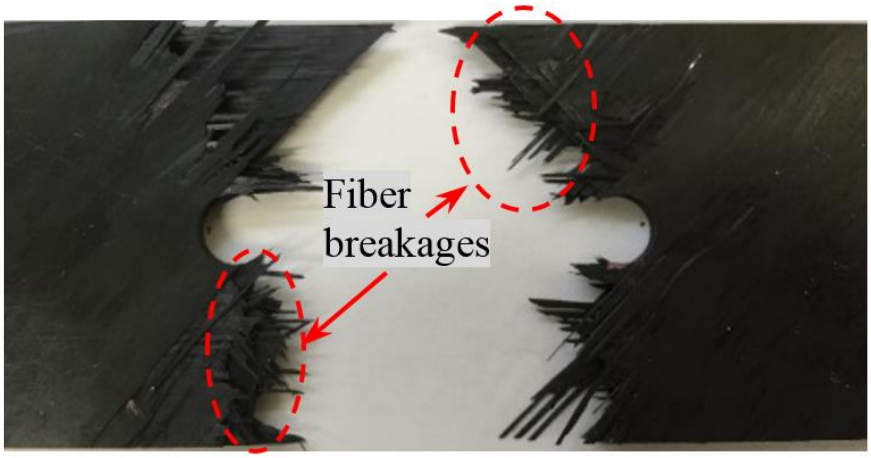

$S = 0.7$

(a) $\theta = 22.5°$

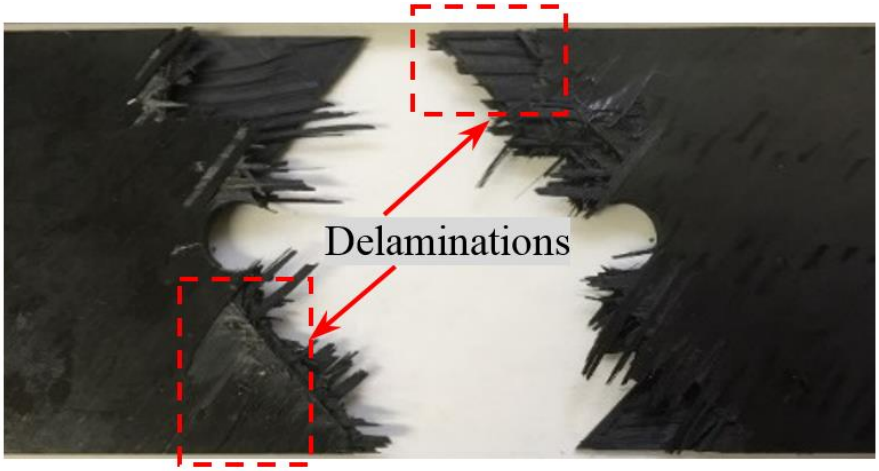

$S = 0.75$

(b) $\theta = 45°$

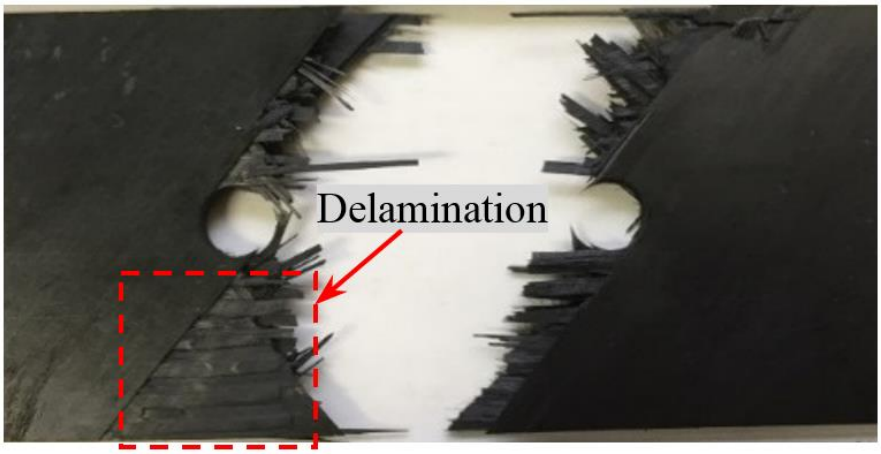

$S = 0.65$

(c) $\theta = 90°$

Figure 3-10: Typical images of fractured specimens of ICF-P laminates with the three θ [72].

3.3.3 Delamination Area at Final Failure

Figure 3-11 shows delamination area for the ICF-A and ICP-P laminates with the three θ at the three N (10^3, 10^4, $5x10^4$ cycles) before final failure. The correlation between the delamination area A_d and N can be fairly well predicted by the following polynomial equation:

$$N = a_0 + a_1 A_d + a_2 A_d^2 + a_3 A_d^3 \quad (1)$$

where a_0, a_1, a_2, and a_3 are the coefficients in the equation and given in Table 3-1. The normalized applied stress S for the six laminates is approximated as the following function of the number of cycles to failure N_f:

$$S = c - d \log_{10} N_f \quad (2)$$

where c and d are the constants determined from Fig. 3-5 and summarized in Table 3-2. Combination of eqs. (1) and (2) yields

$$S = c - d \log_{10} (a_0 + a_1 A_{df} + a_2 A_{df}^{\ 2} + a_3 A_{df}^{\ 3}) \quad (3)$$

where A_{df} denotes A_d just the before final failure ($N = N_f$).

Figure 3-12 shows predicted A_{df} against S for the ICF-A and ICF-P laminates. The arrows in the figures represent the maximum A_d obtained in the experiment (Fig. 3-11).

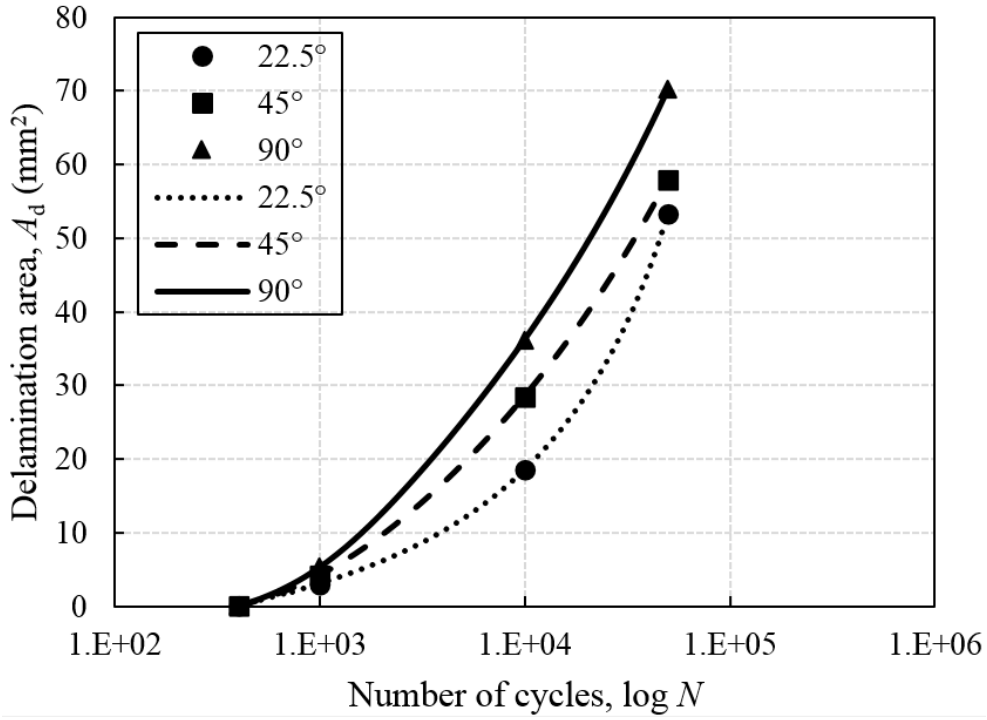

(a) ICF-A

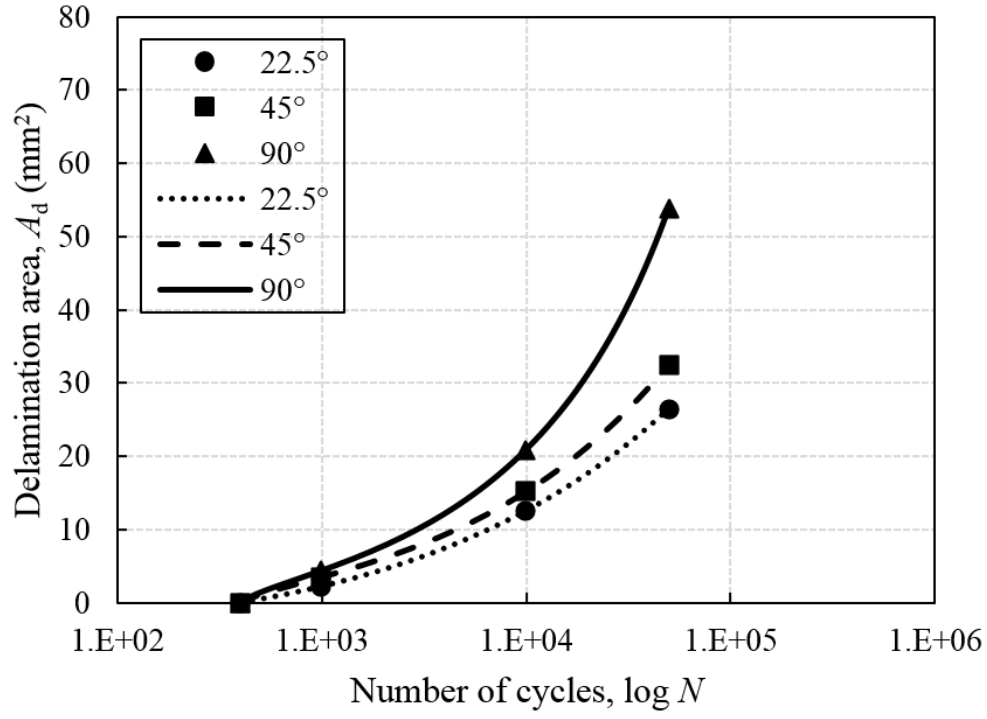

(b) ICF-P

Figure 3-11: Measured and fitted delamination area for the three θ in the (a) ICF-A and (b) ICF-P laminates [72].

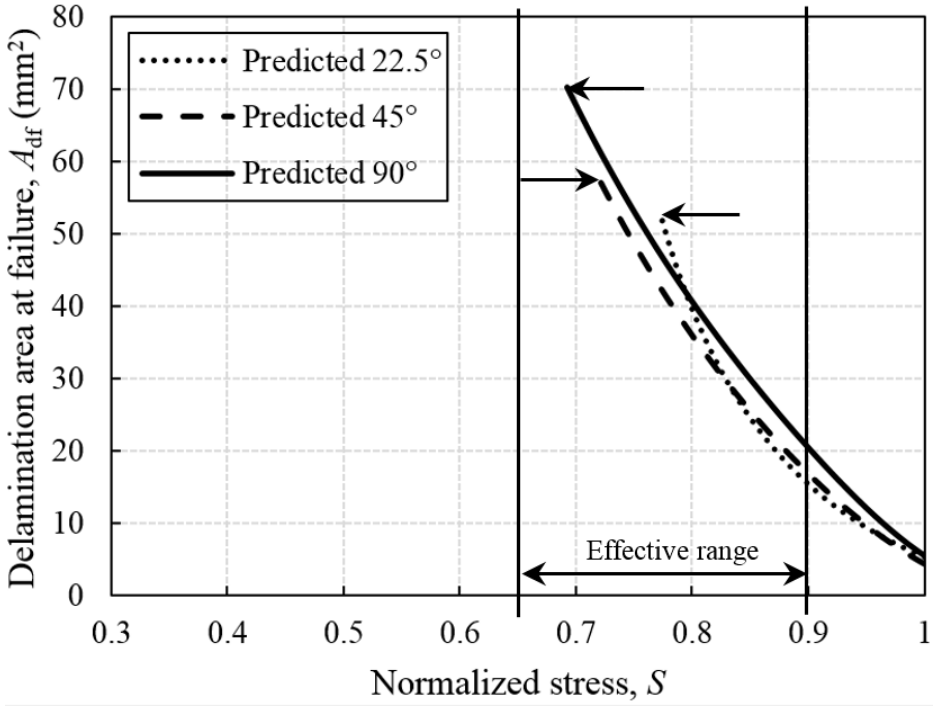

(a) ICF-A

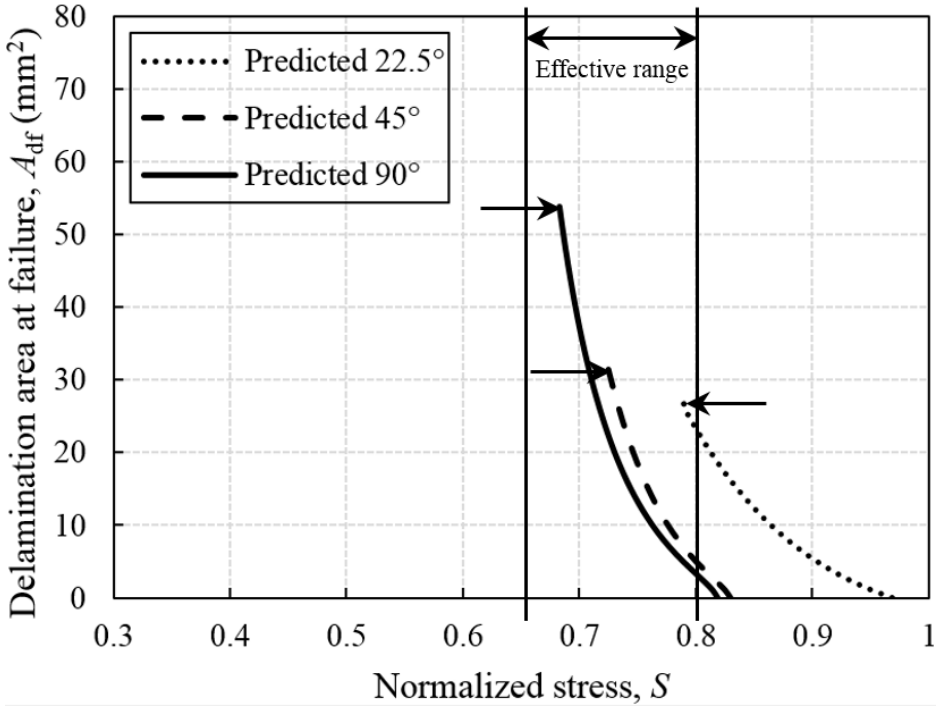

(b) ICF-P

Figure 3-12: Predicted delamination area at failure against the normalized stress for the three θ in the (a) ICF- and (b) ICF-P laminates [72].

The predictions above these values are omitted from the curves. From Fig. 3-6, the effective range of S, which is defined as the range of normalized applied stress, is $0.65 \leq S \leq 0.9$ and $0.65 \leq S \leq 0.8$ for the ICF-A and ICF-P laminates, respectively. In the ICF-A laminates (Fig. 3-12(a)), the delamination growth behavior of the laminates with $\theta =$ 45° and 90° is quite similar. In contrast, the delamination area in the laminate with $\theta =$ 22.5° will be overestimated for $S<0.8$. As mentioned above, the prediction in this region is not significant since it does not always provide a reasonable value of A_{df}. Also in the ICF-P laminates (Fig. 3-12(b)), the delamination growth behavior is similar between the laminates with $\theta =$ 45° and 90°. In contrast, the delamination progress of the laminate with $\theta =$ 22.5° cannot be predicted because the whole curve is out of the effective range

Table 3-1: The coefficients of the polynomial equation for the ICF-A and ICF-P laminates.

Coefficients	ICF-A Laminates			ICP-P Laminates		
	θ = 22.5°	θ = 45°	θ = 90°	θ = 22.5°	θ = 45°	θ = 90°
a_0	400	400	400	400	400	400
a_1	117.17	128.46	111.23	197.87	55.071	40.419
a_2	24.923	2.2371	-0.28952	28.995	32.335	22.421
a_3	-0.18144	0.17745	0.12487	1.3135	0.39783	-0.11286

Table 3-2: The constants of the normalized S-N equation for the ICF-A and ICF-P laminates.

Constants	ICF-A Laminates			ICP-P Laminates		
	θ = 22.5°	θ = 45°	θ = 90°	θ = 22.5°	θ = 45°	θ = 90°
c	1.496	1.4976	1.5469	1.1896	0.961	0.9864
d	0.1543	0.1658	0.1819	0.0852	0.0507	0.0645

of S and A_d. This difference in delamination growth behavior among the three θ suggests that the laminate with $\theta = 22.5°$ fractures in a fiber breakage mode while the other two laminates fail in a delamination mode. Next, comparing the ICF-A and ICF-P laminates, A_{df} in the ICF-A laminates is larger than that in the ICF-P laminates. This is mainly because damages tend to be more easily generated and grow in the ICF laminates having thicker plies [27].

3.4 Conclusions

The fatigue behavior in the open-holed laminates with three different fiber cutting angles is experimentally investigated. The conclusions are summarized below:

1. The *S*-*N* behavior of the ICF laminates was governed by the fiber cutting angle. The highest fatigue strength was obtained in the ICF-P laminate with the smallest θ (22.5°).
2. The ICF laminates with the largest fiber cutting angle (90°) exhibit the greatest delamination growth around the hole.
3. A semi-empirical equation can predict the delamination area just before the final failure in the ICF-A and ICF-P laminates with larger θ (45° and 90°).

Chapter 4

Fatigue Behavior of Non-holed CFRP Laminates with Initially Cut Fibers

In this chapter, we investigated fatigue behavior and damage progress of non-holed CFRP laminates with ICFs having interlayers. Three types of CFRP laminates were employed; a laminate without ICF fabricated using an autoclave (Continuous-A), a laminate with ICF fabricated using an autoclave (ICF-A) and a laminate with ICF fabricated using press molding (ICF-P). First, fatigue test was conducted to obtain *S* (maximum stress)-*N* (the number of cycles to failure) curves in order to reveal fatigue strength. The fatigue tests for several specimens were interrupted at three prescribed numbers of cycles to observe damage progress.

4.1 Introduction

Recently, carbon fiber-reinforced plastics (CFRPs) have been widely applied to be a primary structural material in the fields of transportation (aircraft and automobiles) and other fields replacing metal materials because a large fuel saving becomes possible by making structures light. When CFRP laminates are applied in automobiles structures, these components are frequently subjected to cyclic loads and vibrations, which may cause degradation of structural integrity because of fatigue damage. Note that fatigue fractures are the main cause of the destruction of machinery in metal materials. Thus, it is important to investigate the fatigue characteristics of CFRP for application as a primary structural member in various fields. In addition, for design requirements and functional needs, an automobile is composed of many complexly shaped components.

It is quite difficult to fabricate such components using only conventional CFRP prepreg with continuous fiber owing to its poor formability. In contrast, discontinuous fiber-reinforced plastics fabricated by sheet molding compound (SMC) or injection molding have already been used as automotive parts since they have good molding flowability. However, their strength is much lower than that of composites reinforced with continuous fiber. Therefore, a new material, called unidirectionally arrayed chopped strands, was developed by Taketa et al. [21] by introducing initially cut fibers (ICFs) into

CFRP prepreg. The strength and uniformity of layer structure of the ICF laminate were found to be superior to SMCs.

Several experimental results have been reported on ICF laminates thus far. In the subsequent paper by Taketa et al. [27], the effects of interlaminar toughening on suppression of delamination in ICF laminates were experimentally studied. Yashiro & Ogi [51] investigated the effects of ICFs on fracture behavior in CFRP cross-ply laminates, having alternate or identical ICF angle $\pm\theta$ in the 0° plies. Next, Taketa et al. [52] proposed a technique for enhancing strength and uniformity of layer structure in ICF laminates by introducing ICFs with small angles for the fiber direction. Furthermore, Taketa et al. [28] also investigated mechanical properties of ICF laminates for the application as structural material for complex geometry. They found that the ICF laminates maintain high mechanical properties after forming to complex shapes. Li et al. [29] proposed two newly designed ICF prepregs with discontinuous staggered angled ICFs and discontinuous bi-angled ICFs. Li et al. [30] also studied the damage progression in three kinds of ICF quasi-isotropic (QI) laminates under tension by finite element simulation based on a multiscale analysis. Most of the investigations were concerned with the improvement of mechanical properties (e.g: tensile and modulus strength) and flowability while little attention has been paid to fatigue behavior of CFRP laminates with initially cut fibers.

Meanwhile, the damage and fracture process of laminated composites under cyclic loading is an important issue in the application to load bearing structures. In order to evaluate the damage behavior and strength of laminated composites, many investigations have been carried out on the fatigue strength evaluation [57–60] and the damage initiation and evolution [61–70]. However, most of the above studies on have been performed on continuous CFRP laminates with various stacking sequence while very little attention has been paid to fatigue behavior of CFRP laminates with initially cut fibers.

The present investigation aims at making clear the fatigue strength and damage progress of ICF CFRP laminates with toughened interlayers under tension-tension cyclic loading. Two kinds of QI ICF laminates were fabricated by autoclave and hot press molding methods. For comparison, a QI laminate made of continuous prepreg is also manufactured by the autoclave method. Fatigue tests were carried out on three kinds of laminates to reveal fatigue strength and damage progress. First, S (maximum stress)-N (the number of cycles to failure) curves were measured for the above three laminates. Then, the internal fatigue damage progress was observed using radiography.

4.2 Experimental Procedure

The prepreg used in this study is made of carbon fiber (volume fraction 0.58) and epoxy resin with interlayers, (T800S/#3900-2B, Toray Industries). This prepreg system

contains about 30 μm thick interlayers including tough thermoplastic particles on the 150 μm thick base CFRP layer. A micrograph on the cross-section of the laminate is presented in Fig. 2-1.

In this study, we made ICF sheets as proposed by Taketa et al. [21]. An automatic cutting machine with a special tangential blade was employed to mechanically introduce ICFs into the prepreg. The schematic of the ICF patterns in this study is illustrated in Fig. 2-2. 1 mm-long staggered ICFs were arrayed at an interval of 25 mm in the fiber direction. Two types of ICF laminates with an ICF angle θ of 22.5° were fabricated by using the autoclave method (ICF-A) and press molding method (ICF-P). The ICF plies were prepared by cutting 300 mm and 250 mm square prepreg sheets for the ICF-A and ICF-P laminates, respectively.

An ICF-A QI laminate was built by stacking ICF plies in a sequence of $[45/0/-45/90]_s$ and then cured in the autoclave. The schematic of the press molding process is illustrated in Fig. 2-3. An ICF-P QI laminate was made by stacking ICF plies in a sequence of $[45/0/-45/90]_{2s}$ into a mold (300 mm square) and cured at a pressure of 0.3 MPa and a temperature of 150° C for 30 min, during which its area increases from 70 % to 100 % of the mold. For comparison, a Continuous-A QI laminate was also fabricated by stacking the conventional prepreg (250 mm square) without ICFs in a sequence of $[45/0/-45/90]_s$ and then cured

using autoclave method.

Non hole tension (NHT) specimens were then cut out from laminates according to the ASTM standard (D3039). The dimensions and geometry of NHT specimens are shown in Fig. 4-1. The specimen is 250 mm long and 25 mm wide. GFRP tabs were bonded at grip area on the specimen. Table 4-1 summarizes the stacking sequence, the thickness and static tensile strength of NHT specimens for the Continuous-A, ICF-A and ICF-P laminates.

The tensile fatigue tests were conducted at a room temperature with a sinusoidal waveform under a load-control condition using a hydraulic testing machine (8516

Table 4-1: Stacking sequence, thickness and static tensile strength of NHT specimens.

Laminate	Stacking sequence	Thickness		Static tensile strength (MPa)
		Laminate (mm)	Ply (mm)	
Continuous-A	$[+45/0/-45/90]_s$	1.55	0.194	922.5
ICF-A	$[+45/0/-45/90]_s$	1.56	0.195	613.1
ICF-P	$[+45/0/-45/90]_{2s}$	2.16	0.135	769

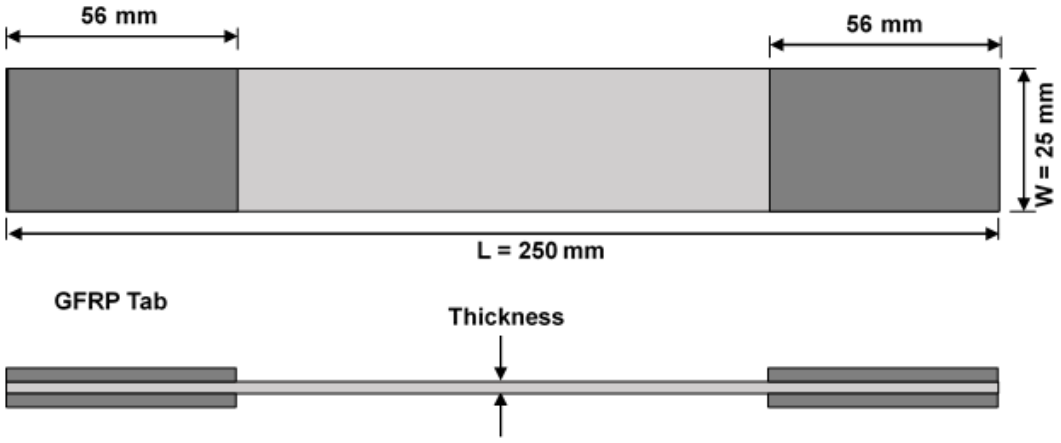

Figure 4-1 Dimensions of the non hole tension (NHT) specimen.

INSTRON). All the tests were performed at a stress ratio of 0.1 and at a frequency of 3 Hz. The maximum stress σ_{max} was varied between 60 and 95 % of the static tensile strength σ_{OHT} of each ICF OHT specimen. The tests were terminated at N of 10^6 cycles even if no failure occurred. In order to quantitatively evaluate the magnitude of damage, fatigue tests (σ_{max} = 0.60 σ_{NHT}) of one specimen for each laminate was interrupted at the prescribed numbers of cycles ($N = 10^2, 10^3, 10^4, 10^5$) before final failure. The internal damage progress during the fatigue test was observed using transmissive radiography (SOFTEX M-100) with the aid of zinc iodide as a contrast medium.

4.3 Result and Discussion

4.3.1 *S-N* Curves

Figure 4-2 shows the *S-N* curves of non-holed CFRP for the Continuous-A, ICF-A and ICF-P laminates. The *S-N* curve behavior of the three laminates was similar and the reduction of fatigue strength for three laminates was approximately by 35% of the static tensile strength at 10^6 cycles. The fatigue strength of Continuous-A laminate was the highest among the three laminates. This suggested that the fatigue strength significantly depends on the static strength of laminates and it higher in the conventional laminate (with prepreg without initial cut fibers). Comparing the results of both ICF laminates and Continuous- laminates, both the static tensile strength and fatigue strength of the ICF-A

and ICP laminates are smaller than those of the Continuous-A laminate. This indicates that damage are easily initiated from ICFs at relatively low stress levels or low numbers of cycles, as shown later in the damage progress of these laminates. Moreover, comparing the ICF-A and ICF-P laminates, both the static tensile strength and fatigue strength of the ICF-P laminate (ply thickness 1.56 mm) were higher than those of the ICF-A laminate (ply thickness 2.16 mm). The main reason for higher strength of the ICF-P laminate is the thinner plies as has been analytically explained by Taketa et al. [21].

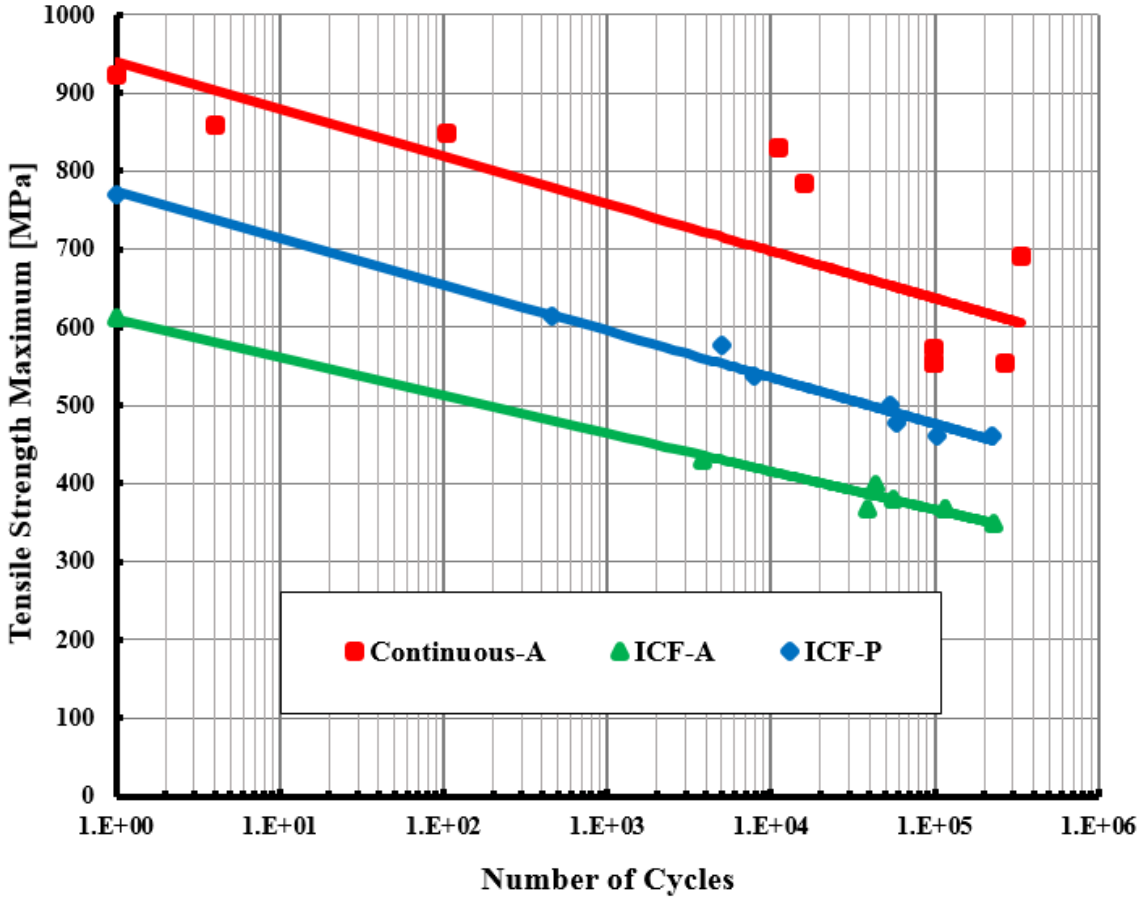

Figure 4-2: *S-N* curves of three types of NHT specimens.

4.3.2 Damage Progress

Figure 4-3, 4-4 and 4-5 show representative damage growth by soft X-ray photography in quasi-isotropic laminates under fatigue loading for Continuous-A, ICF-A and ICF-P laminates, respectively.

At early cycles, at N of 10^2 and N of 10^3 for all the three laminates, transverse cracks in the ±45° and 90° plies that occurred at specimen edges grew in the width direction of the specimen and were multiplied in the specimen with an increase in the number of loading cycles. Comparing both autoclave laminates, the crack density and delamination area in Continuous-A is more prominent than that in ICF-A. This is mainly due to a lot of cracks propagating from the 90° plies. In contrast, the crack density and delamination area in ICF-P laminates are the smallest among the three laminates.

Next, at N of $10^{4,}$ the transverse cracks from the both free edges propagated and were connected with each other across the width of the specimens. In the ICF-A and ICF-P laminates, the new cracks were generated from ICFs and they appears more in ICF-A laminate compared to the ICF-P laminate. This suggested that cracks were difficult to propagate in the ICF-P laminate due to the ply is thinner in the ICF-P laminate.

Finally, at $N = 10^5$, the delamination generated at the specimen edges increases rapidly, especially in the Continuous-A and ICF-A laminates. The delamination propagating in the Continuous-A and ICF-A laminates are more remarkable than that in

the ICF-P laminate as shown in Fig. 4-3 and 4-4. As a result, the ICF-P laminate shows the smallest damage growth among the three laminates. This is because the initiation and propagation of matrix cracking are suppressed as the ply becomes thinner.

From the above damage progress, in the Continuous-A laminate, the damage scenario is as follows: (1) Transverse cracks are initiated in the 90° and ±45° plies. (2) The number of transverse cracks increases with increasing *N*. (3) Adjacent transverse cracks are connected with each other by way of the ply interfaces. (4) Delamination is generated from free edges and extends along the specimen length and across the specimen width. The delaminations are mainly caused by the interlaminar shear stress at the both free edges. On the other hand, the damage progress in the ICF-A and ICF-P laminates are summarized as follows: (1) Transverse cracks independent of ICFs occur in the 90° and ±45° plies. (2) New cracks extend from the tips of ICFs only in the ICF-A laminate. (3) Adjacent transverse cracks are connected with each other through the ply interfaces. (4) Delamination is started from free edges and extends along specimen length and across the specimen width. In particular, the delamination occurs at the ply interfaces at the early stage of cycles.

It is found that the delamination in the Continuous-A laminate is more prominent than that in the ICF-A laminate. Contrarily, relatively small delamination locally extends

in the ICF-P laminate. It is revealed that matrix cracks are relatively difficult to propagate in the ICF-P laminate with thinner plies.

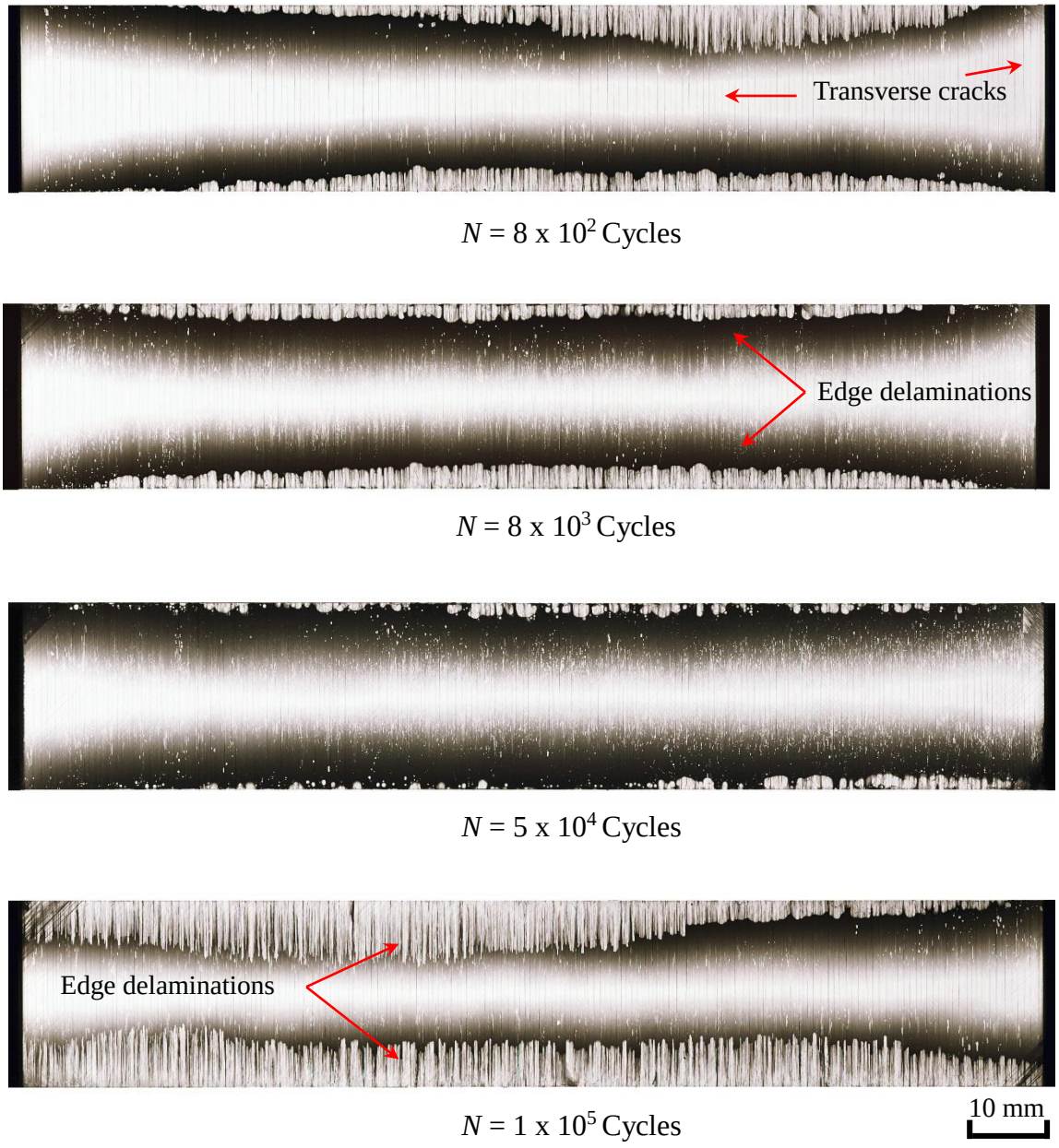

Figure 4-3: Observation of internal damage growth of Continuous-A laminate under applied stress level of $\sigma_{max} = 0.6.\sigma_s$ with soft X-ray photography.

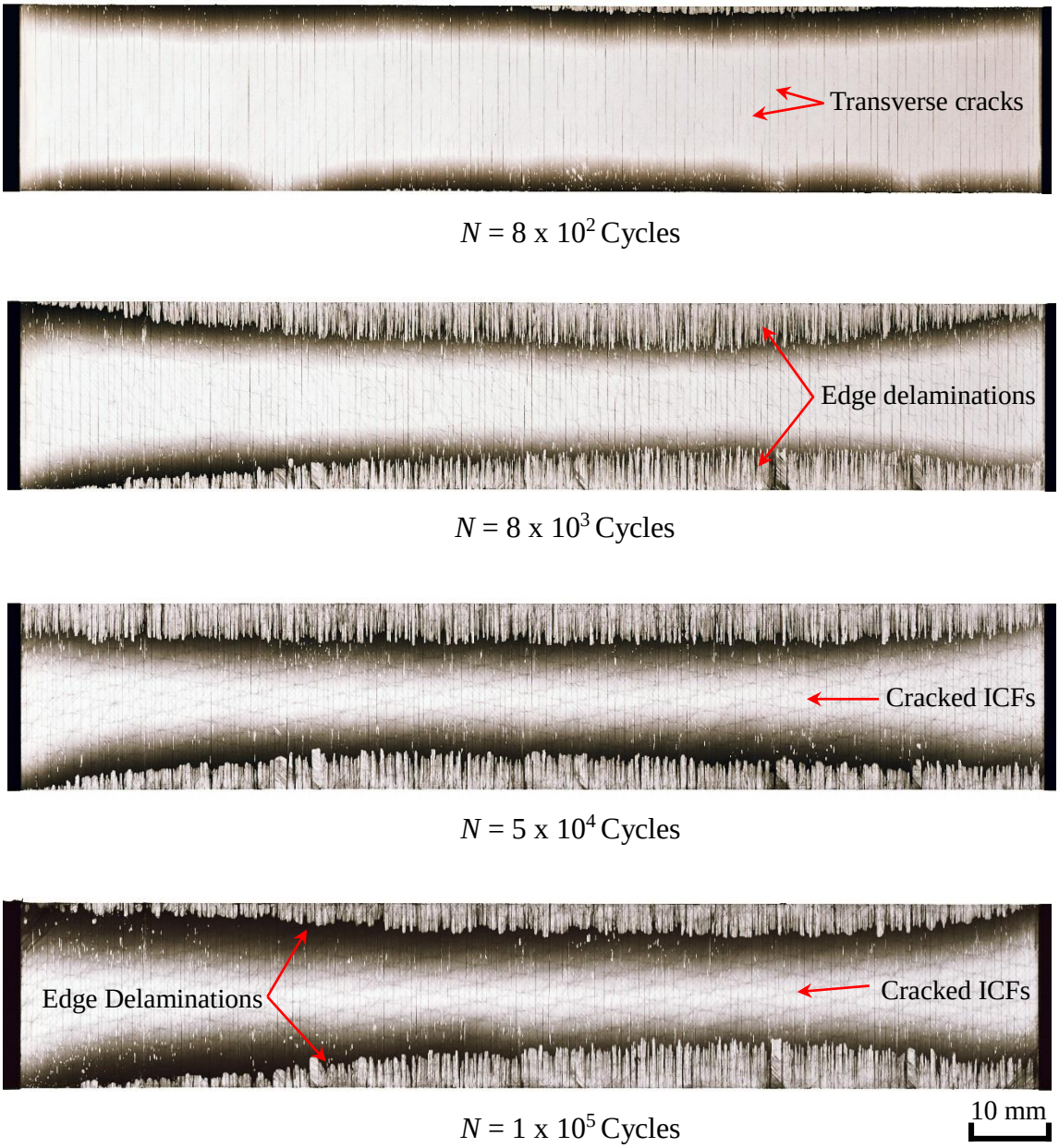

Figure 4-4: Observation of internal damage growth of ICF-A laminate under applied stress level of $\sigma_{max} = 0.6.\sigma_s$ with soft X-ray photography.

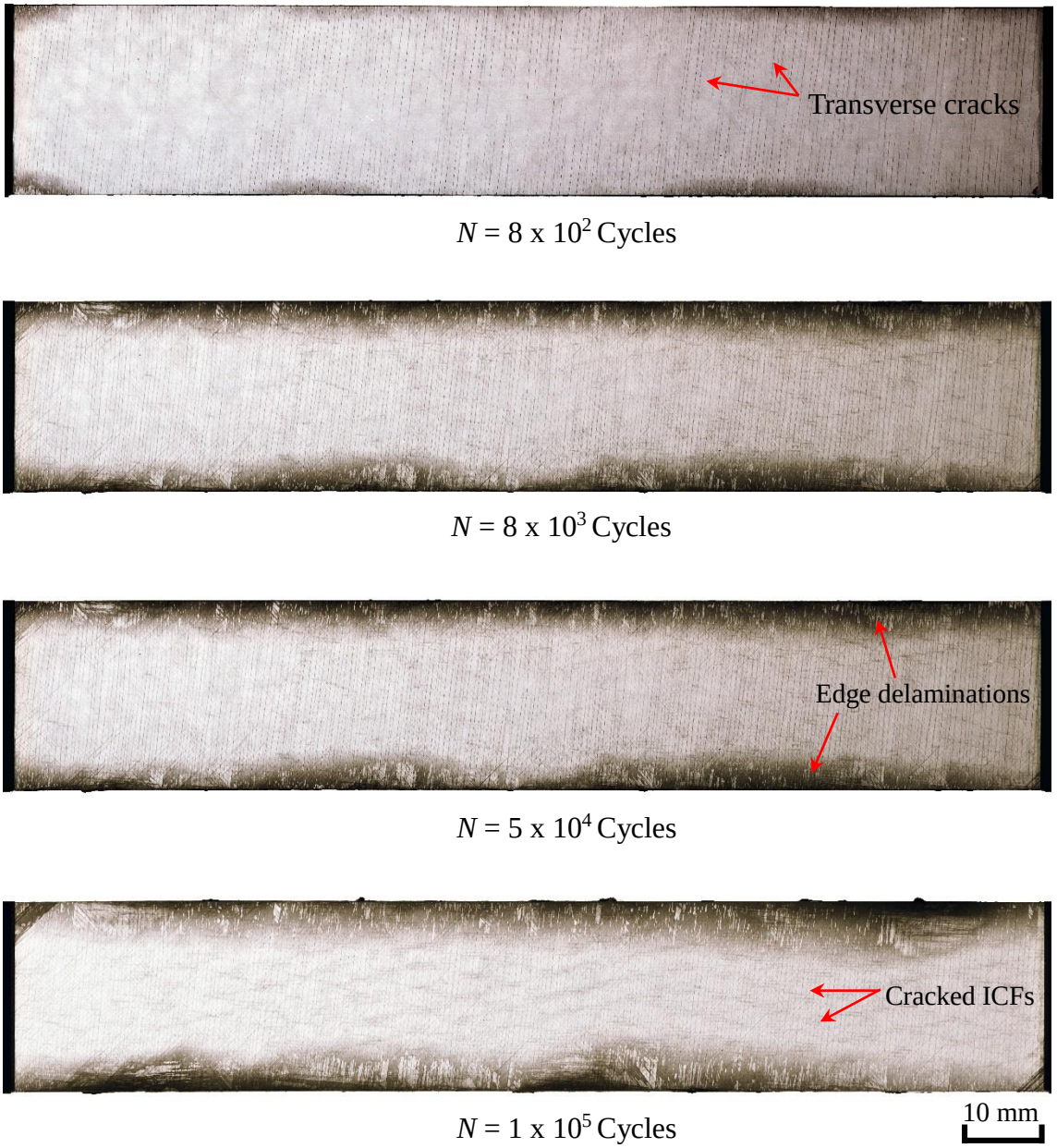

Figure 4-5: Observation of internal damage growth of ICF-P laminate under applied stress level of $\sigma_{max} = 0.6.\sigma_s$ with soft X-ray photography.

4.4 Conclusion

The fatigue behavior and damage progress in non-holed CFRP laminates with ICF toughened with interlayers are presented. From the experimental results, the following conclusions are derived:

1. The fatigue strength of the Continuous-A laminate is the highest among the three laminates while the fatigue strength of the ICF-P laminate is higher than that of the ICF-A laminate. However, the decrease ratio of fatigue strength at N of 10^6 is about 35% of its static strength, which is almost the same in the three laminates.
2. The degree of damage in the ICF-P laminate is the smallest among the three laminates while the increase rate of the crack density and edge delamination is the greatest in the ICF-A laminate with thicker plies.
3. Further work is still required to quantitatively predict fatigue damage development in both non-holed ICF laminates by finite element analysis.

Chapter 5

Conclusions and Future Work

This chapter summarizes the main results of this dissertation and predicts the main research topics which may be concerned with this study in future.

5.1 Conclusions

CFRP laminate with initially cut fibers (ICF) is a new type of short fiber reinforced polymer by introducing regular slits into the conventional prepreg before the fabrication of laminates. In this study, two kinds of ICF CFRP laminates with toughened interlayers are fabricated by autoclave (ICF-A laminate) and press molding (ICF-P laminate). For comparison, a conventional laminate was also fabricated using autoclave (Continuous-A laminate). Fatigue properties and damage progress in the open-holed and non-holed ICF CFRP laminates are investigated by experiment. In addition, the effect of fiber cutting angle on the fatigue behavior of open-holed ICF CFRP laminates is also investigated.

Based on these works, the following conclusions are obtained:

1. The results obtained from the fatigue test and damage progress observation of open-holed CFRP laminates reveal that the fatigue strength of the ICF-P laminate is higher than that of the ICF-A laminate. The decrease ratio of fatigue strength at N of 10^6 is about 30% of its static strength, which is almost the same in the both ICF laminates. However, the fatigue strength of the Continuous-A laminate is the highest among the three laminates with the decrease ratio of fatigue strength at N of 10^6 is only 5% of its static strength. Moreover, the damage progress in the ICF-P laminate is the smallest among the three laminates while the increase rate of the crack density is the greatest

in the ICF-A laminate with thicker plies.

2. The results obtained from fatigue test and damage progress observation of open ICF CFRP laminates with different fiber cutting angle indicated that the *fatigue* behavior of the ICF laminates was governed by the fiber cutting angle. The highest fatigue strength was obtained in the ICF-P laminate with the smallest θ (22.5°). In contrast, the ICF laminates with the largest fiber cutting angle (90°) exhibit the greatest delamination growth around the hole.
3. The results obtained from the fatigue test and damage progress observation of non-holed CFRP laminates indicated that the fatigue strength of the Continuous-A laminate is the highest among the three laminates while the fatigue strength of the ICF-P laminate is higher than that of the ICF-A laminate. However, the decrease ratio of fatigue strength at N of 10^6 is about 35% of its static strength, which is almost the same in the three laminates. In addition, the degree of damage in the ICF-P laminate is the smallest among the three laminates while the increase rate of the crack density and edge delamination is the greatest in the ICF-A laminate with thicker plies.

5.2 Future Work

This study investigated the fatigue behavior of ICF CFRP laminates for open holed and non-holed specimen with different fabrication method and fiber cutting angle,

however, other important mechanical properties such as compression, bending, compression fatigue and impact have not been investigated. Further experimental research and numerical analysis are necessary for the development of practically useful ICF laminates in future.

References

[1] D. Hull, *An introduction to composite materials*. 1981.

[2] M. F. Ashby, *Materials Selection in Mechanical Design*. 2005.

[3] H. G. S. J. Thuis, "Development of a composite cargo door for an aircraft," *Compos. Struct.*, vol. 47, no. 1–4, pp. 813–819, 1999.

[4] M. M. Shokrieh and F. Taheri Behrooz, "Wing instability of a full composite aircraft," *Compos. Struct.*, vol. 54, no. 2–3, pp. 335–340, 2001.

[5] A. C. Okafor, N. Singh, U. E. Enemuoh, and S. V. Rao, "Design, analysis and performance of adhesively bonded composite patch repair of cracked aluminum aircraft panels," *Compos. Struct.*, vol. 71, no. 2, pp. 258–270, 2005.

[6] S. Murugan, E. I. Saavedra Flores, S. Adhikari, and M. I. Friswell, "Optimal design of variable fiber spacing composites for morphing aircraft skins," *Compos. Struct.*, vol. 94, no. 5, pp. 1626–1633, 2012.

[7] Z. Kapidžić, L. Nilsson, and H. Ansell, "Finite element modeling of mechanically fastened composite-aluminum joints in aircraft structures," *Compos. Struct.*, vol. 109, no. 1, pp. 198–210, 2014.

[8] R. Schouwenaars, S. Cerrud, and A. Ortiz, "Mechanical analysis of fracture in an automotive radiator head produced from a nylon ± glass ® bre composite," *Image (Rochester, N.Y.)*, vol. 33, pp. 551–558, 2002.

[9] J. M. Corum, R. L. Battiste, and M. B. Ruggles-Wrenn, "Low-energy impact effects on candidate automotive structural composites," *Compos. Sci. Technol.*, vol. 63, no. 6, pp. 755–769, 2003.

[10] M. B. Ruggles-Wrenn, J. M. Corum, and R. L. Battiste, "Short-term static and cyclic behavior of two automotive carbon-fiber composites," *Compos. Part A Appl. Sci. Manuf.*, vol. 34, no. 8, pp. 731–741, 2003.

[11] D. G. Lee, H. S. Kim, J. W. Kim, and J. K. Kim, "Design and manufacture of an automotive hybrid aluminum/composite drive shaft," *Compos. Struct.*, vol. 63, no. 1, pp. 87–99, 2004.

[12] S. W. Lee and D. G. Lee, "Composite hybrid valve lifter for automotive engines," *Compos. Struct.*, vol. 71, no. 1, pp. 26–33, 2005.

[13] S. Marouani, L. Curtil, and P. Hamelin, “Ageing of carbon/epoxy and carbon/vinylester composites used in the reinforcement and/or the repair of civil engineering structures,” *Compos. Part B Eng.*, vol. 43, no. 4, pp. 2020–2030, 2012.

[14] Z. K. Awad, T. Aravinthan, Y. Zhuge, and F. Gonzalez, “A review of optimization techniques used in the design of fibre composite structures for civil engineering applications,” *Mater. Des.*, vol. 33, no. 1, pp. 534–544, 2012.

[15] P. Böer, L. Holliday, and T. H. K. Kang, “Independent environmental effects on durability of fiber-reinforced polymer wraps in civil applications: A review,” *Constr. Build. Mater.*, vol. 48, pp. 360–370, 2013.

[16] Y. C. Tseng and C. Y. Kuo, “Engineering and construction torsional responses of glass-fiber/epoxy composite blade shaft for a small wind turbine,” *Procedia Eng.*, vol. 14, pp. 1996–2002, 2011.

[17] Z. Lanting, “Research on Structural Lay-up Optimum Design of Composite Wind Turbine Blade,” *Energy Procedia*, vol. 14, pp. 634–642, 2012.

[18] T. Kim, A. M. Hansen, and K. Branner, “Development of an anisotropic beam finite element for composite wind turbine blades in multibody system,” *Renew. Energy*, vol. 59, pp. 172–183, 2013.

[19] The Japan Carbon Fiber Manufacturer Association, “Aircraft and Aerospace Fields.” [Online]. Available: http://www.carbonfiber.gr.jp/english/field/craft.html. [Accessed: 12-Apr-2017].

[20] T. Kondo, “Innovation in Carbon Fiber Business,” pp. 0–24, 2012.

[21] I. Taketa, T. Okabe, and a. Kitano, “A new compression-molding approach using unidirectionally arrayed chopped strands,” *Compos. Part A Appl. Sci. Manuf.*, vol. 39, no. 12, pp. 1884–1890, Dec. 2008.

[22] S. Suresh, *Fatigue of Materials*. Cambridge University Press, 1998.

[23] E. Society for the Advancement of Material and Process Engineering. European Chapter. International Conference (10th : 1989 : Birmingham and S. Benson, *Materials and processing--move into the 90’s : Proceedings of the 10th International European Chapter Conference of the Society for the Advancement of Material and Process Engineering, Birmingham, United Kingdom, July 11-13, 1989*. Elsevier, 1989.

[24] I. Y. Chang and J. F. Pratte, “LDFTM Thermoplastic Composites Technology,” *J. Thermoplast. Compos. Mater.*, vol. 4, no. 3, pp. 227–252, 1991.

[25] P. Feraboli, E. Peitso, T. Cleveland, P. B. Stickler, and J. C. Halpin, “Notched behavior of prepreg-based discontinuous carbon fiber/epoxy systems,” *Compos. Part A Appl. Sci. Manuf.*, vol. 40, no. 3, pp. 289–299, 2009.

[26] P. Feraboli, T. Cleveland, M. Ciccu, P. Stickler, and L. DeOto, “Defect and damage analysis of advanced discontinuous carbon/epoxy composite materials,” *Compos. Part A Appl. Sci. Manuf.*, vol. 41, no. 7, pp. 888–901, 2010.

[27] I. Taketa, T. Okabe, and A. Kitano, “Strength improvement in unidirectional arrayed chopped strands with interlaminar toughening,” *Compos. Part A Appl. Sci. Manuf.*, vol. 40, no. 8, pp. 1174–1178, Aug. 2009.

[28] I. Taketa, N. Sato, a. Kitano, M. Nishikawa, and T. Okabe, “Enhancement of strength and uniformity in unidirectionally arrayed chopped strands with angled slits,” *Compos. Part A Appl. Sci. Manuf.*, vol. 41, no. 11, pp. 1639–1646, Nov. 2010.

[29] H. Li, W. X. Wang, Y. Takao, and T. Matsubara, “New designs of unidirectionally arrayed chopped strands by introducing discontinuous angled slits into prepreg,” *Compos. Part A Appl. Sci. Manuf.*, vol. 45, pp. 127–133, 2013.

[30] H. Li, W.-X. Wang, and T. Matsubara, “Multiscale analysis of damage progression in newly designed UACS laminates,” *Compos. Part A Appl. Sci. Manuf.*, vol. 57, pp. 108–117, 2014.

[31] F. Aymerich and M. S. Found, “Response of notched carbon / PEEK and carbon / epoxy laminates,” pp. 675–683, 2000.

[32] A. Afaghi-Khatibi, L. Ye, and Y. W. Mai, “An experimental study of the influence of fibre-matrix interface on fatigue tensile strength of notched composite laminates,” *Compos. Part BEngineering*, vol. 32, no. 2001, pp. 371–377, 2001.

[33] B. Vieille and W. Albouy, “Fatigue damage accumulation in notched woven-ply thermoplastic and thermoset laminates at high-temperature: influence of matrix ductility and fatigue life prediction,” *Int. J. Fatigue*, vol. 80, pp. 1–9, May 2015.

[34] M. Kawai and T. Shiratsuchi, “Vanishing notch sensitivity approach to fatigue life prediction of notched cross-ply CFRP laminates at room temperature,” *J. Compos. Mater.*, vol. 46, no. 23, pp. 2935–2950, Jan. 2012.

[35] O. J. Nixon-Pearson, S. R. Hallett, P. J. Withers, and J. Rouse, “Damage development in open-hole composite specimens in fatigue. Part 1: Experimental investigation,” *Compos. Struct.*, vol. 106, pp. 882–889, Dec. 2013.

[36] O. J. Nixon-Pearson and S. R. Hallett, “An investigation into the damage development and residual strengths of open-hole specimens in fatigue,” *Compos. Part A Appl. Sci. Manuf.*, vol. 69, pp. 266–278, 2015.

[37] O. J. Nixon-Pearson and S. R. Hallett, “An experimental investigation into quasi-static and fatigue damage development in bolted-hole specimens,” *Compos. Part B Eng.*, vol. 77, pp. 462–473, Aug. 2015.

[38] B. Aidi, M. K. Philen, and S. W. Case, “Progressive damage assessment of centrally notched composite specimens in fatigue,” *Compos. Part A Appl. Sci. Manuf.*, vol. 74, pp. 47–59, Jul. 2015.

[39] S. M. Spearing, P. W. R. Beaumont, and M. T. Kortschot, “The fatigue damage mechanics of notched carbon-fiber peek laminates,” *Composites*, vol. 23, no. 5, pp. 305–311, 1992.

[40] S. M. Spearing and P. W. R. Beaumont, “Fatigue damage mechanics of composite materials. I: Experimental measurement of damage and post-fatigue properties,” *Compos. Sci. Technol.*, vol. 44, no. 2, pp. 159–168, 1992.

[41] T. Mohlin, L. Carlsson, and A. F. Blom, “TEQC83,” 1983, vol. 83, no. September.

[42] S. Kellas, J. Morton, and S. M. Bishop, “Fatigue damage development in a notched carbon fibre composite,” *Compos. Struct.*, vol. 5, no. 2, pp. 143–157, 1986.

[43] J. Morton and S. Kellas, “Damage Characteristics in Notched Carbon Fiber Composites Subjected to Fatigue Loading & mdash ; Environmental Effects,” pp. 657–673, 1987.

[44] S. Kellas, J. Morton, and P. T. Curtis, “A characteristic fatigue parameter for notched composites,” *Int. J. Fatigue*, vol. 13, no. 1, pp. 35–43, 1991.

[45] C. Soutis, N. A. Fleck, and P. A. Smith, “Compression fatigue behaviour of notched carbon fibre-epoxy laminates.” pp. 303–312, 1991.

[46] S. Mall, D. W. Katwyk, R. L. Bolick, A. D. Kelkar, and D. C. Davis, “Tension-compression fatigue behavior of a H-VARTM manufactured unnotched and

notched carbon/epoxy composite," *Compos. Struct.*, vol. 90, no. 2, pp. 201–207, 2009.

[47] S. Yashiro and T. Okabe, "Estimation of fatigue damage in holed composite laminates using an embedded FBG sensor," *Compos. Part A Appl. Sci. Manuf.*, vol. 42, no. 12, pp. 1962–1969, Dec. 2011.

[48] J. S. Huh and W. Hwang, "Fatigue life prediction of circular notched CFRP laminates," *Compos. Struct.*, vol. 44, no. 2–3, pp. 163–168, Feb. 1999.

[49] M. R. Satapathy, B. G. Vinayak, K. Jayaprakash, and N. K. Naik, "Fatigue behavior of laminated composites with a circular hole under in-plane multiaxial loading," *Mater. Des.*, vol. 51, pp. 347–356, Oct. 2013.

[50] O. J. Nixon-Pearson, S. R. Hallett, P. W. Harper, and L. F. Kawashita, "Damage development in open-hole composite specimens in fatigue. Part 2: Numerical modelling," *Compos. Struct.*, vol. 106, pp. 890–898, Dec. 2013.

[51] S. Yashiro and K. Ogi, "Fracture behavior in CFRP cross-ply laminates with initially cut fibers," *Compos. Part A Appl. Sci. Manuf.*, vol. 40, no. 6–7, pp. 938–947, Jul. 2009.

[52] I. Taketa, T. Okabe, H. Matsutani, and a. Kitano, "Flowability of unidirectionally arrayed chopped strands in compression molding," *Compos. Part B Eng.*, vol. 42, no. 6, pp. 1764–1769, Sep. 2011.

[53] R. M. O'Higgins, M. a. McCarthy, and C. T. McCarthy, "Comparison of open hole tension characteristics of high strength glass and carbon fibre-reinforced composite materials," *Compos. Sci. Technol.*, vol. 68, no. 13, pp. 2770–2778, Oct. 2008.

[54] Y. Fujita, H. Matsutani, S. Kawamoto, T. Takehara, and I. Taketa, "Mechanical Property and Flowability of Quasi-Isotropic Uacs Laminates," no. June, pp. 22–26, 2014.

[55] A. Murdani, C. Makabe, and M. Fujikawa, "Fatigue and fracture behavior in notched specimens of C/C composite with fine-woven carbon fiber laminates," *Carbon N. Y.*, vol. 47, no. 14, pp. 3355–3364, Nov. 2009.

[56] T. Okabe and S. Yashiro, "Damage detection in holed composite laminates using an embedded FBG sensor," *Compos. Part A Appl. Sci. Manuf.*, vol. 43, no. 3, pp. 388–397, Mar. 2012.

[57] Z. Hashin and A. Rotem, “A Fatigue Failure Criterion for Fiber Reinforced Materials,” *J. Compos. Mater.*, vol. 7, no. 4, pp. 448–464, 1973.

[58] F. Ellyin and H. El-Kadi, “A fatigue failure criterion for fiber reinforced composite laminae,” *Compos. Struct.*, vol. 15, no. 1, pp. 61–74, 1990.

[59] A. Plumtree and G. X. Cheng, “Fatigue damage parameter for off-axis unidirectional fibre-reinforced composites,” *Int. J. Fatigue*, vol. 21, no. 8, pp. 849–856, 1999.

[60] M. Kawai, “A phenomenological model for off-axis fatigue behavior of unidirectional polymer matrix composites under different stress ratios,” *Compos. Part A Appl. Sci. Manuf.*, vol. 35, no. 7–8, pp. 955–963, 2004.

[61] K. L. Reifsnider and A. Talug, “Analysis of fatigue damage in composite laminates,” *Int. J. Fatigue*, vol. 2, no. 1, pp. 3–11, 1980.

[62] S. Liu and J. A. Nairn, “Fracture Mechanics Analysis of Composite Microcracking: Experimental Results in Fatigue,” *Proc. 5th Tech. Conf. Compos. Mater. Am. Soc. Compos.*, pp. 287–295, 1990.

[63] J. Tong, F. J. Guild, S. L. Ogin, and P. A. Smith, “On matrix crack growth in quasi-isotropic laminates—I. Experimental investigation,” *Compos. Sci. Technol.*, vol. 57, no. 11, pp. 1527–1535, 1997.

[64] J. Tong, F. J. Guild, S. L. Ogin, and P. A. Smith, “on Matrix Crack Growth in Quasi-Isotropic Laminates-Ii. Finite Element Analysis,” *Compos. Sci. Technol.*, vol. 51, no. 97, pp. 1537–1545, 1997.

[65] C. Henaff-Gardin and M. C. Lafarie-Frenot, “The use of a characteristic damage variable in the study of transverse cracking development under fatigue loading in cross-ply laminates,” *Int. J. Fatigue*, vol. 24, no. 2–4, pp. 389–395, 2002.

[66] J. Tong, “Characteristics of fatigue crack growth in GFRP laminates,” *Int. J. Fatigue*, vol. 24, no. 2–4, pp. 291–297, 2002.

[67] A. W. Wharmby and F. Ellyin, “Damage growth in constrained angle-ply laminates under cyclic loading,” *Compos. Sci. Technol.*, vol. 62, no. 9, pp. 1239–1247, 2002.

[68] T. Yokozeki, T. Aoki, and T. Ishikawa, “Fatigue growth of matrix cracks in the transverse direction of CFRP laminates,” *Compos. Sci. Technol.*, vol. 62, no. 9, pp. 1223–1229, 2002.

[69] N. T. Hoang, D. Gamby, and M. C. Lafarie-Frenot, “Predicting fatigue transverse crack growth in cross-ply carbon-epoxy laminates from quasi static strength tests by using iso-damage curves,” *Int. J. Fatigue*, vol. 32, no. 1, pp. 166–173, 2010.

[70] A. Hosoi, K. Takamura, N. Sato, and H. Kawada, “Quantitative evaluation of fatigue damage growth in CFRP laminates that changes due to applied stress level,” *Int. J. Fatigue*, vol. 33, no. 6, pp. 781–787, 2011.

[71] Sudarsono and K. Ogi, “Fatigue Behavior of Open-Holed CFRP Laminates with Initially Cut Fibers,” *Open J. Compos. Mater.*, vol. 7, no. 1, pp. 49–62, 2017.

[72] Sudarsono and K. Ogi, “Effect of Fiber Cutting Angle on The Fatigue Behavior of Open-Holed CFRP Laminates with Initially Cut Fibers,” *Mater. Syst.*, vol. 35, pp. 37–44, 2017.